MODIFIED CROCCO-LEES MIXING THEORY FOR SUPERSONIC SEPARATED AND REATTACHING FLOWS

Thesis by

Herbert S. Glick

In Partial Fulfillment of the Requirements

For the Degree of

Doctor of Philosophy

California Institute of Technology

Pasadena, California

1960

ACKNOWLEDGMENTS

The author wishes to express his appreciation to Professor Lester Lees for his guidance throughout the course of the investigation. He also wishes to thank Mrs. Betty Laue for her enthusiastic and able assistance in carrying out most of the desk computations; Mrs. Truus van Harreveld, Miss Georgette A. Pauwels, and Mr. Andy Chapkis who assisted in the early computations; Mrs. Betty Wood for preparing the figures, and Mrs. Geraldine Van Gieson for her typing of the manuscript.

The author acknowledges with gratitude the receipt of a sabbatical leave grant from the Cornell Aeronautical Laboratory, Inc. of Buffalo, New York for the year 1957-1958, and a fellowship from the Curtiss-Wright Corporation for the year 1958-1959.

ABSTRACT

Re-examination of the Crocco-Lees method has shown that the previous quantitative disagreement between theory and experiment in the region of flow up to separation was caused primarily by the improper $C(\kappa)$ relation assumed. A new $C(\kappa)$ correlation, based on low-speed theoretical and experimental data and on supersonic experimental results, has been developed and found to be satisfactory for accurate calculation of two-dimensional laminar supersonic flows up to separation.

A study of separated and reattaching regions of flow has led to a physical model which incorporates the concept of the "dividing" streamline and the results of experiment. According to this physical model, viscous momentum transport is the essential mechanism in the zone between separation and the beginning of reattachment, while the reattachment process is, on the contrary, an essentially inviscid process. This physical model has been translated into Crocco-Lees language using a semi-empirical approach, and approximate $C(\kappa)$ and $F(\kappa)$ relations have been determined for the separated and reattaching regions. The results of this analysis have been applied to the problem of shock wave-laminar boundary layer interaction, and satisfactory quantitative agreement with experiment has been achieved.

TABLE OF CONTENTS

LIST OF FIGURES

LIST OF SYMBOLS

a	speed of sound $= \sqrt{\gamma RT}$
A	0.44
$\overline{b}$	function defined by Eq. (B-26)
$C(\kappa)$	mixing rate correlation function
$\overline{C}$	average value of $C(\kappa)$ between separation and shock impingement
C_1	value of $C(\kappa)$ in the region from separation to the beginning of the plateau
C_2	value of $C(\kappa)$ in the plateau region
c_f	$\tau_w / \frac{1}{2} \rho_e u_e^2$
d	function defined by Eq. (B-28)
$D(\kappa)$	skin friction correlation function
f	$\dfrac{(\delta - \delta_i^* - \delta_i^{**})\,\delta_i}{(\delta_i - \delta_i^*)^2}$
$\overline{f}$	function defined by Eq. (C-8)
F	$f/\kappa^2 = \left(\dfrac{\delta_i + \delta_i^{**}}{\delta_i - \delta_i^* - \delta_i^{**}}\right)$
$\overline{g}$	function defined by Eq. (C-8)
H	form factor $= \delta^*/\delta^{**}$
I	momentum flux in the x direction $= \int_0^\delta \rho u^2 \, dy$
k	$(d\delta/dx) - \theta$
k_3	function defined by Eq. (C-8)
K	$\dfrac{(3\gamma - 1)}{2(\gamma - 1)}$
$\overline{L}$	characteristic length

m	mass flux in the x direction = $\int_0^\delta \rho\, u\, dy$
$\dot{m}$	$m\, a_t$
M	Mach number = u/a
$\hat{M}_e$	$\frac{1}{2}(M_{esh} + M_{\infty f})$
n	Cohen-Reshotko velocity profile shape parameter
p	pressure
R	gas constant
Re	Reynolds number
S_w	Cohen-Reshotko wall enthalpy parameter
t	$(1 - \frac{\gamma - 1}{2} w_e^2) = T_e/T_t$
T	temperature
u	velocity in x direction
w	u/a_t
x, y	coordinates along, and normal to, the wall
L, N, P, Q	functions defined by Eq. (39)
a, b, v	constants
$\tilde{m}_i, \tilde{k}_i, \tilde{C}(K)_i$	quantities defined by Eqs. (D-1) and (D-2)
α, β	constants in linear relation, $F = \alpha K + \beta$
γ	ratio of specific heats = c_p/c_v
δ	a length which measures the thickness of the viscous layer
δ^*	displacement thickness
δ^{**}	momentum thickness
Δx_R	reattachment length scale
Δ^*	$(\delta_i^*/\xi)\sqrt{Re_i \frac{(n+1)}{2}}$

ε	$(M_e - M_\infty)$
ζ	a kind of local Reynolds number = $m/\mu_t a_t$
$\bar{\eta}$	F_s/F_b
θ	streamline direction relative to the wall at $y = \delta$
κ	Crocco-Lees velocity profile shape parameter
λ	velocity profile shape parameter
μ	coefficient of viscosity
ξ, η	incompressible coordinates along, and normal to, the wall
$\bar{\xi}$	$\xi/\bar{L}$
ρ	density
$\sigma(\kappa)$	$\frac{D(\kappa)}{2(1-\kappa)C(\kappa)}$
τ	shear stress
ϕ_e	$\frac{(1 - \frac{\gamma-1}{2} w_e^2)}{\gamma w_e}$
ϕ_1	$(T_1/T_t)(1/\gamma w_1)$
χ	$\theta \zeta_s/2\bar{C}$
ψ	function defined by Eq. (67)
Ω	F_b/K_b
ω	K_{sh}/K_b

Subscripts

b	Blasius flat plate conditions
e	conditions at $y = \delta$
i	incompressible conditions
R	conditions at reattachment

s	conditions at separation
sh	conditions at shock impingement
t	free stream stagnation conditions
w	conditions at the wall
$\ulcorner$	conditions at the beginning of the plateau region
1	mean value of viscous region
∞	free stream conditions
∞f	conditions far downstream of interaction

I. INTRODUCTION

The main object of the present research is to advance the development of the Crocco-Lees "mixing" theory[1]* so that it can be used to treat flows that contain separated and reattaching regions. The problem of separated flows is an old one, and many examples of such flows are observed in everyday experience, as well as in diverse technical problems. For example, the relatively calm air pocket that is found on the upstream side of a house during a windstorm[2] and the "dead water" zones behind large rocks in a swiftly flowing river are familiar examples of separated regions. Knowledge of separated flows is important to the engineer in such technical problems as the prevention of wing stall, the calculation of diffuser and compressor efficiencies, the prediction of losses in overexpanded rocket nozzles, and the estimation of the effectiveness of aerodynamic control surfaces. In order to solve his problems, the engineer has been obliged to use experimental data almost entirely, since a practical theoretical method of treating such flows is not available.

Separated and reattaching flows can occur under a variety of circumstances. For example, the flow may be laminar or turbulent, steady or unsteady, and subsonic or supersonic. But in all cases, the main cause of the phenomenon of separation can be traced to the inability of the low energy viscous region adjacent to a body to adjust to the imposed inviscid pressure distribution. More specifically, consider subsonic laminar flow about a bluff body, such as a cylinder or sphere, in a high Reynolds number stream. Such a flow generally contains a region

---

* Superscripts denote references at the end of the text.

in which there is a fairly large positive pressure gradient. The no-slip boundary condition of continuum flow implies that the boundary layer fluid upstream of the positive pressure gradient region is deficient in energy and momentum, and this deficiency is especially serious for the fluid particles near the wall. As the boundary layer fluid enters the region of positive pressure gradient, momentum is transferred to the low energy fluid near the wall from the more energetic fluid further out by molecular transport. For turbulent boundary layers, the momentum transport is mainly due to macroscopic turbulent eddies. In either the laminar or the turbulent case, this momentum transfer enables the low energy fluid near the wall to continue flowing downstream. At the same time, the boundary layer velocity profile is distorted in such a way that the velocity gradient normal to the wall, and thus the wall shear stress, is reduced. The distortion of the velocity profile is therefore associated with two effects which allow the boundary layer fluid to continue flowing downstream, namely the transport of momentum from high energy to low energy regions and the reduction of the wall shear stress.

However, the amount of velocity profile distortion that is possible is limited. After the flow has progressed sufficiently into the region of positive pressure gradient, the slope of the velocity profile becomes zero at the wall, so that the wall shear stress is zero. At that point, for the two-dimensional and axi-symmetric cases, the flow "separates" from the wall. For general three-dimensional flows, the phenomenon of separation is more complex[3], and the vanishing of the wall shear stress is only a necessary, but not a sufficient, condition for separation. However, in all cases, if the flow field is divided into two regions by a stream surface

starting at the body such that one region consists of all the fluid particles upstream of the body and the second region is an isolated "dead water" region, the flow is generally regarded to be a separated one. When the flow separates, the actual pressure distribution is always markedly different from the inviscid distribution, and in such a way as to reduce the values of the positive pressure gradients. Thus, the phenomenon of separation is caused by the limited ability of the flow to supply sufficient momentum to the low energy portions of the flow that are adjacent to the body, thereby necessitating a change in the effective body shape, which is achieved by the fluid "separating" from the body. Increasing the capacity for momentum transfer would of course tend to delay separation. This deduction is readily verified by the well-known experimental fact that turbulent boundary layers can penetrate more deeply into positive pressure gradient fields without separating than laminar boundary layers can.[2]

It is often found that separated flows will return to the surface, and "reattach". The sequence of separation and reattachment traps a separated dead water region between the body and the outer flow. Examples of this phenomenon are found in separation "bubbles" on wing surfaces[4], and in shock wave-boundary layer interactions[5-9]. The details of the reattachment process are more obscure than those in the case of separation, and experimental studies of reattachment are only now beginning to provide a real understanding of the process[7].

It is clear from the above discussion that the details of separated flow phenomena are quite complex, even for laminar flow. The Navier-Stokes equations, which describe general laminar continuum flow with

satisfactory accuracy, also in principle describe the subclass of laminar separated flows. Unfortunately, the Navier-Stokes equations are a highly non-linear set of partial differential equations that have been solved only in a relatively few simple cases. The flow geometries and boundary conditions of separated and reattaching flows are so complicated that a direct solution of the problem using the Navier-Stokes equations directly does not seem to be feasible. This realization, and the practical importance of separated flows, has led to a search for approximate methods.

It has been observed experimentally that various types of separated flows have many similarities, and indeed, it has been possible to correlate the behavior of separated flows with widely different flow geometries[7]. The observed similarities suggest that an approximate method that is applicable to general separated flows may be feasible. Several attempts have been made to formulate such an approximate method, but unfortunately, the results of these efforts, while showing some agreement with experiment, have been either severely restricted in generality or quantitatively unsatisfactory[1, 10-12]. Of the various approximate methods that have been formulated, the method of Crocco and Lees[1] appears to be the most general and promising.

The Crocco-Lees method is similar in many respects to approximate integral methods that have been developed for the treatment of attached boundary layers[13-17]. However, these approximate methods of attached boundary layer theory, with the exception of the method of Tani[17], employ a parameter that, while satisfactory for attached boundary layers, is not appropriate for separated flows. The choice of an alternate

parameter that is satisfactory for the treatment of separated flows largely determines the essential differences between the Crocco-Lees method and the other approximate integral methods.

In order to describe the main conceptual aspects of the Crocco-Lees method, as well as to show the specific differences between it and the other approximate integral methods, we will briefly consider the general approach and concepts of integral methods for the case of attached boundary layers. The original idea stems from the von Kármán momentum integral equation. For steady two-dimensional flow, this equation is as follows:

$$(\partial/\partial x)\int_0^\delta \rho u^2\, dy - u_e(\partial/\partial x)\int_0^\delta \rho u\, dy = -\tau_w - \delta(dp/dx) \qquad (1)$$

where

ρ = density

u_e = velocity in the x direction at $y = \delta = u_e(x)$

τ_w = wall shear stress $= \mu(\partial u/\partial y)_{y=0}$

p = pressure $= p(x)$

δ = a length which measures the boundary layer thickness

x, y = the coordinates along, and normal to, the wall.

This equation is simply an expression of Newton's second law averaged over the boundary layer thickness, δ. By means of this averaging process, the original second-order partial differential equation for the x-momentum and the equation of continuity are converted into a single first-order differential equation for the dependent variable, $\delta(x)$, or for an integral parameter, such as the momentum thickness, δ^{**}.

Suppose we consider the case of low-speed, isothermal flow. By defining the displacement and momentum thicknesses as follows:

$$\delta_i^* = \text{displacement thickness} \equiv \int_0^{\delta_i} \left(1 - \frac{u}{u_e}\right) dy$$

$$\delta_i^{**} = \text{momentum thickness} \equiv \int_0^{\delta_i} (u/u_e)\left(1 - \frac{u}{u_e}\right) dy \qquad (2)$$

the von Kármán momentum integral equation can be written as

$$u_e \frac{d\delta_i^{**}}{dx} + 2\delta_i^{**} \frac{du_e}{dx}\left(2 + \frac{\delta_i^*}{\delta_i^{**}}\right) = 2\frac{\mu}{\rho u_e}\delta_i^{**}\left(\frac{\partial u}{\partial y}\right)_{y=0} \qquad (3)$$

In the usual approximate integral methods[13-17], the velocity profile is represented as

$$\frac{u(x,y)}{u_e} = g\left(\frac{y}{\ell}, \lambda\right) \qquad (4)$$

where λ is a velocity profile shape parameter and ℓ is either δ_i or δ_i^{**}. In the Pohlhausen[13] and Thwaites[14-16] methods, a second relation is obtained by satisfying the boundary layer x-momentum equation at the surface, which gives the following relation

$$\frac{\mu}{\rho}\left(\frac{\partial^2 u}{\partial y^2}\right)_{y=0} = \frac{\mu u_e}{\rho \ell^2} g''(0,\lambda) = -u_e \frac{du_e}{dx} \quad . \qquad (5)$$

If the parameter λ is defined as

$$\lambda \equiv -\frac{\ell^2 \rho}{\mu}\frac{du_e}{dx} = g''(0,\lambda) \quad , \qquad (6)$$

then Eqs. (1) and (6) provide two independent relations for the dependent variables, λ and ℓ, and the method is completely formulated. If the

velocity profile is expressed in terms of more than one shape parameter, then the additional parameters must be related to δ_i or δ_i^{**} by the boundary conditions, or else additional relations must be supplied. Thus, if an approximate integral method uses only the von Kármán momentum integral equation and a second relation analogous to Eq. (6), then such a method generally implies, and is inseparable from, a one-parameter description of the flow.

According to Eq. (6), the shape of the velocity profile is directly related to the local gradient of the external stream velocity. Such a formulation may be more or less satisfactory for attached boundary layers, but it is completely inadequate for separated and reattaching flows. It implies, for example, that the profile must coincide with the Blasius flat plate profile whenever $(du_e/dx) \longrightarrow 0$. In the case of shock wave - laminar boundary layer interaction (Figure 1), the pressure gradient downstream of separation decreases steadily and is practically zero in the plateau region, but the velocity profile bears no resemblance to the Blasius flow. Similar anomalies occur in the reattachment region. In order to avoid this difficulty, the Crocco-Lees method utilizes a shape parameter, κ, which is a non-dimensional ratio of the momentum flux to the mass flux in the viscous region. This parameter, κ, is not explicitly related to (du_e/dx) and is also not uniquely determined by δ. A second relation, in addition to Eq. (1), is required to complete the mathematical formulation of the method, and this relation is obtained from a physical model. The flow, according to this physical model, is divided into two regions -- an external, inviscid region and an internal viscous zone (Figure 2). These two regions interact by the momentum transfer associated with the

"mixing", or mass entrainment, of fluid from the high energy external flow into the low energy viscous region. A continuity equation, expressing the rate of mixing, or entrainment, of fluid from the external region into the internal region is the second relation between k and δ in the Crocco-Lees method, and basically distinguishes it from the other approaches.

Another aspect which characterizes the Crocco-Lees method is that the external and internal flows interact, so that the change in the thickness of the viscous region affects the external inviscid flow. The earlier discussion of the phenomenon of separation shows that a separated flow certainly falls into this category. However, it is well-known that for attached subsonic flows, the effect of the increase in boundary layer thickness on the flow field is small, at least at high Reynolds number, and can be neglected as far as the determination of the pressure distribution is concerned. But if the flow does separate, the whole flow field is strongly affected. Thus, subsonic interaction is generally either trivial or drastic. In the supersonic case, the situation is the opposite, with a relatively small thickening of the viscous region causing large effects locally in the external flow field, especially for the case of non-cooled walls. Also, if the flow separates, the effect on the external flow field is rather localized. These considerations and the simplicity of the relation between flow angle and velocity given by the Prandtl-Meyer equation show that the problem of supersonic separated flow is much more amenable to solution than the subsonic problem, and all calculations that have been performed using the Crocco-Lees method have been for the former case.

The Crocco-Lees mixing theory is not the only possible way in

which separated and reattaching flows can be treated. By multiplying the x-momentum equation by u^m and integrating across the boundary layer, one obtains a series of first-order moment equations, with the von Kármán momentum integral equation characterized by $m = 0$. This n-moment method ($n = m + 1$) thus provides n independent relations that can be used in the formulation of an approximate method. In the case of attached boundary layers, Tani[17], following an idea of Walz[18], does not use Eq. (6), but employs a formulation in which $n = 2$. He therefore obtains a pair of first-order ordinary differential equations, instead of the single differential equation and algebraic equation of the Pohlhausen and Thwaites methods. Since Tani does not use Eq. (6), his method could be used beyond separation and therefore constitutes a possible alternate two-moment method for treating separated and reattaching flows.

An n-moment method for $n > 2$ offers the possibility of characterizing the velocity profile by more than a single shape parameter. The use of more than one parameter to characterize the velocity profile clearly implies an increase in the mathematical complexity of the method, and can really be justified only by the failure of one-parameter methods. The complexity of separated and reattaching flows suggests that a one-parameter approach may not be adequate, and the present study is to a large extent an investigation aimed at determining whether or not the one-parameter Crocco-Lees method is satisfactory for treating separated and reattaching flows.

In this study, only laminar flows will be considered since the present aim is to examine relatively well-understood cases with the method to determine if the present formulation is basically adequate.

The extension of the method to turbulent flows is discussed in References 1 and 19. Also only two-dimensional cases will be considered in the same spirit of keeping the equations as simple as possible, but the generalization of the method to axi-symmetric flows can be carried out in essentially the same way as in Reference 16. In addition to the above assumptions, it will also be assumed for the present that the heat transfer to the body is zero. The extension of the method to include heat transfer is not obvious, but approaches such as that used in Reference 16 may be employed.

The problem of two-dimensional laminar supersonic flow over insulated bodies has been studied both experimentally[5-9] and by the Crocco-Lees method[20, 21]. Qualitative agreement between theory and experiment has been achieved, but the quantitative agreement has been unsatisfactory even for attached flows[21] where the assumptions of the method are least open to question. In the present study, the attached region of flow will be investigated first with the aim of determining the reason for the previous quantitative disagreement between theory and experiment. Then the problem of the separated and reattaching regions of flow will be investigated. A physical model of separated flows will be developed and translated into the language of the Crocco-Lees method. Finally several calculations of shock wave-laminar boundary layer interaction will be carried out and shown to predict a complex separated and reattaching flow with satisfactory quantitative accuracy.

II. CROCCO-LEES METHOD

Since important changes in concepts and content of the Crocco-Lees method have been developed here, it is the purpose of this section to re-examine in detail the physical and mathematical formulation of the method. The flow is divided into two regions -- an outer region which is assumed to be essentially non-dissipative, and an inner region in which viscosity is assumed to play an important role (Figure 2). The extent of the viscous region is measured by the length, δ, which for the case of a body in a high Reynolds number stream is the usual boundary layer thickness, and for a wake, is the extent of the non-uniform flow in the direction transverse to the external flow direction. Clearly, the definition of the length, δ, is artificial, and physical quantities, such as pressure, interaction distance, etc. should not be sensitive to the definition of δ. In several previous studies using the Crocco-Lees method[1, 19-21], the artificiality of the length, δ, was not appreciated and studies were carried out to determine the proper method of defining δ. It has been found in the present study and in the work of Gadd and Holder[22] that physical quantities do not depend on the definition of δ as long as the definition is a reasonable one that is sensitive to velocity profile shape. Indeed, for the limiting case of weak hypersonic interaction, which is discussed in Appendix B, it is shown explicitly that several different definitions of δ give identically the same result.

Once some criterion for determining δ is selected, the equations of motion for the viscous region can be written. The complete equations describing attached, separated, and reattaching flows are too formidable

to allow mathematical analysis, so many simplifying assumptions have to be made. The assumptions will now be listed, but a discussion of their validity will be postponed until Section V. The assumptions can be grouped roughly into two categories depending on their importance and inherent necessity. The major assumptions of the method are as follows:

(1) The gradients of viscous or Reynolds stresses in the flow direction are negligible compared with the static pressure gradient in the flow direction.

(2) The pressure gradient transverse to the stream direction is negligible.

(3) The flow is steady.

In addition to these major assumptions, the following secondary assumptions have been made in the present study in order to simplify the problem:

(4) The external flow is a plane, isentropic, supersonic flow over a flat, adiabatic wall oriented in the free stream direction, with the flow direction at $y = \delta$ given by the Prandtl-Meyer relation.

(5) Prandtl number is unity.

(6) Viscosity is proportional to the absolute temperature.

(7) Flow angles relative to the wall are small.

(8) The gas is thermally and calorically perfect.

(9) The stagnation temperature is constant throughout the whole flow.

(10) The viscous region is laminar.

The equations describing the flow can now be written. The momentum equation for the viscous region in the x direction is

$$dI/dx = u_e (d\bar{m}/dx) - (\delta dp/dx) - \tau_w \qquad (7)$$

where

I = momentum flux in x direction $\equiv \int_0^\delta \rho u^2 \, dy$

u_e = absolute value of flow velocity at $y = \delta$

$\bar{m}$ = mass flux in x direction $\equiv \int_0^\delta \rho u \, dy$

p = static pressure of viscous region at a streamwise location

τ_w = shear stress at the wall.

The continuity equation for the viscous region can be written as

$$(d\bar{m}/dx) = \rho_e u_e \left(\frac{d\delta}{dx} - \theta \right) \qquad (8)$$

where

ρ_e = density at $y = \delta$

θ = streamline direction angle relative to the wall at $y = \delta$ (Figure 2)

Since the external flow is assumed to be isentropic, the Bernoulli equation can be written as

$$(1/p)(dp/dx) = -(1/\phi_e)(dw_e/dx) \qquad (9)$$

where

$a_t \equiv$ stagnation speed of sound $= \sqrt{\gamma R T_t}$

$$\phi_e \equiv \frac{\left(1 - \frac{\gamma - 1}{2} w_e^2 \right)}{\gamma w_e}$$

$$w_e \equiv (u_e/a_t)$$

With these basic assumptions and equations, it is now possible to cast the equations into the language of the Crocco-Lees method. First, the basic parameter of the method, and the one used to characterize the flow in the viscous region is defined as follows:

$$K \equiv \frac{\text{momentum flux}}{\text{mass flux x local external velocity}} = \frac{I}{\bar{m}\, u_e}$$

$$= \frac{\text{actual momentum flux}}{\text{momentum flux of mass flux moving at } u = u_e} \qquad (10)$$

$$= u_1/u_e$$

where

$u_1 \equiv$ "average" velocity of viscous region.

It is now convenient to introduce some definitions to facilitate the writing of the equations. Let

$$\delta^* \equiv \int_0^\delta \left(1 - \frac{\rho u}{\rho_e u_e}\right) dy = \text{displacement thickness}$$

$$\delta^{**} \equiv \int_0^\delta \left(\rho u/\rho_e u_e\right)\left(1 - \frac{u}{u_e}\right) dy = \text{momentum thickness} \qquad (11)$$

$$\rho_1 \equiv \text{mean density of the viscous region} \equiv \bar{m}/u_1\delta$$

$$T_1 \equiv \text{mean temperature of the viscous region} \equiv p/\rho_1 R \quad .$$

The definitions of ρ_1 and T_1 are made for convenience and no thermodynamical significance is attributed to these quantities, except for the trivial case of uniform flow conditions in the viscous region. We also define the following convenient quantities:

$$\phi_1 \equiv (T_1/T_t)(1/\gamma w_1)$$

$$c_f \equiv (\tau_w/\tfrac{1}{2}\rho_e u_e^2) \tag{12}$$

$$m \equiv \bar{m}\, a_t$$

Using these relations, it can be shown[1] that

$$\kappa = \left(\frac{\delta - \delta^* - \delta^{**}}{\delta - \delta^*} \right) \tag{13}$$

$$(\rho_1/\rho_e) = (T_e/T_1) = \frac{(\delta - \delta^*)^2}{\delta(\delta - \delta^* - \delta^{**})} \tag{14}$$

The flow equations written in terms of these newly-defined quantities are

$$(d/dx)(m\kappa w_e) = w_e\,(dm/dx) - \delta(dp/dx) - (pw_e/\phi_e)(c_f/2) \tag{15}$$

$$dm/dx = p/\phi_e \left(\frac{d\delta}{dx} - \theta \right) \tag{16}$$

$$dp/p = -(dw_e/\phi_e) \tag{17}$$

$$m = p\delta/\phi_1 \tag{18}$$

For supersonic flow, the Prandtl-Meyer relation furnishes another equation:

$$\theta = \theta(w_e) \tag{19}$$

When p and θ are eliminated from the system of equations by using Eqs. (17) and (19), there are three remaining independent relations for the six unknowns δ, m, κ, w_e, c_f, and ϕ_1. Therefore, three additional relations are required to complete the mathematical formulation of the method. The three additional relations will be taken to be of the following form:

$$\phi_1 = \phi_1(\kappa, w_e, m, \delta)$$

$$c_f = c_f(\kappa, w_e, m, \delta) \qquad (20)$$

$$k \equiv (d\delta/dx) - \theta = k(\kappa, w_e, m, \delta)$$

These additional relations are of the same type as those employed in the integral correlation methods of Thwaites[14], Rott and Crabtree[15], and Cohen and Reshotko[16]. It should be emphasized that the data necessary to obtain these correlation relations must come from other sources, either theoretical or experimental. For attached flows, detailed theoretical and experimental data are available, while for separated flows, only experimental data of a very restricted nature are known. This qualitative difference between attached and separated flow data will necessitate separate approaches in obtaining the correlation relations ϕ_1, c_f, and k. In order to avoid confusion, the discussion of the problem beyond separation will be postponed until Section IV. It is nevertheless clear that the same basic information is necessary in all regions of flow, and the apparent differences in approach for the two flow regimes are dictated by the present ignorance of separated flows.

For attached flows, the theoretical studies of Thwaites[14], Howarth[23], Falkner and Skan[24], and Hartree[25], and the experimental study of flow over an ellipse by Schubauer[26] provide detailed incompressible flow data on attached boundary layers for different external velocity distributions. This detailed data can be examined with a view toward finding relations for ϕ_1, c_f, and k in terms of the variables κ, w_e, m, and δ which are similar for the several flows. If such relations can be found, interpolated

curves for ϕ_1, c_f, and k in the κ, w_e, m, and δ space can be selected to represent flows of the same general class. These interpolated curves are the "universal" curves characteristic of correlation methods.

The errors introduced by selecting "universal" curves are not obvious and are generally found by comparison with experiment and exact solutions. If the correlation curves for the various experiments and exact solutions can be made to agree closely, the correlation method should give good results. Therefore, one problem is to try to optimize the correlation relations to give such agreement (See Appendix D.). No systematic procedure for such an optimization is known, and the general method of determining correlation functions is to try the simplest functions consistent with theoretical and experimental knowledge. The general experience of correlation methods seems to be that a skin friction correlation can be found that is quite "universal", while the other correlations are not as satisfactory.

With this discussion of the concepts, aims, and problems in obtaining correlations for ϕ_1, c_f, and k, we now proceed to the methods by which they have been determined in the present study for the attached part of the flow. In order to determine the ϕ_1 correlation (related to the mean temperature function of Reference 1), it is necessary to introduce the Stewartson transformation[27], relating a compressible boundary layer flow with a prescribed variation of external velocity to an equivalent incompressible boundary layer with a transformed external velocity distribution.

The Stewartson transformation is defined by the relations

$$\xi \equiv \int_0^x (a_e/a_t)(\rho_e/\rho_t)\, dx$$

$$\eta \equiv (a_e/a_t) \int_0^y (\rho/\rho_t)\, dy \qquad (21)$$

where ξ , η are incompressible coordinates, x, y are the associated compressible coordinates, and the subscript t refers to the compressible free stream stagnation conditions (chosen as reference values). In Reference 1, it is shown that if u is the compressible velocity in the x direction and u_i is the transformed, or incompressible, velocity, then

$$\left.\begin{aligned} (u_i/a_t) &= (u/a_e) \\ (u_i/u_{ie}) &= (u/u_e) \\ (\delta_i - \delta_i^*) &= \frac{\rho_e a_e}{\rho_t a_t} (\delta - \delta^*) \\ (\delta_i - \delta_i^* - \delta_i^{**}) &= \frac{\rho_e a_e}{\rho_t a_t} (\delta - \delta^* - \delta^{**}) \\ m_i &= m \end{aligned}\right\} \qquad (22)$$

so that

$$\kappa = \frac{(\delta - \delta^* - \delta^{**})}{(\delta - \delta^*)} = \frac{(\delta_i - \delta_i^* - \delta_i^{**})}{(\delta_i - \delta_i^*)} \quad . \qquad (23)$$

Thus κ can be evaluated from the incompressible equivalent of the compressible flow. It is also shown in Reference 1 that

$$\delta = \frac{\rho_t a_t T_t}{\rho_e a_e T_e} \left[\delta_i - \frac{\gamma - 1}{2} w_e^2 (\delta_i - \delta_i^* - \delta_i^{**}) \right] \qquad (24)$$

and from the definition of T_1 given in Eq. (14), one finds that

$$(T_1/T_t) = f - \frac{\gamma - 1}{2} \kappa^2 w_e^2 \tag{25}$$

where

$$f \equiv \frac{(\delta_i - \delta_i^* - \delta_i^{**})\,\delta_i}{(\delta_i - \delta_i^*)^2} = \frac{\kappa\,\delta_i}{(\delta_i - \delta_i^*)} \quad . \tag{26}$$

For a uniform viscous region, δ_i^* and $\delta_i^{**} = 0$, so that f and κ approach unity and the relation for T_1/T_t is the familiar one-dimensional result. The deviations of f and κ from unity thereby measure, in a certain sense, the non-uniformity of the velocity profile.

It will be convenient to define an alternate function for f, defined as follows:

$$F \equiv (f/\kappa^2) - 1 = \frac{(\delta_i^* + \delta_i^{**})}{(\delta_i - \delta_i^* - \delta_i^{**})} \quad . \tag{27}$$

Since F and κ are defined by incompressible boundary layer parameters, for every incompressible velocity profile there are unique values of F and κ, so that the ϕ_1 correlation that is sought is

$$\phi_1 = \frac{1}{\gamma \kappa w_e} \left[f(\kappa) - \frac{\gamma - 1}{2} w_e^2 \kappa^2 \right]$$

or

$$\phi_1 = \frac{\kappa}{\gamma w_e} \left[F(\kappa) + t \right] \tag{28}$$

where

$$t \equiv 1 - \frac{\gamma - 1}{2} w_e^2 = (T_e/T_t) \quad .$$

It should be noted that the compressibility effects are separated out in an explicit way, since F and κ do not depend on w_e. Thus the problem of finding the ϕ_1 correlation essentially reduces to the determination of the $F(\kappa)$ correlation.

During the present study it was noticed that, for a given value of the form factor, H_i, where $H_i = (\delta_i^*/\delta_i^{**})$, the mean-temperature parameter f is maximum for a finite value of δ_i, while κ generally has the property that it increases monotonically towards unity with increasing δ_i. By choosing δ_i such that f is maximum, one obtains a simple analytic expression for $f(\kappa)$, which is

$$f(\kappa) = \frac{\kappa^2}{(2\kappa - 1)} \qquad \text{(See Appendix A.)}$$

or

$$F(\kappa) = \frac{2(1 - \kappa)}{(2\kappa - 1)} \quad . \tag{29}$$

For attached flows, the function $F(\kappa)$ derived from this maximization method agrees fairly well with the curve obtained from Falkner-Skan solutions when δ_i is defined by the condition $\frac{u(\delta_i)}{u_e} = 0.95$ (Figure 3). This $F(\kappa)$ relation also agrees closely with experimental turbulent data. No physical explanation of the suitability of this $F(\kappa)$ relation has been found as yet.

The maximum method of defining δ_i not only leads to a simple $F(\kappa)$ relation, but also greatly helps in obtaining the mixing rate correlation, k, from experimental studies, such as the Schubauer ellipse experiment. The reason this method of defining δ_i assists in reducing experimental data is because it is possible to calculate the extent of the viscous layer using well-defined experimental integral quantities (H_i and δ_i^*), instead of a velocity ratio, thereby determining the mass flux in the viscous region at given streamwise station without large experimental uncertainty. Inasmuch as k is determined from experiment by finding differences in mass flux between adjacent flow stations, small errors in

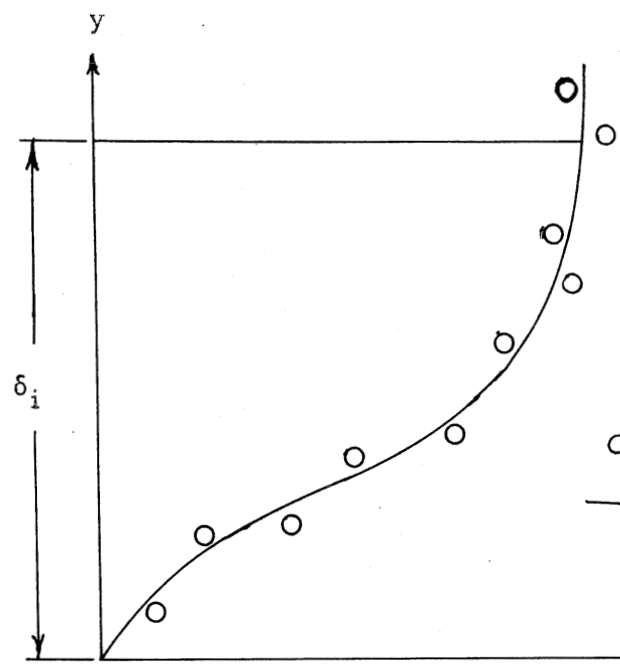

$$\delta_i = \delta_i^* \frac{(H_i + 1)}{(H_i - 1)} \qquad (A\text{-}14)$$

○ Experimental Point

—— Faired Curve

SKETCH A

---

determining the area under a velocity profile curve can easily make it impossible to determine mixing rates. (See Sketch A.)

The other two correlation relations necessary to complete the formulation of the Crocco-Lees method can be obtained by using the Stewartson transformation [Eq. (21)] to eliminate compressibility effects and then examining known incompressible solutions. From Eqs. (21) and (22), it follows that

$$d\bar{m}/dx = (a_e p_e / a_t p_t)\,(d\bar{m}_i/d\xi) \quad . \qquad (30)$$

For incompressible flow,

$$\bar{m}_i = \rho_t u_{ie} (\delta_i - \delta_i^*) \quad . \tag{31}$$

In order to obtain the functional form of the correlation relations, similarity solutions, such as those obtained by Falkner-Skan[24], have been employed. For such solutions, $u_{ie} \sim \xi^v$ and

$$\delta_i - \delta_i^* = \left(\frac{2 C \mu_t}{\rho_t u_{ie}} \right)^{\frac{1}{2}} \quad , \tag{32}$$

where C is a function of the shape of the velocity profile, i. e., $C = C(K)$. It is shown in Reference 1 that

$$k \equiv \frac{1}{\rho_e u_e} \frac{d\bar{m}}{dx} = C(k) \frac{\mu_e}{\bar{m}}$$

and (33)

$$k_i \equiv \frac{1}{\rho_t u_{ie}} \frac{d\bar{m}_i}{d\xi} = C(K) \frac{\mu_t}{\bar{m}_i}$$

A similar treatment can be given for the skin friction correlation. In Reference 1, it is shown that

$$c_f = \frac{D(K) \mu_e}{\bar{m}} \quad \text{and} \quad c_{f_i} = \frac{D(K) \mu_t}{\bar{m}_i} \quad , \tag{34}$$

where $D(K)$ is a function of the shape of the velocity profile.

In previous studies using the Crocco-Lees method, the $C(K)$ and $D(K)$ relations that have been used were those obtained from the Falkner-Skan solutions. However, by investigating other theoretical and experimental results for attached boundary layers, it is found that although the Falkner-Skan relation for c_f appears general (Figure 4), the relation for k is not universal. In fact, the Falkner-Skan values differ qualitatively as well as quantitatively from the other boundary layer results (Figure 5).

Roughly speaking, $C(\mathcal{K})$ for the Falkner-Skan solutions is essentially constant from separation to the Blasius flow condition, while the other theoretical solutions[14, 23, 24, 25] and the experimental Schubauer ellipse data[26] show a trend in which $C(\mathcal{K})$ drops sharply going from the Blasius condition to separation.

The reason that the $C(\mathcal{K})$ correlation for the Falkner-Skan solutions is qualitatively different from the other boundary layer solutions may be seen by expressing the definition of k so that the formal difference between Falkner-Skan flows and the other flows is brought out. From Eqs. (8), (11), (20), and (21), we obtain

$$k_i \equiv \frac{1}{\rho_t u_{ie}} \frac{d\overline{m}_i}{d\xi} = (\delta_i - \delta_i^*)\left[\frac{1}{\delta_i}\frac{d\delta_i}{d\xi} + \frac{1}{u_{ie}}\frac{du_{ie}}{d\xi}\right] - \delta_i \frac{d}{d\xi}\left(\frac{\delta_i^*}{\delta_i}\right) \quad . \quad (35)$$

For a general separating flow,

$$\begin{aligned} &(d\delta_i/d\xi) > 0 \\ &(du_{ie}/d\xi) < 0 \\ &(d/d\xi)(\delta_i^*/\delta_i) \geq 0 \quad . \end{aligned} \quad (36)$$

For a Falkner-Skan similarity solution, $(d/d\xi)(\delta_i^*/\delta_i) \equiv 0$. Therefore, for Falkner-Skan flows, the last term is zero, and the remaining two terms are of opposite sign. By numerically evaluating k_i for the Falkner-Skan case, it is found that the first term, which is positive, is the larger. It is therefore seen that the term that is missing in the Falkner-Skan case tends, in the general case, to reduce the value of k_i as separation is approached. This tendency is enhanced by the fact that as separation is

approached, the ratio, $(\delta_i - \delta_i^*)/(\delta_i)$, is about 0.4. In Figure 6, the variation of δ_i^*/δ_i with distance is shown for the Schubauer ellipse velocity distribution (Figure 7). The term $(d/d\xi)(\delta_i^*/\delta_i)$ is essentially zero near the Blasius flat plate condition, but becomes appreciable near separation. It is thus clear why the $C(\mathcal{K})$ correlations for Falkner-Skan and other boundary layer flows are similar near the Blasius condition and are different near separation. This difference is associated with the physical fact that Falkner-Skan flows are similar flows which do not have "histories" and do not reflect the essential change in shape of the velocity profile prior to separation, while the velocity profiles of the other boundary layer flows change in the streamwise direction.

As discussed previously, the definition of the length, δ_i, should not affect physical quantities, such as separation pressures, interaction distances, etc. However, the correlation functions $F(\mathcal{K})$, $C(\mathcal{K})$, and $D(\mathcal{K})$ are strongly dependent on the method of defining δ_i. This dependence is seen in Figure 3, where for laminar flows it is found that the $F(\mathcal{K})$ curves differ appreciably depending, for example, on the value chosen for the $u(\delta_i)/u_e$ ratio. The same sort of sensitivity is found in the $C(\mathcal{K})$ and $D(\mathcal{K})$ curves[1, 19]. It should be emphasized that since the method of defining δ_i is artificial, no physical significance can be associated with the fact that different methods of defining δ_i lead to different numerical values of $F(\mathcal{K})$, $C(\mathcal{K})$, and $D(\mathcal{K})$ for the same velocity profile. It is therefore clear that the choice of the method of defining δ_i is tantamount to choosing a method of bookkeeping. However, it can be expected that physical statements such as "the mixing rates between separation and

shock impingement increase to high values", will be reflected numerically for any definition of δ_i. These considerations of the artificiality of δ_i and the non-uniqueness of the $F(\kappa)$, $C(\kappa)$, and $D(\kappa)$ relations make it clear that what is to be sought is a self-consistent method of bookkeeping in which the behavior of flows which are of the same general type can be understood and interpreted within the Crocco-Lees framework, so as to allow reliable and relatively simple flow calculations and analyses to be performed.

III. FLOW PROBLEM UPSTREAM OF SEPARATION

The problem of two-dimensional laminar supersonic flow upstream of separation can be approached in several different ways. In 1949, Lees[10] treated the problem of shock wave-laminar boundary layer interaction using a modified von Kármán-Pohlhausen method. Cheng and Bray[20], Cheng and Chang[21], and Gadd and Holder[22] have made similar calculations using the Crocco-Lees method, with correlation functions derived from the Falkner-Skan similar solutions. As mentioned previously, these studies showed qualitative agreement with experiment, but the quantitative agreement was generally poor.

In the present study, the problem of two-dimensional laminar supersonic flows upstream of separation has been treated by two methods. First, the Cohen-Reshotko method[16] was modified to introduce interaction between the external and viscous flows by equating the "external flow" direction with the gradient of the displacement thickness. (See Appendix C.) Second, the problem has been studied using the Crocco-Lees method with correlation functions obtained by the maximum principle, and a new $C(\kappa)$ relation based on boundary layers that have "histories".

In order to determine the sensitivity of the theoretical results to the $C(\kappa)$ relation, calculations were performed for a separating flow at a free stream Mach number of 2.0 and a separation Reynolds number of 2.87×10^5 using several $C(\kappa)$ relations, corresponding to the curves shown in Figure 5. The $F(\kappa)$ relation used in the calculations was the one obtained by the maximum principle, and the $D(\kappa)$ relation used was that obtained by assuming that $D(\kappa)$ decreases linearly from the Blasius

value at $K = 0.693$ to zero at $K = 0.630$, the Howarth value of K at separation. Thus,

$$F(K) = \frac{2(1-K)}{(2K-1)}$$
$$D(K) = 22.2\,(K - .630) \tag{37}$$

If the variable, $\sigma(K)$, is defined as

$$\sigma(K) = \frac{D(K)}{2(1-K)\,C(K)} \tag{38}$$

the Crocco-Lees equations, when linearized with regard to Mach number, i.e., $M = M_\infty + \varepsilon$ and $\varepsilon << M_\infty$, become (See Appendix B.):

$$(dK/d\zeta) = -L\left[\frac{P}{\zeta} - \varepsilon\right]$$
$$(d\varepsilon/d\zeta) = -N\left[\frac{Q}{\zeta} - \varepsilon\right] \tag{39}$$

where

$\zeta = (m/\mu_t a_t) = \bar{m}/\mu_t$ is a kind of local Reynolds number ,

$$L \equiv \frac{2K(1-K)(2K^2-1)\sqrt{M_\infty^2-1}}{4M_\infty K(1-K)(2K^2-2K+1)\left(1+\frac{\gamma-1}{2}M_\infty^2\right)C(K)\left[1-\frac{\gamma M_\infty^2(2K-1)^2}{2(2K^2-2K+1)\left(1+\frac{\gamma-1}{2}M_\infty^2\right)}-\frac{(2K-1)^3(M_\infty^2-1)}{4(2K^2-2K+1)(1-K)\left(1+\frac{\gamma-1}{2}M_\infty^2\right)^2}\right]}$$

$$N \equiv \frac{L M_\infty}{K F(K)} = \frac{L M_\infty (2K-1)}{2K(1-K)}$$

$$P \equiv \frac{C(K)M_\infty}{\sqrt{M_\infty^2-1}}\left[\sigma(1-K)+\frac{(2K-1)(1-\sigma)}{2K}\left\{\frac{2\gamma K(1-K)M_\infty^2}{(2K-1)}+K\left(\frac{\gamma+1}{2}\frac{M_\infty^2}{1+\frac{\gamma-1}{2}M_\infty^2}-1\right)\right\}-\frac{2K(1-K)\left(1+\frac{\gamma-1}{2}M_\infty^2\right)}{(2K-1)}\right]$$

$$Q \equiv \frac{C(K)M_\infty}{\sqrt{M_\infty^2-1}}\left[\sigma(1-K)-\frac{2(1-K)K\left(1+\frac{\gamma-1}{2}M_\infty^2\right)}{(2K-1)}\left\{1-\frac{(1-\sigma)(2K^2-2K+1)}{K(2K-1)}\right\}\right]$$

In calculating a separating flow problem, the free stream Mach number, M_∞, is given and the quantities L, N, P, and Q are first plotted as a function of κ. A value of ζ is chosen at the separation point, which is equivalent to selecting the value of the separation Reynolds number. Then trial values of ε at separation are chosen, and the equations are numerically integrated in the upstream direction. The correct eigenvalue for ε at separation is obtained when the integrated quantities approach the weak hypersonic interaction limit[19, 20, 21, 28]. The results are then transformed back into the physical plane using the continuity equation and performing a single quadrature. (See Appendix B.)

The pressure distributions obtained by four such integrations are shown in Figure 8 along with a calculation of the same case using the Cohen-Reshotko method. The point at which the pressure starts to rise is roughly independent of the $C(\kappa)$ relation. It is found that the larger the value of $C(\kappa)$ near separation is, the larger are the values of the separation pressure rise and the separation pressure gradient. Also shown in Figure 8 is the slope of the experimental pressure distribution near separation (See Figure 9.) at the same free stream Mach number and roughly the same separation Reynolds number. By comparing the experimental and theoretical separation pressure gradients one sees that even for Case D, the theoretical separation pressure gradient is too great. In order to obtain a theoretical lower limit for the separation pressure gradient, a calculation was performed in which $C(\kappa)$ was assumed to be zero throughout the range of integration (Case F). Although this assumption is in error near the Blasius condition, it is seen to give a separation pressure gradient that is in good agreement with the experimental value.

This result suggests that $C(\kappa)$ is essentially zero for some, as yet undetermined, range of κ. The reason that only the experimental separation pressure gradient and not the pressure distribution is compared with calculations is seen in Figure 9 where experimental results obtained by Chapman, Kuehn, and Larson[7] are compared with those of Hakkinen, Greber, Trilling, and Abarbanel[8] at the same free stream Mach number and approximately the same Reynolds number. The experimental pressure distributions have similar shapes, with the major difference being a shift of the distributions in the streamwise direction. The reason the distributions are shifted is quite clearly the uncertainty in determining the separation point. In the experiments of Chapman, Kuehn, and Larson, the separation point was determined by an oil film technique, while in the experiments of Hakkinen, et al, the separation point was obtained from Stanton tube measurements. It is not clear which, if either, of these methods reliably determines the separation point, especially since the interaction distance in which the separation pressure rise takes place in many of the experiments is only a small fraction of an inch. These experimental difficulties have prevented the use of experimentally-determined parameters that depend directly on the determination of the separation point for comparison with the results of theoretical calculations. In Figure 8, for example, the experimental separation pressure, as measured by the two methods, indicates only that separation pressures calculated using a Falkner-Skan $C(\kappa)$ correlation are too high, but does not distinguish among the other $C(\kappa)$ relations.

Also, the uncertainty in locating the separation point prevents

the determination of the range of K near separation for which $C(K)$ can be set equal to zero. For this reason, an approximate $C(K)$ curve has been selected for the present calculations. The $C(K)$ relation that has been chosen is one that decreases linearly from the Blasius value of $C(K)$ at $K = 0.693$ to zero at the separation value of K, which is $K = 0.630$, i.e.,

$$C(K) = 36.2\,(K - .630) \quad . \tag{40}$$

Calculations of the pressure distributions up to separation for two different cases of shock wave-laminar boundary layer interaction have been carried out using this linear $C(K)$ relation, and the results are shown in Figures 10 and 11. It is seen that the agreement between theory and experiment is quite good for the case shown in Figure 10, while it is less satisfactory for the case shown in Figure 11. The scatter of the experimental data in the latter case is appreciable, and it is not certain whether the disagreement between theory and experiment is significant. Based on these calculations, it is felt that although the linear $C(K)$ relation is not an optimum, it is capable of predicting pressure distributions for a separating flow with an accuracy that is consistent with the present status of experimental data.

A re-examination of the Crocco-Lees theory up to separation has revealed that the major reason for the previous disagreement between theory and experiment for two-dimensional laminar supersonic separating flows[1, 20-22] is that the flow is characterized by low values of $C(K)$ near separation, and not by the Falkner-Skan values. The determination of an approximate $C(K)$ relation which seems to be consistent with low speed and supersonic data completes, albeit roughly, the solution of the problem up to the separation point.

IV. FLOW PROBLEM BEYOND SEPARATION

IV. 1. Physical Discussion

The problem of separated and reattaching flows must be treated in a manner that is different from the way in which the problem up to separation was studied, since no detailed theoretical studies of separated and reattaching flows exist. In order to focus on the main aspects of the problem, consider the case of the steady two-dimensional interaction between an incident oblique shock wave and the laminar boundary layer on a flat plate (Figure 1). In a fictitious inviscid fluid, the static pressure on the plate surface remains constant up to the point of shock impingement, rises suddenly at this point to the level predicted by the Rankine-Hugoniot shock relations, and remains constant thereafter. But in a real fluid, a portion of the overall pressure rise is communicated upstream through the boundary layer. Unless the shock wave is rather weak, the laminar boundary layer separates from the surface upstream of shock impingement. The static pressure distribution has the familiar doubly-inflected shape, with the region of pressure rise extending over a distance equivalent to hundreds of boundary layer thicknesses.

In the following paragraphs, it will be shown that in the region between separation and shock impingement the main physical process is the momentum enrichment of the viscous region through mass entrainment from the external inviscid flow. Thus the flow is "prepared" for the additional pressure rise during reattachment. The reattachment process itself will be shown to be an essentially isentropic, inviscid recompression in which mass entrainment is not important. This

general picture of the flow beyond separation is consistent with experimental observations and well-established physical concepts.

In the present discussion of the flow beyond separation, a key concept is Chapman's idea[7, 29] of the "dividing (or zero) streamline"*, which may be briefly expressed as follows: for steady flow, the fluid particle which is adjacent to the wall at separation must be adjacent to the wall at reattachment. Thus the flow is divided into two zones -- the first being a by-pass flow which includes all the fluid upstream of separation, and the second being a circulating region of flow that always consists of the same fluid particles, if diffusion is neglected (Figure 1).

In order to see how the dividing streamline idea contributed to the present understanding of flow beyond separation, it is necessary to

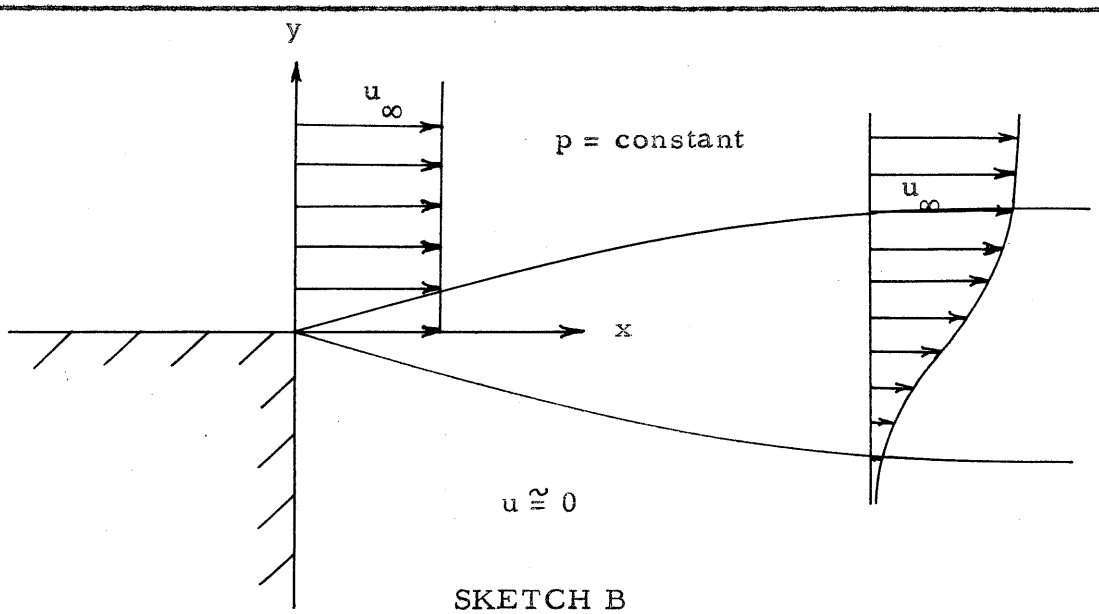

SKETCH B

* This concept was also discovered independently for turbulent separated and reattaching flows by Korst, Page, and Childs.[30]

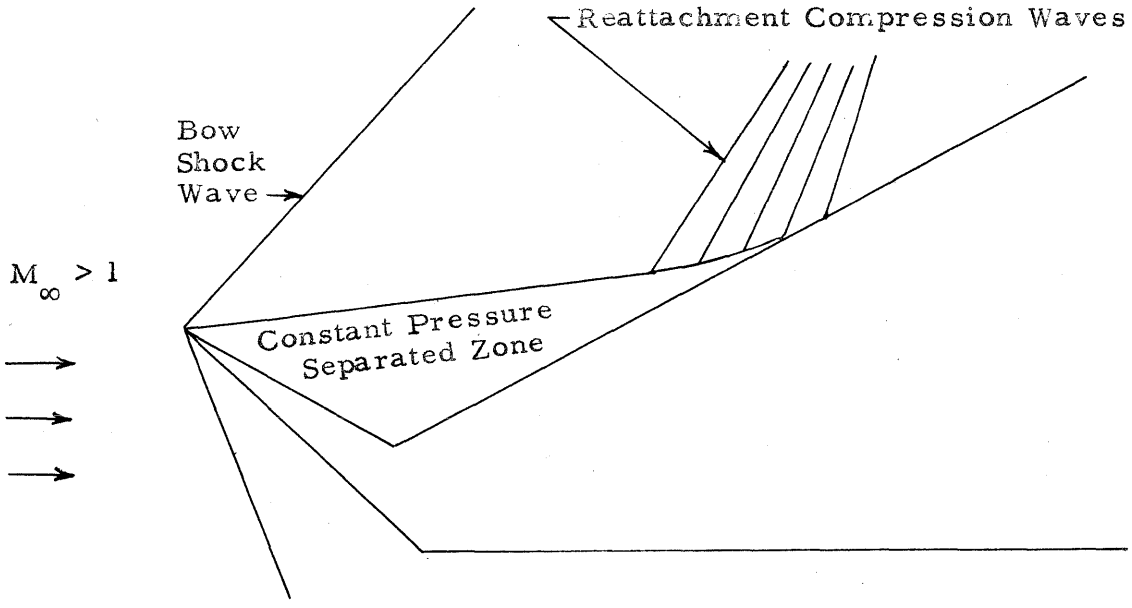

SKETCH C

discuss briefly a special separated and reattaching flow that was investigated theoretically and experimentally by Chapman and his co-workers. In a theoretical study[29], Chapman examined the mixing region that is formed when a uniform stream passes beyond a semi-infinite rearward-facing step. (See Sketch B on page 32.) This flow configuration is of course similar to that of a parallel jet streaming into a stagnant mass of gas. Chapman calculated the velocity profile of the mixing, or transition, region for the case of constant pressure and uniform flow at the end of the step, i. e., $\delta^* = \delta^{**} = 0$, using the ordinary boundary layer equations with the usual no-slip boundary condition replaced by the condition that the velocity be zero at $y = -\infty$. Chapman's result is a similarity solution in which the velocity along the dividing streamline changes impulsively from the initial uniform velocity to a value which is 0.587 of the initial uniform velocity, and remains at this value

thereafter.

In the experimental study of reattaching flows by Chapman, Kuehn and Larson[7], a flow configuration was devised which approximated the boundary conditions of Chapman's theoretical study, so that a separated flow with a known velocity profile was generated. The geometry of the model, shown in Sketch C on page 33, insured an essentially zero thickness boundary layer ($\delta^* = \delta^{**} = 0$) at the beginning of the separated zone and a constant pressure mixing region up to the beginning of reattachment, which is indicated by the appearance of compression waves. The semi-infinite aspect of the theoretical model was approximated roughly by a steep slope on the model face just downstream of separation. The separated flow thus generated was then allowed to reattach on a flat wall, and it was found that the observed pressure rise during reattachment corresponded to isentropic deceleration to rest of the fluid along the dividing streamline. These experiments therefore indicate that reattachment is an isentropic process in which viscous effects do not seem to be important. This conclusion is further substantiated by the fact that the reattachment pressure rise was observed to be independent of Reynolds number. Thus, it is seen that the most important phenomena in the reattachment process are the deceleration of the flow and the contraction of the viscous region, and not mixing -- a fact which will be important in later discussions.

For a general separating flow, the velocity profile at separation is of course far from uniform, but the dividing streamline concept is still valid. The conclusion that mixing is not important during reattachment should also apply for more general reattaching flows. These con-

ditions, and the experimental observation that beyond separation the static pressure rises monotonically, determine to a large extent the major physical phenomena that must occur in general separated and reattaching flows. Consider the fluid particle just above the dividing streamline at the separation point (Figure 1). This fluid particle in general has a negligible velocity, so that its stagnation pressure is essentially equal to the static separation pressure. According to the dividing streamline idea, this fluid particle has to reattach at a higher stagnation pressure. In order for this reattachment to occur, work must be done on this fluid element, and it is clear that this work is done by the external flow through viscous momentum transfer. In other words, the external flow does work on the fluid along the dividing streamline, and thereby loses momentum. This loss of momentum of the external flow is reflected as mixing, or mass entrainment. From the reattachment experiments of Chapman, Kuehn, and Larson, it is clear that this viscous momentum transfer must occur prior to the beginning of reattachment, and therefore must take place in the region between separation and the beginning of reattachment.

This physical picture is further substantiated by the experiments of Hakkinen et al[8], where it is found that the reattachment pressure rise increases with the distance between separation and shock impingement (Figure 12). Since viscous momentum transport is envisioned as the essential physical mechanism in this region, it is clear that the longer the region, the higher the stagnation pressure of the fluid element adjoining the dividing streamline, and therefore the higher the reattachment pressure rise necessary to stagnate the fluid below the dividing

streamline.

From the above discussion, it is clear that the flow region before reattachment begins is a zone in which mixing is the dominant physical phenomenon. Chapman, in his similarity solution, finds that the viscous mixing zone grows roughly three times as fast as an equivalent Blasius flow, indicating high mixing rates based on a δ which includes the external and inducted flows. Since Chapman's solution assumes that the velocity is always positive, the velocity profiles do not contain the reverse flow regions which are known to exist for separated and reattaching flows. Therefore, no accurate quantitative conclusions can be drawn from Chapman's profiles. However, the qualitative conclusion that the mixing rates beyond separation are high will be seen to be consistent with the ideas and methods of the present study.

In Chapman's idealized case, the reattachment pressure rise for laminar flow is independent of Reynolds number because the flow velocity of the dividing streamline is always 0.587 of the free stream velocity. The length scale of the reattachment process must also be independent of Reynolds number since the process of reattachment is seen to be essentially inviscid. However, we shall show by a simplified analysis that for general separated flows the length scale for the reattachment process must depend on Reynolds number through δ_s. On the other hand, certain important features of the flow upstream of the beginning of reattachment are virtually independent of Reynolds number and of the agency causing separation.

The physical picture that has been developed for separated and

reattaching flows may therefore be summarized as follows: after separation, the flow is essentially divided into two parts by the dividing streamline -- one part includes all the fluid upstream of separation and the other part is a steady circulating flow in which the fluid elements continuously undergo a cycling action. The fluid along the dividing streamline is accelerated by viscous momentum transfer in the region between separation and the beginning of reattachment, and is thereby "prepared" for the forthcoming reattachment pressure rise in which fluid along the dividing streamline is isentropically stagnated. This physical picture is quantitatively translated into Crocco-Lees language in the next section.

IV. 2. Crocco-Lees Method

In re-examining the formulation of the Crocco-Lees method beyond separation, it became clear that in order to determine the correlation relations quantitatively, experimental results must be used, since no satisfactory theoretical data are available. The case of shock wave-laminar boundary layer interaction has been selected as a representative example of separating and reattaching flows, since it embodies many of the general characteristics which are observed in other separated flows (Figure 1). The experiment selected to provide the necessary detailed data was performed at a free stream Mach number of 2.45 and at a free stream Reynolds number per inch of 6×10^4 (Figure 13)[7]. This particular experiment was chosen because of the small scatter of the data, and because the Reynolds number was the lowest available from experiments of shock wave-laminar boundary layer interaction,

so that the flow is most apt to be laminar throughout the whole interaction region.

The physical parameters of shock wave-laminar boundary layer interaction may be readily determined from the limiting inviscid case, i.e., $Re \longrightarrow \infty$. The parameters are clearly the free stream conditions, the shock impingement point, and the incident shock strength (or overall pressure ratio). The principal features of shock wave-laminar boundary layer interaction are as follows (Figure 1): (1) the pressure rise up to separation; (2) the pressure rise up to the plateau; (3) the pressure rise during reattachment; and (4) the length scales of the various regions. The present task is to relate the correlation functions, $F(\kappa)$ and $C(\kappa)$, in the regions downstream of separation to these main features of the flow, in the hope that the "universal" behavior of the functions can be determined. *

Since the flow configuration that is produced in the case of shock wave-laminar boundary layer interaction is so complex, it is instructive to discuss qualitatively what determines the various pressure rises and length scales. According to the previous physical discussion, the separation point must move upstream as the overall pressure ratio is increased. This response is due to two factors -- (1) the separation pressure rise increases as the separation Reynolds number decreases,[7] and (2) as the distance between separation and shock impingement is increased, the energy of fluid particles along the dividing streamline

---

* The skin friction is small in this region, and $D(\kappa)$ is taken to be zero between separation and reattachment in a first approximation.

is generally increased, thus making it possible to support a larger reattachment pressure rise. Therefore the location of the separation point is intimately connected with the various pressure rises, and the flow responds chiefly to an overall pressure ratio by properly adjusting the position of the separation point.

IV. 2. 1. Simplified Analysis

It was shown in the previous discussion that the various regions of shock wave-laminar boundary layer interaction are connected and that the problem must be treated as a whole. By making several simplifications, it is possible to treat the whole shock wave-laminar boundary layer interaction problem analytically, and thereby obtain explicitly the effects of Mach and Reynolds numbers on the main features of the flow. In this section, such a simplified treatment will be given and in subsequent paragraphs the method will be refined to enable more accurate determination of the details of the flow.

It is clear from the physical discussion given in Section IV. 1. that the pressure rise during reattachment is determined largely by the momentum of the viscous layer at shock impingement, i. e., largely by $\mathcal{K}_{sh}$. Although the mixing rate, or $C(\mathcal{K})$, is expected to rise continuously from zero near separation (Section III.) to a high value upstream of shock impingement, suppose one takes $C(\mathcal{K}) = \bar{C}$ = constant for this region. In this same spirit, at first we ignore the pressure rise between separation and shock impingement. The momentum equation, Eq. (15), becomes

$$(d\mathcal{K}/dx) = (1 - \mathcal{K})(1/m)(dm/dx) \quad . \tag{41}$$

Therefore,

$$(1 - \kappa)m = \text{constant} = (1 - \kappa_s)m_s \quad , \tag{42}$$

and to this approximation,

$$\kappa_{sh} = 1 - (1 - \kappa_s)(m_s/m_{sh}) \quad . \tag{43}$$

It is seen from this expression for κ_{sh} that when $m_{sh} >> m_s$, $\kappa_{sh} \longrightarrow 1$. Eq. (43) thus clearly shows that when the high energy external flow mixes with the relatively low energy viscous flow, the average energy and momentum levels of the viscous region are raised. This same behavior is present in constant pressure wake flows, where the low stagnation pressures of the wake region are increased at the expense of the external flow.

From Eqs. (16), (20), and (33), we have

$$(dm/dx) = \frac{\rho_e u_e \mu_e}{m} a_t^2 C(\kappa) \quad , \tag{44}$$

and by integrating this equation from separation to shock impingement under the assumptions of constant $C(\kappa)$ and uniform external flow, we obtain

$$\frac{m_{sh}}{m_s} = \sqrt{1 + \frac{2 Re_{\Delta x} \bar{C}}{\zeta_s^2 (1 + \frac{\gamma - 1}{2} M_e^2)^2}} \tag{45}$$

where

$$Re_{\Delta x} = \frac{\rho_e u_e \Delta x}{\mu_e}$$

$$\zeta_s = \frac{m_s a_t}{\mu_t}$$

$\bar{C}$ = average value of $C(\kappa)$

$\Delta x = x_{sh} - x_s$.

It is shown in Appendix B that

$$\zeta_s\left(1+\frac{\gamma-1}{2}M_e^2\right) \simeq \frac{\sqrt{Re_{x_s}}\,A}{(1-K_s)} \quad , \tag{46}$$

where A = 0.44. From Eqs. (43), (45), and (46), it follows that

$$K_{sh} = 1 - \frac{(1-K_s)}{\sqrt{1+\frac{2(1-K_s)^2\bar{C}}{A}\frac{\Delta x}{x_s}}} \quad . \tag{47}$$

Therefore, Eq. (47) shows that K_{sh} depends mainly on the <u>product</u> $\bar{C}\,(\Delta x/x_s)$ and only very weakly on Mach and Reynolds number. If an explicit relation between reattachment pressure rise and K_{sh} can now be developed, then by selecting a <u>single</u> experimental case of shock wave-laminar boundary layer interaction, and measuring the reattachment pressure rise and the length ratio, $(\Delta x/x_s)$, the value of $\bar{C}$ is obtained. This value of $\bar{C}$ is then regarded as "universal", and is employed in the analysis of all other separating flows.

So far the $F(K)$ relation has not entered the discussion. However, the pressure rise during reattachment and the length of the reattachment zone depend to some extent on the $F(K)$ relation. (See Section IV. 2. 3.) Since there are five original dependent variables (F, K, w_e, m, and δ) and five equations [Eqs. (9) to (14)], the first rough approximation, i. e., $C(K) = \bar{C}$, w_e = constant, between separation and shock impingement specifies a unique relation between F and K in this region. By eliminating δ and m from Eqs. (16), (18), (20), (33), and (42), the following differential equation for $F(K)$ results:

$$\frac{dF}{dK} + \frac{F}{K(1-K)} = \frac{\theta\zeta_s(1-K_s)}{\bar{C}}\,\frac{1}{K(1-K)^2} \quad . \tag{48}$$

This equation can be readily integrated to give

$$F(K) = F_s\left[\left(\frac{1-K}{1-K_s}\right)\frac{K_s}{K} + \frac{\theta\zeta_s}{2\bar{C}F_s}\,\frac{1}{K}\left(\frac{1-K_s}{1-K}\right)\left(1-\left\{\frac{1-K}{1-K_s}\right\}^2\right)\right] \quad . \tag{49}$$

If we define a parameter, χ, as

$$\chi \equiv \theta\zeta_s/2\bar{C} \quad , \tag{50}$$

then the $F(K)$ relation given by Eq. (49) can be exhibited for a range of values of χ. By using the Prandtl-Meyer relation and the separation pressure correlation of Chapman, Kuehn, and Larson[7], it can be shown that

$$\chi \sim \frac{[Re\,(M_e^2-1)]^{1/4}}{(1+\frac{\gamma-1}{2}M_e^2)} \quad . \tag{51}$$

It is found that the values of χ for the cases studied in the present investigation are of the order of unity. Eq. (51) shows that χ is rather insensitive to Mach and Reynolds number for the Mach number range below five, so that a range of χ from 0.1 to 10 may be expected to cover a fairly wide experimental range. The $F(K)$ curves for this range of χ are given in Figure 14, and show that $F(K)$ is approximately constant for values of χ on the order of unity. This analysis, while admittedly crude, suggests that $F(K)$ may be approximately constant in the region between separation and shock impingement, a result which is opposite to the one previously assumed by Crocco and Lees[1]. This question will be discussed again in Section IV. 2. 2.

If it is assumed that $F(K)$ remains constant in the region between separation and shock impingement, then $F_{sh} = F_s$. The determination of

F_{sh} and $\mathcal{K}_{sh}$ fixes the starting point in the F- $\mathcal{K}$ plane from which reattachment starts. Since the terminal point, the Blasius flow condition, is also known, the trajectory of the reattachment process is largely determined. It has been assumed that the reattachment trajectory is a straight line in the F- $\mathcal{K}$ plane of the form:

$$F = a\mathcal{K} + \beta \quad , \tag{52}$$

where a and β are constants depending on the values of F_{sh} and $\mathcal{K}_{sh}$. It can be readily shown that

$$a = \Omega(\bar{\eta} - 1)/(\omega - 1) \tag{53}$$

$$\beta = F_b(\omega - \bar{\eta})/(\omega - 1) \quad , \tag{54}$$

where

$$\Omega \equiv (F_b/\mathcal{K}_b) \cong 2.30$$

$$\bar{\eta} \equiv (F_s/F_b) \cong 1.79 \quad , \text{ since } F_s = F_{sh}$$

$$\omega \equiv \mathcal{K}_{sh}/\mathcal{K}_b \quad .$$

In the present simplified analysis, we shall tentatively assume that the mixing term in the momentum equation, Eq. (15), is negligible so that the momentum equation for reattaching flow is

$$d\mathcal{K} = \mathcal{K} F (dM_e/M_e) \quad . \tag{55}$$

Since $F = a\mathcal{K} + \beta$, Eq. (55) can be integrated to give the result

$$M_e = M_{\infty f}\left[\frac{\mathcal{K}}{\mathcal{K}_b}\left(\frac{\mathcal{K}_b + \beta/a}{\mathcal{K} + \beta/a}\right)\right]^{1/\beta} \quad , \tag{56}$$

where $M_{\infty f}$ = given final flow Mach number far downstream of the interaction and $\mathcal{K}_b$ = Blasius value of $\mathcal{K}$ = 0.693.

Evaluating this expression for M_e at the shock impingement point gives

$$M_{e_{sh}} = M_{\infty f}\left[\left(\frac{K_{sh}}{K_b}\right)\left(\frac{K_b + \beta/\alpha}{K_{sh} + \beta/\alpha}\right)\right]^{1/\beta} \quad . \tag{57}$$

Substituting Eqs. (53) and (54) into Eq. (57), we obtain

$$M_{e_{sh}} = M_{\infty f}\left(\frac{\omega}{\bar{\eta}}\right)^{-\frac{(\omega-1)}{F_b(\bar{\eta}-\omega)}} \quad , \tag{58}$$

where

$$\omega \equiv \frac{K_{sh}}{K_b} = \frac{1}{K_b}\left[1 - \frac{(1-K_s)}{\sqrt{1 + \frac{2(1-K_s)^2\bar{C}}{A}\frac{\Delta x}{x_s}}}\right] \quad , \tag{59}$$

and $\bar{\eta}$, A, K_s, K_b, F_b, F_s, and $M_{\infty f}$ are known constants. From isentropic flow relations, we have

$$\frac{p_t}{p} = \left[1 + \frac{\gamma-1}{2}M_e^2\right]^{\frac{\gamma}{\gamma-1}} \quad , \tag{60}$$

so that

$$\frac{p_{\infty f}}{p_{sh}} = \left[\frac{1 + \frac{\gamma-1}{2}M_{\infty f}^2\left(\frac{\omega}{\bar{\eta}}\right)^{-\frac{2(\omega-1)}{F_b(\bar{\eta}-\omega)}}}{1 + \frac{\gamma-1}{2}M_{\infty f}^2}\right]^{\frac{\gamma}{\gamma-1}} \quad . \tag{61}$$

Eq. (61) shows that $p_{\infty f}/p_{sh}$ is only a function of ω which, in turn, is only a function of the product $\bar{C}(\Delta x/x_s)$ [Eq. (59)]. Thus by measuring the reattachment pressure ratio, $p_{\infty f}/p_{sh}$, and the lengths Δx and x_s for a single experiment of shock wave-laminar boundary layer interaction (Figure 13), the value of $\bar{C}$ is determined.

This simplified analysis can also be employed to obtain approximate expressions for the Mach and Reynolds number dependences of the important features of shock wave-laminar boundary layer interaction.

It has been found experimentally by Chapman, Kuehn, and Larson[7] that

$$p_{sh}/p_o \cong 1 + \frac{1.24\, M_\infty^2}{\left[(M_\infty^2-1)\, Re_{x_o}\right]^{1/4}} \quad , \tag{62}$$

where the subscript o denotes conditions at the point where the pressure first starts to rise. This functional relation has also been obtained by rough theoretical considerations[7, 8, 10, 31]. Since the parameter $p_{\infty f}/p_o = (p_{\infty f}/p_{sh})(p_{sh}/p_o)$ is a constant that is determined by the incident shock strength for a given interaction problem, the following relation results:

$$\frac{p_{\infty f}}{p_o} = \left[\frac{1 + \frac{\gamma-1}{2} M_{\infty f}^2 \left(\frac{\omega}{\bar{\eta}}\right)^{-\frac{2(\omega-1)}{F_b(\bar{\eta}-\omega)}}}{1 + \frac{\gamma-1}{2} M_{\infty f}^2}\right]^{\frac{\gamma}{\gamma-1}} \left[1 + \frac{1.24\, M_\infty^2}{\left[(M_\infty^2-1)\, Re_{x_o}\right]^{1/4}}\right] \quad . \tag{63}$$

From Eqs. (59) and (62), it is seen that the only unknowns in Eq. (63) are x_o and x_s since $\bar{C}$ is now assumed to be known. Another independent relation between x_o and x_s has been found experimentally[7] and can be justified by rough theoretical arguments[7, 10]. This expression is

$$\frac{x_s - x_o}{\delta_o^*} \sim \left[\frac{Re_{x_o}}{M_\infty^2 - 1}\right]^{1/4} \quad . \tag{64}$$

If we define

$$\tilde{Re}_{x_{sh}} \equiv \frac{\rho_\infty u_\infty x_{sh}}{\mu_\infty} \quad , \tag{65}$$

then by using the experimental data of Chapman, Kuehn, and Larson[7] and Eq. (C-8), it can be shown that

$$x_s/x_o \cong 1 + \frac{0.93\,(1.73 + 2.39\,\frac{\gamma-1}{2}\,M_\infty^2)}{\left[(M_\infty^2 - 1)\,\tilde{Re}_{x_{sh}}\right]^{1/4}}\,(x_{sh}/x_o)^{1/4} \quad . \tag{66}$$

If we define

$$\Psi \equiv \frac{0.93\,(1.73 + 2.39\,\frac{\gamma-1}{2}\,M_\infty^2)}{\left[(M_\infty^2 - 1)\,\tilde{Re}_{x_{sh}}\right]^{1/4}} \quad , \tag{67}$$

then

$$x_s/x_o \cong 1 + \Psi\,(x_{sh}/x_o)^{1/4} \quad . \tag{68}$$

Solving for x_s, and substituting the result into Eq. (59), we obtain the condition that

$$\frac{p_{\infty f}}{p_o} = \left[\frac{1 + \frac{\gamma-1}{2}M_{\infty f}^2\left(\frac{\omega}{\eta}\right)^{-\frac{2(\omega-1)}{(\eta-\omega)F_b}}}{1 + \frac{\gamma-1}{2}M_{\infty f}^2}\right]^{\frac{\gamma}{\gamma-1}}\left[1 + \frac{1.24M_\infty^2}{\left[(M_\infty^2-1)\tilde{Re}_{x_{sh}}\right]^{1/4}}\left(\frac{x_{sh}}{x_o}\right)^{1/4}\right] , \tag{69}$$

where

$$\omega = \frac{1}{K_b}\left[1 - \frac{(1-K_s)}{\sqrt{1 - \frac{2(1-K_s)^2\bar{C}}{A}\left[\frac{x_{sh}/x_o}{1+\Psi x_{sh}/x_o} - 1\right]}}\right] \quad . \tag{70}$$

Thus Eq. (69) determines the value of the quantity x_o/x_{sh}, and since x_{sh} is a given parameter, the value of x_o. After x_o is determined, the value of $p_{\infty f}/p_{sh}$, p_{sh}/p_o, and x_s can be readily computed from Eqs. (61), (62), and (66).

The remaining major property to be determined is the reattachment length scale, Δx_R. The order of magnitude of Δx_R can be estimated by

$$\Delta x_R/x_{sh} \cong \frac{(\delta_{sh}/x_{sh})}{\theta_{sh}} \quad , \tag{71}$$

where θ_{sh} is obtained by the Prandtl-Meyer relation and is a function only of $M_{e_{sh}}$ [See Eq. (57).] , and δ_{sh} is found from Eq. (B-13) to be

$$\delta_{sh} = \frac{m_{sh} K_{sh} \left[F_s + t_{sh} \right]}{\gamma p_{sh} w_{esh}} \quad . \tag{72}$$

This equation can be put in the more explicit form

$$\frac{\delta_{sh}}{x_{sh}} = \omega \left(\frac{m_{sh}}{m_s} \right) \left(\frac{x_s}{x_{sh}} \right) \left(\frac{\delta_s}{x_s} \right) \left(1 - \frac{\delta_s^*}{\delta_s} \right) K_b \left(\frac{M_{es}}{M_{esh}} \right) \left[\frac{1 + \frac{\gamma-1}{2} M_{esh}^2}{1 + \frac{\gamma-1}{2} M_{es}^2} \right]^{\frac{\gamma+1}{2(\gamma-1)}} \left[F_s \left(1 + \frac{\gamma-1}{2} M_{esh}^2 \right) + 1 \right] \tag{73}$$

where m_{sh}/m_s , $M_{e_{sh}}$, x_s/x_{sh} , ω , and $(1 - \delta_s^*/\delta_s)$ can be obtained from Eqs. (45), (58), (68), (70), and (A-26). Using Eq. (C-8), it can be shown that

$$\frac{\delta_s}{x_s} = \left(\frac{\delta_s}{\delta_s^{**}} \right) \left(\frac{\delta_s^*}{x_s} \right) = \left[1 - \left(1 - \frac{\delta_s^*}{\delta_s} \right) \right]^{-1} \sqrt{\frac{A}{Re_{x_s}}} \left\{ \left(1 + \frac{\gamma-1}{2} M_\infty^2 \right) \left(H_{is} + 1 \right) - 1 \right.$$
$$\left. + \varepsilon_s \left[\frac{(\gamma-1) M_\infty}{1 + \frac{\gamma-1}{2} M_\infty^2} + \frac{(3\gamma-1)}{4} \frac{M_\infty}{\left(1 + \frac{\gamma-1}{2} M_\infty^2 \right)} \left(\left(1 + \frac{\gamma-1}{2} M_\infty^2 \right) \left(H_{is} + 1 \right) - 1 \right) \right] \right\} \tag{74}$$

where

$$Re_{x_s} = \frac{\rho_\infty u_\infty x_s}{\mu_\infty}$$

$$M_{e_s} \cong \tfrac{1}{2} \left(M_{e_{sh}} + M_\infty \right) \quad .$$

This simplified analysis shows that parameters upstream of shock impingement, as well as the reattachment pressure rise, are rather insensitive to Reynolds number. However, it is seen from Eqs. (71), (73), and (74) that the Reynolds number variation of Δx_R is roughly $Re^{-\frac{1}{2}}$. This variation is obtained by noting that the quantities m_{sh}/m_s , ω , and x_s/x_{sh} have small Reynolds number variation, and tend to

oppose each other. Thus the term, δ_s/x_s, which is proportional to $Re^{-\frac{1}{2}}$ is expected to account for most of the Reynolds number variation of Δx_R.

The simplified analysis shows explicitly, although approximately, how the various pressure rises and length scales are related when the viscous region is subjected to a given overall pressure rise. This discussion is not only useful in showing the unity of the whole interaction and in bringing out the Mach and Reynolds number dependences of the various features of the flow, but also aids in an understanding of the more refined analysis that is given in the next subsection.

IV. 2. 2. Refined Analysis

In the simplified analysis, attention is concentrated on the pressure rise during reattachment, and the pressure rise between separation and shock impingement is neglected. By employing the approximations that $C(\kappa) = \bar{C}$ and $F(\kappa) = F_s$, one can now go back and calculate the pressure rise from separation up to the plateau (Figure 1). However, if a single value of $C(\kappa) = \bar{C}$ is employed in the region between separation and shock impingement, one finds that the calculated pressure rise between separation and the plateau is too large when compared with the selected shock wave-laminar boundary layer interaction experiment. Thus, in order to obtain the proper pressure rise in the region between separation and the plateau, we introduce the additional refinement of a two-step $C(\kappa)$ curve, i. e.,

$$C(\kappa) = C_1 \quad \text{for } x_s \leq x \leq x_\Gamma$$

$$C(\kappa) = C_2 \quad \text{for } x_\Gamma \leq x \leq x_{sh} \quad ,$$

where x_Γ is the distance from the leading edge at which the calculated pressure gradient is negligibly small, and is therefore the beginning of the plateau region (Figure 1).

Using a two-step $C(K)$ relation for the region between separation and shock impingement, an attempt has been made to determine the validity of the assumption that $F(K) = F_s$, which was employed in the simplified analysis given in Section IV. 2. 1. Two linear $F(K)$ relations passing through the point (F_s, K_s) have been assumed, one with a positive slope and the other with a negative slope. For each $F(K)$ relation, a given value of C_1 yields a unique pressure rise from separation to the plateau if the conditions at the separation point are specified. (See Appendix B.) By comparing the calculated pressure rise with the pressure rise observed in the selected shock wave-laminar boundary layer interaction experiment, the value of C_1 corresponding to each assumed $F(K)$ relation is determined. The proper $F(K)$ relation and C_1 value can then be found by matching the length scales of the computed and experimental pressure distributions.

The $F(K)$ relations used in these exploratory calculations were

(A) $F(K) = 3.851\,K + 0.424$

(B) $F(K) = F_s = 2.85$

(C) $F(K) = -1.926\,K + 4.063$,

and the corresponding values of C_1 which approximately yielded the experimental pressure rise were

(A) $C_1 = 7.94$

(B) $C_1 = 11.0$

(C) $C_1 = 13.7$.

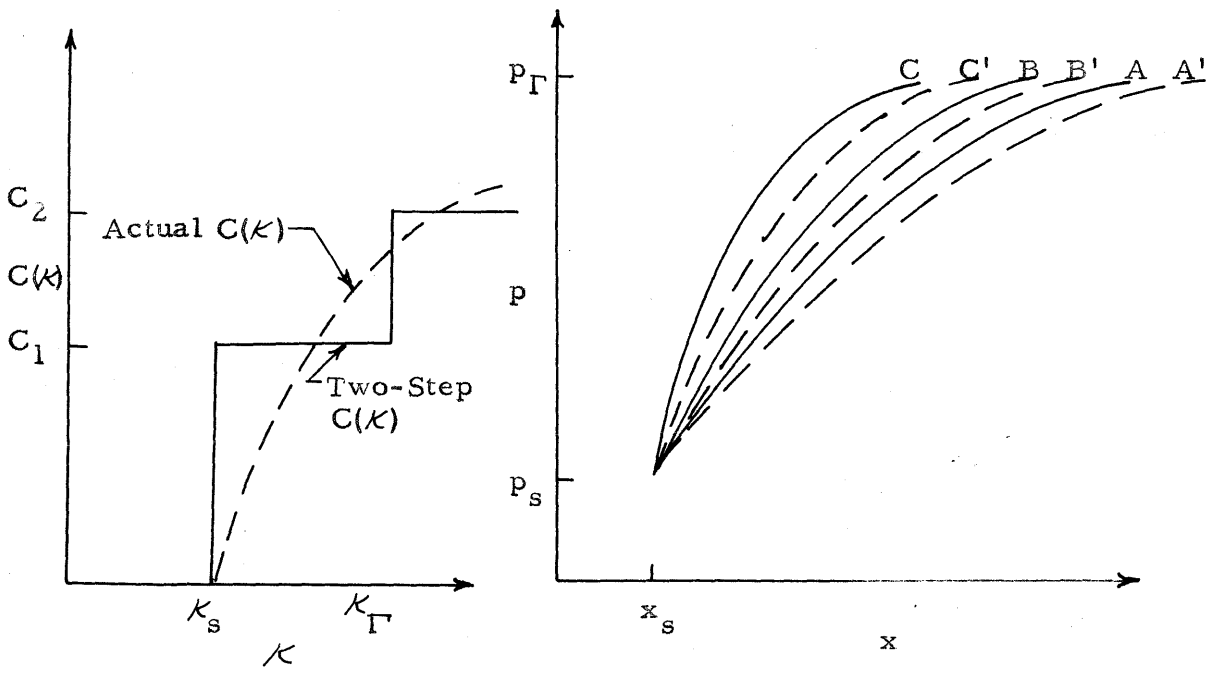

SKETCH D

The results of the calculations are given in Figure 15. It might appear that Case A gives better agreement with experiment, but if a more accurate $C(\kappa)$ relation had been used, the curves in Figure 15 would be displaced to the right as shown in Sketch D. Thus, the results of this exploratory calculation do not select the proper $F(\kappa)$ relation for the region beyond separation since the length scale is not very sensitive to the choice of $F(\kappa)$ within the limits defined by the three cases A, B, and C.

The insensitivity of the pressure distribution to the $F(\kappa)$ relation requires a more precise analysis. If the separation point could be unequivocally determined in an experimental case, and the

pressure distribution accurately measured, the $F(\kappa)$ and $C(\kappa)$ curves for the region between separation and the plateau could be determined by assuming linear $F(\kappa)$ and $C(\kappa)$ relations, with the slopes of the curves as parameters, and finding the best combination of slopes to match the observed pressure distribution. Because of the present experimental uncertainties associated with the location of the separation point, such optimizing calculations are probably premature. In the present study, the simplest assumption has been made, namely that $F(\kappa) = F_s$ in this region. The assumption that $F_{sh} = F_s$ is found to give good agreement between theory and experiment in the reattaching zone, and may be some justification for assuming that $F(\kappa) = F_s$ in the whole region between separation and shock impingement.

In the plateau region, the constant pressure results given in the simplified analysis (Section IV. 2. 1.) can be used to calculate κ_{sh}, with the separation quantities designated by the subscript s replaced by the quantities at the beginning of the plateau region, designated by the subscript Γ. Thus

$$\kappa_{sh} = 1 - \frac{(1 - \kappa_\Gamma)}{\left[1 + \frac{2\,Re_{\Delta x_\Gamma}\; C_2}{\zeta_\Gamma^2 \left(1 + \frac{\gamma-1}{2} M_{e_\Gamma}^2\right)^2}\right]^{1/2}} \tag{75}$$

where

$$Re_{\Delta x_\Gamma} = \frac{\rho_{e\Gamma} u_{e\Gamma} (x_{sh} - x_\Gamma)}{\mu_{e\Gamma}}$$

$$\zeta_\Gamma = \frac{m_\Gamma a_t}{\mu_t}$$

C_2 = value of $C(\kappa)$ for $x_\Gamma \leq x \leq x_{sh}$.

The value of C_2 is determined from the reattachment pressure rise in the selected case of shock wave-laminar boundary layer interaction just as $\bar{C}$ was determined in the simplified analysis (Section IV. 2. 1.).

IV. 2. 3. Reattachment

As has been mentioned several times in the previous discussions, it is believed that during reattachment viscous effects are not important. The main justification for this belief is found in the reattachment experiments of Chapman, Kuehn, and Larson. However, other considerations also suggest, but do not prove, that viscous momentum transfer may not be important during reattachment. When skin friction is negligible, the momentum equation can be written as

$$d\mathcal{K} = (1 - \mathcal{K})(dm/m) + \mathcal{K}F(dMe/Me) \quad , \tag{76}$$

where the first term on the right hand side gives the increase in $\mathcal{K}$ caused by mixing and the second term represents the decrease in $\mathcal{K}$ associated with a positive pressure gradient. The mixing term shows that for a given change in mass flux, the effect on $\mathcal{K}$ is directly proportional to $(1 - \mathcal{K})$, which essentially measures the relative fractional improvement obtained per unit of high energy mass, and is inversely proportional to m, which measures the "inertia" of the layer. The ratio of the mixing term to the pressure gradient term can be evaluated for a specific case if the value of $C(\mathcal{K})$ is known. It is found for the three shock wave-laminar boundary layer interaction cases calculated in this study that the ratio of the mixing term to the pressure gradient term is about $0.1\ C(\mathcal{K})$. Therefore, if $C(\mathcal{K})$ is of the order of unity, the effect of mixing is small.

In the present analysis it is assumed, on the basis of the above discussions, that mixing is negligible during reattachment and that Eqs. (55) through (57) are valid. Therefore, by measuring the reattachment pressure rise in the selected shock wave-laminar boundary layer interaction experiment, the value of $\frac{C_2 \, Re_{\Delta x_\Gamma}}{\zeta_\Gamma^2 \left(1 + \frac{\gamma-1}{2} M_{e_\Gamma}^2\right)^2}$ is determined. [See Eqs. (61) and (75).] Since all the quantities designated by the subscript 1 have been determined by the integration of the equations from separation up to the beginning of the plateau, and $\Delta x_\Gamma = (x_\Gamma - x_{sh})$ can be measured in the selected experiment, the value of C_2 is determined, and has been found to have a value of 15.

In order to obtain the pressure distribution in the physical plane, the continuity equation [Eq. (16)] is used. Since

$$k = \frac{C(K)\mu_e}{\bar{m}} = 0 = (d\delta/dx) - \theta \quad , \tag{77}$$

we obtain the relation

$$dx = (d\delta/\theta) \quad . \tag{78}$$

Thus,

$$x/x_{sh} = 1 + \int_{\delta_{sh}/x_{sh}}^{\delta/x_{sh}} \frac{d(\delta/x_{sh})}{\theta} \quad . \tag{79}$$

The explicit integration of the equation determining x is carried out as follows:

$$\delta = \frac{m K (F + t)}{\gamma \, p \, w_e} \quad . \tag{B-13}$$

This equation can then be written in the form

$$\frac{\delta}{x_{sh}} = \frac{M_{esh}}{M_e}\left(1+\frac{\gamma-1}{2}M_e^2\right)^2\left[\frac{1+\frac{\gamma-1}{2}M_e^2}{1+\frac{\gamma-1}{2}M_{esh}^2}\right]^{\frac{3-\gamma}{2(\gamma-1)}}\left(\frac{m_{sh}}{m_s}\right)\frac{\zeta_s K (F+t)}{Re_{x_{sh}}} \quad . \quad (80)$$

From this equation, it follows that

$$d\left(\frac{\delta}{x_{sh}}\right) = \frac{\delta}{x_{sh}}\left\{\left[\frac{(3\gamma-1)M_e}{2\left(1+\frac{\gamma-1}{2}M_e^2\right)} - \frac{1}{M_e} - \frac{1}{(F+t)}\frac{(\gamma-1)M_e}{\left(1+\frac{\gamma-1}{2}M_e^2\right)2}\right]dM_e + \left[\frac{1}{K}+\frac{1}{(F+t)}\frac{dF}{dK}\right]dK\right\} \quad . \quad (81)$$

Using the approximation that $F = \alpha K + \beta$ and that $M_e \cong \hat{M}_e$ where $\hat{M}_e \equiv \frac{1}{2}(M_{e_{sh}} + M_{\infty f})$, as well as the momentum equation [Eq. (55)], it can be shown that

$$d\left(\frac{\delta}{x_{sh}}\right) = \frac{M_{esh}}{\hat{M}_e}\left(1+\frac{\gamma-1}{2}\hat{M}_e^2\right)^2\left[\frac{1+\frac{\gamma-1}{2}\hat{M}_e^2}{1+\frac{\gamma-1}{2}M_{esh}^2}\right]^{\frac{3-\gamma}{2(\gamma-1)}}\left(\frac{m_{sh}}{m_s}\right)\frac{\zeta_s K(F+\hat{t})}{Re_{x_{sh}}}x$$

$$\left\{\left[\frac{(3\gamma-1)\hat{M}_e}{2\left(1+\frac{\gamma-1}{2}\hat{M}_e^2\right)} - \frac{1}{\hat{M}_e} - \frac{(\gamma-1)\hat{M}_e}{(F+\hat{t})\left(1+\frac{\gamma-1}{2}\hat{M}_e^2\right)2}\right]\frac{\hat{M}_e}{KF} + \frac{1}{K} + \frac{\alpha}{(F+\hat{t})}\right\}dK \quad . \quad (82)$$

By substituting this expression into Eq. (79) and using the results of the integration of the momentum equation, the value of x/x_{sh} is determined for every value of K, and therefore for every value of M_e and p. Since x_{sh} is a known parameter of the flow problem, the pressure distribution for a reattaching flow is determined by the above equations.

In the above analysis of reattaching flows, it has been assumed that the $F(K)$ relation is a linear one joining the points (F_{sh}, K_{sh}) and (F_b, K_b), and that $C(K)$ is negligibly small. It should be emphasized that these assumptions are to be regarded only as a first approximation

to the actual $F(\kappa)$ and $C(\kappa)$ relations for reattaching flows. It is clear, for example, that between flow reattachment and the Blasius condition, skin friction becomes important and the positive pressure gradient tends to zero, so that the relative importance of mixing increases. The general momentum equation is

$$d\kappa = \kappa F (dM_e/M_e) + (1 - \kappa)(1 - \sigma) (dm/m) \quad . \quad \text{(B-12)}$$

At the Blasius flow condition, $\sigma = 1$, so the momentum equation is the same as the equation for $C(\kappa) = 0$, which is the equation assumed for reattaching flow. Since the momentum equations at both ends of the region between reattachment and Blasius flow are the same, it is felt that this equation is approximately correct throughout the region. If this assumption is true, the pressure rise is unaffected by the simultaneous advent of skin friction and mixing, which seems possible since the effects of these two phenomena on κ are in opposite directions.

In the parts of the interaction that are furthest downstream, the flatness of the pressure distribution prevents an accurate determination of the onset of the region in which the effects of mixing appear. Figures 16 and 17 show the $F(\kappa)$ and $C(\kappa)$ trajectories for a complete shock wave-laminar boundary layer interaction. The last part of the $C(\kappa)$ trajectory, i.e., the region between reattachment and the final Blasius condition, is schematically indicated as a dashed curve. It is hoped that accurate experiments in the downstream parts of shock wave-laminar boundary layer interactions will enable the determination of this part of the $C(\kappa)$ trajectory. It is clear however that the assumption $C(\kappa) = 0$ for the region downstream of shock impingement gives excellent quantitative agreement with experiment for the major part of the pressure rise. (See Figures 13 and 18.)

V. DISCUSSION AND APPLICATIONS

In previous sections, the Crocco-Lees method has been re-examined and approximate correlation functions for the attached, separated, and reattaching regions have been determined. The Crocco-Lees method, using these new correlation relations, is now applied to two cases of shock wave-laminar boundary layer interaction. Case A, which corresponds to an experimental case[8], is calculated for a free stream Mach number of 2.0 and a separation Reynolds number of 2.3×10^5. Case B is calculated for a free stream Mach number of 5.8 and a separation Reynolds number of 1×10^5. No experimental data are presently available at the hypersonic conditions of Case B.

In Figure 18, the results of the calculation of Case A are compared with experiment. It should be emphasized that the parameters of the problem are the free stream conditions, the shock impingement point, and the overall pressure ratio. It is seen that the Crocco-Lees method, with the new correlation functions, predicts a pressure distribution that is in good general agreement with experiment. It should be noted that the pressure rise up to the shock impingement point is accurately determined, and that excellent agreement is obtained for the reattaching part of the flow. The agreement with experiment in the region near separation is only fair, and it is not known whether the differences between theory and experiment are significant, or caused by the scatter of the experimental data. In any event, it is clear that the method is able to predict a complicated separated and reattaching flow with good quantitative accuracy.

The results of the hypersonic calculation (Case B) are shown in

Figures 19 and 20. Again the parameters of the problem are the free stream conditions, the shock impingement point, and the overall pressure ratio. The separation Reynolds number in Case B has a value between that of Case A and that of the experiment used to determine C_1 and C_2. Thus, this calculation essentially shows the effect of high Mach number. The general shape of the pressure distribution is seen to be similar to the cases shown in Figures 13 and 18, indicating that no pathological changes have occurred at the higher value of Mach number.

After re-examining the Crocco-Lees method and comparing the results of calculations with experiment, it is appropriate to discuss the various assumptions that have been made in formulating the method. The various initial assumptions are listed on page 12, and subsequent ones, such as the $F(\kappa)$, $C(\kappa)$, and $D(\kappa)$ correlation relations beyond separation, are discussed in Section IV. Since the various initial assumptions largely stemmed from attached boundary layer theory, they are mainly in question only for the separated parts of the flow. For laminar flow, it is believed that assumptions 1 to 10 are reasonably accurate for separated regions and do not introduce serious errors. The ignorance of the $F(\kappa)$, $C(\kappa)$, and $D(\kappa)$ relations for the separated region is considered to be far more serious. In the present study, all the ignorance of the separated part of the flow is gathered into the constants, C_1 and C_2, and the assumed $F(\kappa)$ relation. It is clear that until the $F(\kappa)$, $C(\kappa)$, and $D(\kappa)$ relations for the separated and reattaching parts of the flow are firmly established, either by theory or by experiment, the effects of assumptions 1 to 10 cannot be accurately assessed.

The agreement between theory and experiment for the case of shock wave-laminar boundary layer interaction does not prove that the method will be applicable to general separated flows, since the values of C_1 and C_2 were obtained from the same sort of experiment at roughly the same free stream Mach number. However, the separation Reynolds number in Case A and in the experiment used to determine C_1 and C_2 differed by over an order of magnitude, and it is believed that the observed agreement is therefore significant. In order to establish the generality of the method, calculations of other separated flow geometries, such as those obtained with forward-and rearward-facing steps, corners, ramps, cutouts, etc. must be carried out and the results of calculations compared with experiment. Since many experimental studies of separated flow have been carried out recently, it appears that such a calculation program can be used to determine the general validity of the assumptions that have been employed in the present study of shock wave-laminar boundary layer interactions.

The extension of the Crocco-Lees method to turbulent flow problems has been considered by several investigators[1,19], and some success has been achieved in cases involving no heat transfer. The physical model developed in the present study for laminar separated and reattaching flows seems to be appropriate for the turbulent case also, and it is believed that the same procedures that have been used in the laminar case can be employed in the turbulent case, and an analogous formulation developed.

The introduction of heat transfer into the Crocco-Lees method has been tried for laminar flow by Gadd and Holder[22], but rather poor

quantitative agreement between theory and experiment was obtained. The method by which Gadd and Holder included heat transfer was not indicated in their paper so that it is difficult to determine reasons for the discrepancies. One possible way of introducing heat transfer into the Crocco-Lees method is to employ an additional parameter, analogous to the wall enthalpy parameter, S_w, of the Cohen-Reshotko method[16]. However, on the basis of the present study of the adiabatic case, it is believed that it would be inappropriate to use the similar solutions of Reference 16 to obtain the mixing rate correlation relation. Rather, it is felt that an additional set of solutions which describe boundary layers with "histories" must be generated. Howarth's linearly-decreasing external velocity distribution, for example, might be used to obtain such solutions. The extension of the correlation relations beyond separation may pose some difficulty, but the present adiabatic results should permit the determination of approximate non-adiabatic correlations for this region.

The n-moment method, which was described in Section I, is a direct theoretical technique for treating separated and reattaching zones. Since the viscous region beyond separation seems to have two characteristic lengths, i. e., the distance from the wall to the dividing streamline, $\bar{\delta}$, and the distance from the dividing streamline to the external inviscid stream, $\tilde{\delta}$, a two-moment method with the integral condition that $\int_0^{\bar{\delta}} \rho u \, dy = 0$ fulfills the minimum requirements. A two-moment treatment of a typical separated and reattaching flow is a challenging problem, but there is nothing in principle to prevent it from being carried out.

VI. CONCLUSIONS

Re-examination of the Crocco-Lees method has shown that the previous quantitative disagreement between theory and experiment in the region of flow up to separation was caused primarily by the improper $C(K)$ relation assumed. A new $C(K)$ correlation, based on low-speed theoretical and experimental data and on supersonic experimental results, has been developed and found to be satisfactory for accurate calculation of two-dimensional laminar supersonic flows up to separation. Another result of the study of the Crocco-Lees method for attached regions of flow has been the demonstration that the length, δ, is artificial and that physical quantities are not sensitive to the definition of δ.

A study of separated and reattaching regions of flow has led to a physical model which incorporates the concept of the "dividing" streamline and the results of experiment. According to this physical model, viscous momentum transport is the essential mechanism in the zone between separation and the beginning of reattachment, while the reattachment process is, on the contrary, an essentially inviscid process. This physical model has been translated into Crocco-Lees language using a semi-empirical approach, and approximate $C(K)$ and $F(K)$ relations have been determined for the separated and reattaching regions. The results of this analysis have been applied to the problem of shock wave-laminar boundary layer interaction, and satisfactory quantitative agreement with experiment has been achieved.

The present study, it is hoped, has also helped to formulate more clearly the major problems that must be solved in order to

establish the validity and generality of the Crocco-Lees method. It is felt that the formulation of the method up to separation is now satisfactory, although not optimum. Beyond separation, it is believed that the main phenomena are understood, but that many of the present results, such as the $F(\kappa)$, $C(\kappa)$, and $D(\kappa)$ relations, are to be regarded only as first approximations.

REFERENCES

1. Crocco, L. and Lees, L.: A Mixing Theory for the Interaction Between Dissipative Flows and Nearly Isentropic Streams. Journal of the Aeronautical Sciences, Vol. 19, No. 10, pp. 649-676, October, 1952.

2. Goldstein, S.: Modern Developments in Fluid Dynamics. Vol. I, Oxford University Press, London, 1938.

3. Oswatitsch, K.: Die Ablösungsbedingung von Grenzschichten. Proceedings of the Freiburg Symposium on Boundary Layer Research, pp. 357-367, August, 1957.

4. Gault, D. E.: An Experimental Investigation of Regions of Separated Laminar Flow. NACA TN 3505, 1955.

5. Liepmann, H. W.: The Interaction between Boundary Layer and Shock Waves in Transonic Flow. Journal of the Aeronautical Sciences, Vol. 13, No. 12, pp. 623-637, December, 1946.

6. Ackeret, J.; Feldmann, F.; and Rott, N.: Investigations of Compression Shocks and Boundary Layers in Gases Moving at High Speed. NACA TM 1113, 1947.

7. Chapman, D. R.; Kuehn, D. M.; and Larson, H. K.: Investigation of Separated Flows in Supersonic and Subsonic Streams with Emphasis on the Effect of Transition. NACA Report 1356, 1958.

8. Hakkinen, R. J.; Greber, I.; Trilling, L.; and Abarbanel, S. S.: The Interaction of an Oblique Shock Wave with a Laminar Boundary Layer. NASA Memo 2-18-59W, March, 1959.

9. Gadd, G. E.; Holder, D. W.; and Regan, J. D.: An Experimental Investigation of the Interaction Between Shock Waves and Boundary Layers. Proceedings of the Royal Society of London, Series A, Vol. 226, pp. 227-253, 1954.

10. Lees, L.: Interaction between the Laminar Boundary Layer over a Plane Surface and an Incident Oblique Shock Wave. Princeton University, Aeronautical Engineering Laboratory, Report 143, January 24, 1949.

11. Honda, M.: Theoretical Investigation of the Interaction between Shock Waves and Boundary Layers. Journal of the Aeronautical Sciences, Vol. 25, No. 11, pp. 667-678, November, 1958.

12. Gadd, G. E.: A Theoretical Investigation of Laminar Separation in Supersonic Flow. Journal of the Aeronautical Sciences, Vol. 24, No. 10, pp. 759-771, October, 1957.

13. Pohlhausen, K.: Zur näherungsweisen Integration der Differentialgleichung der laminaren Grenzschicht. Z. a. M. M., Bd. 1, Heft 4, pp. 252-268, August, 1921.

14. Thwaites, B.: Approximate Calculation of the Laminar Boundary Layer. Aeronautical Quarterly, Vol. I, pp. 245-280, May-February, 1949-1950.

15. Rott, N. and Crabtree, L. F.: Simplified Laminar Boundary Layer Calculations for Bodies of Revolution and for Yawed Wings. Journal of the Aeronautical Sciences, Vol. 19, No. 8, pp. 553-565, August, 1952.

16. Cohen, C. B. and Reshotko, E.: The Compressible Laminar Boundary Layer with Heat Transfer and Arbitrary Pressure Gradient. NACA Report 1294, 1956.

17. Tani, I.: On the Approximate Solution of the Laminar Boundary Layer Equations. Journal of the Aeronautical Sciences, Vol. 21, No. 7, pp. 487-504, July, 1954.

18. Walz, A.: Anwendung des Energiesatzes von Wieghardt auf einparametrige Geschwindigkeitsprofile in laminarer Grenzschichten. Ingenieur-Archiv, Vol. 16, pp. 243-248, 1948.

19. Crocco, L.: Considerations on the Shock-Boundary Layer Interaction. Proceedings of the Conference on High-Speed Aeronautics, held at the Polytechnic Institute of Brooklyn, January 20-22, 1955.

20. Cheng, S. I. and Bray, K. N. C.: On the Mixing Theory of Crocco and Lees and Its Application to the Interaction of Shock Wave and Laminar Boundary Layer. Part I. Generals and Formulation. Princeton University, Department of Aeronautical Engineering, Report 376, AFOSR TN 57-283, May, 1957.

21. Cheng, S. I. and Chang, I. D.: On the Mixing Theory of Crocco and Lees and Its Application to the Interaction of Shock Wave and Laminar Boundary Layer. Part II. Results and Discussion. Princeton University, Department of Aeronautical Engineering, Report 376, AFOSR TN 58-3, November, 1957.

22. Gadd, G. E. and Holder, D. W.: The Behavior of Supersonic Boundary Layers in the Presence of Shock Waves. Institute of the Aeronautical Sciences, Paper No. 59-138, presented at the 7th Anglo-American Aeronautical Conference, October 5-7, 1959.

23. Howarth, L.: On the Solution of the Laminar Boundary Layer Equations. Proceedings of the Royal Society, Series A, Vol. 164, January-February, 1938.

24. Falkner, V. M. and Skan, S. W.: Some Approximate Solutions of the Boundary Layer Equations. British Reports and Memoranda No. 1314, April, 1930.

25. Hartree, D. R.: A Solution of the Boundary Layer Equation for Schubauer's Observed Pressure Distribution for an Elliptic Cylinder. Aeronautical Research Council, Report 3966, 1939.

26. Schubauer, G. B.: Air Flow in a Separating Laminar Boundary Layer. NACA Report 527, pp. 369-380, 1935.

27. Stewartson, K.: Correlated Incompressible and Compressible Boundary Layers. Proceedings of the Royal Society, Series A, Vol. 200, pp. 84-100, December, 1949.

28. Hayes, W. D. and Probstein, R. F.: Hypersonic Flow Theory, Academic Press, New York and London, 1959.

29. Chapman, D. R.: Laminar Mixing of a Compressible Fluid. NACA Report 958, 1950.

30. Korst, H. H.; Page, R. H.; and Childs, M. E.: A Theory for Base Pressures in Transonic and Supersonic Flow. University of Illinois, Engineering Experimental Station, Mechanical Engineering Department, TN 392-2, March, 1955.

31. Gadd, G. E.: A Theoretical Investigation of the Effects of Mach Number, Reynolds Number, Wall Temperature and Surface Curvature on Laminar Separation in Supersonic Flow. Report No. FM 2415, British A. R. C., June, 1956.

32. Lees, L.: Hypersonic Flow, Proceedings of the 5th International Aeronautical Conference, Los Angeles, Institute of the Aeronautical Sciences, New York, pp. 241-276, 1955.

33. Lees, L. and Probstein, R. F.: Hypersonic Viscous Flow over a Flat Plate. Princeton University, Aeronautical Engineering Laboratory, Report No. 195, April 20, 1952.

34. Smith, A. M. O.: Improved Solutions of the Falkner and Skan Boundary Layer Equation. SMF Fund Paper No. FF-10, March, 1954.

APPENDIX A

MAXIMUM CORRELATION METHOD

It is the purpose of this Appendix to derive several relations that have been used in the present study to obtain the correlation functions for the attached part of the flow. It is shown in Section II. that

$$K = \frac{\delta_i - \delta_i^* - \delta_i^{**}}{\delta_i - \delta_i^*} \tag{A-1}$$

$$f = \frac{(\delta_i - \delta_i^* - \delta_i^{**})\ \delta_i}{(\delta_i - \delta_i^*)^2} = \frac{K\,(\delta_i/\delta_i^*)}{(\delta_i/\delta_i^* - 1)} \quad . \tag{A-2}$$

Solving for (δ_i/δ_i^*) from Eq. (A-2), we obtain

$$\delta_i/\delta_i^* = (f/f - K) \quad . \tag{A-3}$$

Substituting this equation for δ_i/δ_i^* into Eq. (A-1), it can be shown that

$$f = K\left[H_i\,(1 - K) + 1\right] \quad , \tag{A-4}$$

where

$$H_i = (\delta_i^*/\delta_i^{**}) \quad .$$

If it is assumed that a boundary layer profile is characterized by the value of H_i, then for a given profile, H_i may be taken as constant, and thus

$$\left.\frac{df}{dK}\right|_{H_i} = H_i + 1 - 2\,H_i\,K \quad . \tag{A-5}$$

It can be shown from Eq. (A-1) that

$$K = 1 - \frac{1}{H_i}\frac{1}{\left(\frac{\delta_i}{\delta_i^*} - 1\right)} \tag{A-6}$$

so that

$$\left.\frac{dK}{d\delta_i}\right|_{H_i} = -\frac{1}{H_i}\frac{1}{\left(\frac{\delta_i}{\delta_i^*}-1\right)^2}\left(\frac{\delta_i}{\delta_i^*}\right)^2 \frac{d}{d\delta_i}\left(\frac{\delta_i^*}{\delta_i}\right) \quad , \tag{A-7}$$

since

$$\delta_i^* \equiv \int_0^{\delta_i}\left(1-\frac{u_i}{u_{ie}}\right)d\eta \quad , \tag{A-8}$$

then

$$\frac{d(\delta_i^*/\delta_i)}{d\delta_i} = \frac{1}{\delta_i}\left[\frac{1}{\delta_i}\int_0^{\delta_i}\frac{u_i}{u_{ie}}\,d\eta - \frac{u_i(\delta_i)}{u_{ie}}\right]$$

$$= -\frac{u_i(\delta_i)}{u_{ie}}\frac{1}{\delta_i}\left[1-\int_0^{'}\frac{u_i}{u_i(\delta_i)}d\left(\frac{\eta}{\delta_i}\right)\right] < 0 \quad . \tag{A-9}$$

Thus,

$$\left.\frac{dK}{d\delta_i}\right|_{H_i} > 0 \quad . \tag{A-10}$$

Therefore, K increases monotonically with δ_i. This conclusion is also obvious from the definition of K as the ratio of the momentum to the mass flux.

It is clear however from Eq. (A-5) that

$$\left.\frac{df}{dK}\right|_{H_i} = 0 \quad , \quad \text{if} \quad H_i + 1 - 2H_i K = 0 \quad , \tag{A-11}$$

so that

$$\left.\frac{df}{d\delta_i}\right|_{H_i} = \left.\frac{df}{dK}\right|_{H_i}\left.\frac{dK}{d\delta_i}\right|_{H_i} = 0 \quad , \text{ if } \quad H_i + 1 - 2H_i K = 0 \quad . \tag{A-12}$$

Thus it is seen that, for every H_i, there exists a δ_i such that f is an extremum (a maximum), and in the present study, this condition has been used to determine δ_i. From Eq. (A-11), we find that

$$H_i = 1/(2K - 1) \quad \text{or} \quad K = (H_i + 1)/2H_i \quad . \tag{A-12}$$

Substituting this relation back into Eq. (A-4), we obtain

$$f = \frac{K^2}{(2K-1)} = \frac{(H_i+1)^2}{4H_i}$$

or

$$F = \frac{2(1-K)}{(2K-1)} = H_i - 1 \tag{A-13}$$

where

$$F \equiv f/K^2 - 1 \quad .$$

In the present study, the values of δ_i^*, δ_i^{**}, and H_i that have been used have been those tabulated for $\delta_i \longrightarrow \infty$. Although this procedure is not strictly consistent with the definitions of δ_i^*, δ_i^{**}, and H_i, it can be shown that the errors introduced by this approximation are small since the values of δ_i obtained by the maximum method roughly correspond to those obtained for $u(\delta_i)/u_{ie} = 0.95$.

With the above relations, it is now possible to relate the boundary layer thickness, δ_i, with δ_i^* and δ_i^{**}. It is found, for example, that

$$\delta_i = \delta_i^* \frac{(H_i + 1)}{(H_i - 1)} = \frac{K \delta_i^*}{(1 - K)} \quad . \tag{A-14}$$

The $C(K)$ correlations have been obtained in the present study by first finding the values of $\bar{m}_i$ at successive stations, where

$$\bar{m}_i = \rho_t u_{ie} \delta_i^* \left(\frac{\delta_i}{\delta_i^*} - 1 \right) = \frac{2 \rho_t u_{ie} \delta_i^*}{(H_i - 1)} \quad , \tag{A-15}$$

and then fitting a polynomial in ξ through these values of $\bar{m}_i$. The derivative of this polynomial essentially gives the value of $C(K)$ at each

station, and this value of $C(\mathcal{K})$ is then correlated with $\mathcal{K} = (H_i + 1)/2H_i$ to give the desired $C(\mathcal{K})$ relation.

Determination of $(1 - \delta_s^*/\delta_s)$

In several of the calculations, the quantity $(1 - \delta_s^*/\delta_s)$ is required. The value of this quantity can be found using the above relations and Eq. (23) as follows:

$$\mathcal{K} = \left(\frac{\delta - \delta^* - \delta^{**}}{\delta - \delta^*} \right) = \left(\frac{\delta_i - \delta_i^* - \delta_i^{**}}{\delta_i - \delta_i^*} \right) . \qquad \text{(A-16)}$$

It can be readily shown that

$$H \left[(\delta/\delta^*) - 1 \right] = H_i \left[(\delta_i/\delta_i^*) - 1 \right] . \qquad \text{(A-17)}$$

Solving for δ^*/δ, and using Eq. (A-14), we obtain

$$\left(1 - \frac{\delta^*}{\delta}\right) = \left[1 + \frac{H(1-\mathcal{K})}{H_i(2\mathcal{K}-1)}\right]^{-1} . \qquad \text{(A-18)}$$

The next step is to evaluate H. It is shown in Reference 1 that

$$m\mathcal{K}\left[(F + t)\right] = \gamma p w_e \delta . \qquad \text{(A-19)}$$

Using Eqs. (23) and (A-19), it can be shown that

$$\delta/\delta^{**} = \mathcal{K}(F+t)/t(1-\mathcal{K}) . \qquad \text{(A-20)}$$

If we write $\mathcal{K}$ in the form

$$\mathcal{K} = \frac{\delta/\delta^{**} - H - 1}{\delta/\delta^{**} - H} , \qquad \text{(A-21)}$$

and substitute the expression for δ/δ^{**} given by Eq. (A-20), it is found that

$$H = \frac{\mathcal{K}\left[F\left(1 + \frac{\gamma-1}{2} M_e^2\right) + 1\right] - 1}{(1 - \mathcal{K})} . \qquad \text{(A-22)}$$

Thus,

$$H_i = \frac{\kappa F}{1-\kappa} - 1 = F + 1 \quad . \tag{A-23}$$

Solving for F from Eq. (A-23) and substituting the result into Eq. (A-22), we obtain

$$H = (H_i + 1)\left(1 + \frac{\gamma-1}{2} M_e^2\right) - 1 \quad . \tag{A-24}$$

This result has also been reported by Rott and Crabtree[15] and Cohen and Reshotko[16]. Therefore, the equation for $(1 - \delta^*/\delta)$ is

$$\left(1 - \frac{\delta^*}{\delta}\right) = \left\{1 + \frac{[(H_i+1)(1+\frac{\gamma-1}{2}M_e^2) - 1]\,(1-\kappa)}{H_i \qquad (2\kappa-1)}\right\}^{-1} \quad . \tag{A-25}$$

Evaluating this equation at the separation point, we obtain

$$\left(1 - \frac{\delta_s^*}{\delta_s}\right) = \left\{1 + \frac{[(H_{is}+1)(1+\frac{\gamma-1}{2}M_{es}^2) - 1]\,(1-\kappa_s)}{H_{is} \qquad (2\kappa_s-1)}\right\}^{-1} \quad , \tag{A-26}$$

where the Howarth values of κ_s and H_{is} have been used.

APPENDIX B

CROCCO-LEES METHOD

The purpose of this Appendix is to show how the basic equations given in Section II are reduced to two non-linear first order ordinary differential equations. These equations will then be linearized with regard to Mach number for use in regions in which the difference between the local and free stream Mach numbers is small compared with the free stream Mach number. The linearized equations will then be examined for the two flow regimes up to the plateau. Finally, the limiting case of weak hypersonic interaction will be discussed to show how this particular result is independent of the definition of the viscous layer thickness, δ.

The basic equations given in Section II are

Momentum Equation

$$(d/dx)(m K w_e) = w_e (dm/dx) - \delta (dp/dx) - \frac{p w_e c_f}{2 \phi_e} \qquad (B\text{-}1)$$

Continuity Equation

$$dm/dx = (p/\phi_e) \left(\frac{d\delta}{dx} - \theta \right) \qquad (B\text{-}2)$$

Bernoulli Equation

$$dp/p = - (dw_e/\phi_e) \qquad (B\text{-}3)$$

Mean-Temperature Equation

$$m = p\delta/\phi_1 \qquad (B\text{-}4)$$

In addition to these equations, the three correlation relations are

$$F = F(K)$$

$$\mathcal{K} \equiv (d\delta/dx) - \theta = C(K)\mu_e a_t/m \qquad \text{(B-5)}$$

$$c_f = D(K)\mu_e a_t/m \quad .$$

Expanding the momentum equation, and using the Bernoulli equation to eliminate the pressure gradient term, we find

$$\frac{dK}{dx} = (1-K)\frac{1}{m}\frac{dm}{dx} + \left(\frac{\phi_1}{\phi_e} - K\right)\frac{1}{w_e}\frac{dw_e}{dx} - \frac{p}{\phi_e m}\frac{C_f}{2} \quad . \text{(B-6)}$$

It can be readily shown, using the equations given in Section II, that

$$\left(\frac{\phi_1}{\phi_e} - K\right) = KF/t$$

$$(1/w_e t)\ dw_e = (1/M_e)\ dM_e \quad , \qquad \text{(B-7)}$$

so the momentum equation becomes

$$\frac{dK}{dx} = (1-K)\frac{1}{m}\frac{dm}{dx} + \frac{KF}{M_e}\frac{dM_e}{dx} - \frac{p}{\phi_e m}\frac{C_f}{2} \quad . \text{(B-8)}$$

Introducing the definition

$$\zeta \equiv m/a_t\mu_t \quad , \qquad \text{(B-9)}$$

it is found that the momentum equation can be written as

$$\frac{dK}{dx} = (1-K)\frac{1}{\zeta}\frac{d\zeta}{dx} + \frac{KF}{M_e}\frac{dM_e}{dx} - \frac{\rho_e u_e t^2}{2\mu_e}\frac{D(K)}{\zeta^2} \quad . \text{(B-10)}$$

The continuity equation can be written as

$$\frac{1}{\zeta}\frac{d\zeta}{dx} = \frac{C(K)\rho_e u_e t^2}{\zeta^2 \mu_e} \quad . \text{(B-11)}$$

Inserting this form of the continuity equation into the momentum equation and using the definition $\sigma(K) \equiv \frac{D(K)}{2(1-K)\,C(K)}$, it is found that

$$\frac{dK}{dx} - \frac{KF}{M_e}\frac{dM_e}{dx} = (1-\sigma)(1-K)\frac{1}{\zeta}\frac{d\zeta}{dx} = (1-\sigma)(1-K)\frac{1}{m}\frac{dm}{dx} \quad . \text{(B-12)}$$

It is shown in Reference 1 that

$$\delta = \frac{m\,K(F+t)}{\gamma\, p\, w_e} \quad . \text{(B-13)}$$

Since

$$d\delta/dx = \theta + k = \theta + \frac{C(K)}{\zeta}\,(T_e/T_t) \quad , \text{(B-14)}$$

and introducing the definition $t \equiv (T_e/T_t) = \frac{1}{\left(1 + \frac{\gamma-1}{2} M_e^2\right)} = 1 - \frac{\gamma-1}{2} w_e^2$,

it can be shown, using Eqs. (B-13) and (B-14), that

$$\left[F + t + K\frac{dF}{dK}\right]\frac{dK}{dx} - \left[K(F+t)\left(1 - \frac{3\gamma-1}{2} w_e^2\right) + Kt(\gamma-1)w_e^2\right]\frac{1}{M_e}\frac{dM_e}{dx} = \frac{\rho_e u_e}{\mu_e}\frac{1}{\zeta}\, t^2\left[\theta + \frac{C}{\zeta}\left(t - K(F+t)\right)\right] \quad \text{(B-15)}$$

It is to be noted that x appears in Eqs. (B-12) and (B-15) only in the derivatives, and can therefore be eliminated. Solving these equations simultaneously, we get the following set of non-linear first order ordinary differential equations:

$$\frac{dK}{d\zeta} = -\frac{KF}{C}\,\frac{\left\{\frac{C}{\zeta}\left[t - K(F+t) - \frac{(1-K)(1-\sigma)}{KF}\left(K(F+t)\left(1 - \frac{3\gamma-1}{2} M_e^2 t\right) + KM_e^2 t^2(\gamma-1)\right)\right] + \theta\right\}}{\left\{K(F+t)\left(1 - \frac{3\gamma-1}{2} M_e^2 t\right) + K(\gamma-1)M_e^2 t^2 - KF\left(F + t + K\frac{dF}{dK}\right)\right\}} \quad \text{(B-16)}$$

$$\frac{dM_e}{d\xi} = -\frac{M_e}{C}\frac{\left\{\frac{C}{5}\left[t - K(F+t) - \frac{(1-K)(1-\sigma)}{KF}\left(K(F+t)\left(1-\frac{3\gamma-1}{2}M_e^2t\right)+(\gamma-1)KM_e^2t^2\right)\right]+\theta\right\}}{\left\{K(F+t)\left(1-\frac{3\gamma-1}{2}M_e^2t\right)+(\gamma-1)KM_e^2t^2-KF\left(F+t+K\frac{dF}{dK}\right)\right\}} \qquad \text{(B-17)}$$

These general equations will now be specialized to the various flow regions. The first region to be considered is the zone from the beginning of the interaction up to separation. In this zone, the maximum correlation method will be used so that

$$F(K) = \frac{2(1-K)}{(2K-1)} \quad . \text{ (See Appendix A.)} \qquad \text{(B-18)}$$

The equation for $D(K)$ is obtained by noting from Figure 4 that a linear representation of $D(K)$ appears reasonable. The Blasius value of $D(K)$ is chosen to be 1.40 at $K = 0.693$. It is assumed, following Thwaites, that $D(K)$ is zero when the Howarth separation value of $K = 0.630$ is reached. Therefore, the equation assumed for $D(K)$ is

$$D(K) = 22.2\,(K - .630) \quad . \qquad \text{(B-19)}$$

The equation for $C(K)$ is also assumed to be linear. However, the scatter in the $C(K)$ curves shown in Figure 5 does not allow an accurate determination of the $C(K)$ relation. Since the experimental separation pressure gradient seems to agree with calculations assuming that $C(K)$ near separation is zero (Figure 8), it has been assumed that $C(K)$, like $D(K)$, is zero at the separation value of K. In order to determine another point for the linear $C(K)$ relation, it is assumed that $\sigma(K)$ is equal to unity at $K = 0.693$. This assumption is usually made for flows with zero pressure gradient and insures that the Crocco-Lees method will give the same weak hypersonic interaction result which is obtained by the Cohen and Reshotko method (Appendix C) and which has been

found in earlier investigations[32, 33]. The equation for $C(K)$, thus defined, is

$$C(K) = 36.2\,(K - .630) \quad . \tag{B-20}$$

The general equations are now linearized with respect to Mach number. It is assumed that $M = M_\infty + \varepsilon$, where $\varepsilon << M_\infty$, and

$$\vartheta = - \frac{\sqrt{M_\infty^2 - 1}\;\varepsilon}{M_\infty \left(1 + \frac{\gamma-1}{2} M_\infty^2\right)} \quad \text{(linearized Prandtl-Meyer relation)} . \tag{B-21}$$

If terms of order ε are kept, it is found that the equations can be cast into the following form:

$$\begin{aligned} dK/d\zeta &= - L \left[\frac{P}{\zeta} - \varepsilon\right] \\ d\varepsilon/d\zeta &= - N \left[\frac{Q}{\zeta} - \varepsilon\right] \end{aligned} \tag{B-22}$$

where

$$L = \frac{2K(1-K)(2K^2-1)\sqrt{M_\infty^2-1}}{4M_\infty K(1-K)(2K^2-2K+1)\left(1+\frac{\gamma-1}{2}M_\infty^2\right)C(K)\left[1 - \frac{\gamma M_\infty^2 (2K-1)^2}{2(2K^2-2K+1)\left(1+\frac{\gamma-1}{2}M_\infty^2\right)} - \frac{(2K-1)^3(M_\infty^2-1)}{4(2K^2-2K+1)(1-K)\left(1+\frac{\gamma-1}{2}M_\infty^2\right)^2}\right]}$$

$$N = \frac{LM_\infty}{KF(K)} = \frac{LM_\infty(2K-1)}{2K(1-K)}$$

$$P = \frac{C(K)M_\infty}{\sqrt{M_\infty^2-1}}\left[\sigma(1-K) + \frac{(2K-1)(1-\sigma)}{2K}\left\{\frac{2\gamma K(1-K)M_\infty^2}{(2K-1)} + K\left(\frac{\gamma+1}{2}\frac{M_\infty^2}{1+\frac{\gamma-1}{2}M_\infty^2} - 1\right)\right\} - \frac{2K(1-K)\left(1+\frac{\gamma-1}{2}M_\infty^2\right)}{(2K-1)}\right]$$

$$Q = \frac{C(K)M_\infty}{\sqrt{M_\infty^2-1}}\left[\sigma(1-K) - \frac{2(1-K)K\left(1+\frac{\gamma-1}{2}M_\infty^2\right)}{(2K-1)}\left\{1 - \frac{(1-\sigma)(2K^2-2K+1)}{K(2K-1)}\right\}\right]$$

The results of numerical integrations using Eqs. (B-22) may be

transformed back to the physical plane using the continuity equation as follows:

$$dm/dx = \frac{\rho_e u_e a_t^2}{m} C(K) = \frac{\rho_e u_e t}{\zeta} C(K) \quad . \tag{B-23}$$

This equation can be integrated and put into the form

$$\frac{x_s - x}{x_s} = \frac{1}{Re_{x_s}} \left(1 + \frac{\gamma-1}{2} M_\infty^2\right) \int_{\zeta}^{\zeta_s} \frac{\zeta \, d\zeta}{C(K)} \frac{M_\infty}{M_e} \left[\frac{1 + \frac{\gamma-1}{2} M_e^2}{1 + \frac{\gamma-1}{2} M_\infty^2}\right]^{\frac{(3\gamma-1)}{2(\gamma-1)}} \quad . \tag{B-24}$$

where

$$Re_{x_s} \equiv \frac{\rho_\infty u_\infty x_s}{\mu_\infty} \quad .$$

The remaining equation to complete the formulation of the problem up to separation involves the skin friction, or wall shear, distribution. From the correlation equation for c_f, we have

$$c_f = \frac{D(K)\mu_e}{\bar{m}} = \frac{D(K)}{\zeta} \frac{1}{\left(1 + \frac{\gamma-1}{2} M_e^2\right)} \quad . \tag{B-25}$$

Since every ζ corresponds to known values of M_e, K, and x, the skin friction distribution is therefore determined. Calculations of the skin friction distribution for three shock wave-laminar boundary layer interaction cases are given in Figures 10, 11, and 20.

In the region between separation and the beginning of the plateau, the following assumptions have been made and are discussed in Section IV:

(1) F = constant = value of F at separation

(2) $\sigma = 0$, since c_f is assumed negligible in separated flow

(3) $C(K) = C_1 = 11$ (by comparison with a selected experiment)

(4) $\theta = - \frac{\sqrt{M_\infty^2 - 1} \quad \varepsilon}{M_\infty \left(1 + \frac{\gamma-1}{2} M_\infty^2\right)}$.

Substituting these conditions into the general linearized equations, we obtain

$$\frac{d\kappa}{d\zeta} = \frac{-F_s\sqrt{M_\infty^2-1}}{M_\infty(1+\frac{\gamma-1}{2}M_\infty^2)C_1 b}\left[\frac{C_1 M_\infty(1+\frac{\gamma-1}{2}M_\infty^2)}{\sqrt{M_\infty^2-1}\ \zeta}\left(\frac{F_s^2-(1-\kappa)b}{F_s}\right)+\varepsilon\right]$$

$$\frac{d\varepsilon}{d\zeta} = \frac{-\sqrt{M_\infty^2-1}}{\kappa(1+\frac{\gamma-1}{2}M_\infty^2)C_1 b}\left[\frac{C_1 M_\infty(1+\frac{\gamma-1}{2}M_\infty^2)F_s}{\sqrt{M_\infty^2-1}\ \zeta}+\varepsilon\right] \qquad \text{(B-26)}$$

where

$$b \equiv F_s^2 + \frac{\gamma F_s M_\infty^2}{(1+\frac{\gamma-1}{2}M_\infty^2)} + \frac{(M_\infty^2-1)}{(1+\frac{\gamma-1}{2}M_\infty^2)^2}$$

These equations are integrated in the same manner as Eqs. (B-22), using as initial conditions the values at separation found in the solution of the eigenvalue problem for ε_s. The transformation of the results back to the physical plane is carried out using Eq. (B-24).

Weak Hypersonic Interaction

If $\sigma(\kappa)$ is set equal to unity, corresponding to Blasius flow, it is seen that Eqs. (B-16) and (B-17) reduce to

$$d\kappa/d\zeta = (-\kappa F/Cd)\left\{\frac{C\left[t-\kappa(F+t)\right]}{\zeta}+\theta\right\} \qquad \text{(B-27)}$$

$$dM_e/d\zeta = (-M_e/Cd)\left\{\frac{C\left[t-\kappa(F+t)\right]}{\zeta}+\theta\right\} = (M_e/\kappa F)(d\kappa/d\zeta), \qquad \text{(B-28)}$$

where

$$d \equiv \kappa(F+t)\left(1-\frac{3\gamma-1}{2}M_e^2\,t\right)+\kappa(\gamma-1)M_e^2\,t^2-\kappa F\left(F+t+\kappa\frac{dF}{d\kappa}\right).$$

Therefore, if $(dM_e/d\zeta)$ and $d\kappa/d\zeta$ are assumed to be of lower order than

either of the terms on the right-hand sides of Eqs. (B-27) and (B-28), then the following relation is obtained:

$$\theta = - \left. \frac{C\left[t - K(F + t)\right]}{\zeta} \right|_{K=K_b} , \qquad \text{(B-29)}$$

since the condition, $\sigma(K) = 1$, implies $K = K_b$. It is shown in Reference 19 that

$$\zeta = (t \, \mathrm{Re}_{\delta^{**}})/(1 - K) , \qquad \text{(B-30)}$$

and from Eqs. (A-24) and (C-8), it follows that

$$\mathrm{Re}_{\delta^{**}} \cong \sqrt{A} \sqrt{\mathrm{Re}_x} . \qquad \text{(B-31)}$$

Using Eqs. (B-21), (B-29), (B-30), and (B-31), it is found that

$$\varepsilon_b = \left. \frac{M_\infty \left(1 + \frac{\gamma-1}{2} M_\infty^2\right) C(K)(1-K)^2}{\sqrt{M_\infty^2 - 1}\sqrt{A}\sqrt{\mathrm{Re}_x}} \left(1 - \frac{KF}{(1-K)}\left(1 + \frac{\gamma-1}{2} M_\infty^2\right)\right) \right|_{K=K_b} . \qquad \text{(B-32)}$$

In the hypersonic limit, i.e., $M_\infty >> 1$, we obtain

$$\lim_{M_\infty >> 1} \varepsilon_b = - \left. \frac{C(K)(1-K)^2 \left(\frac{\gamma-1}{2}\right)^2 M_\infty^4}{\sqrt{A}\sqrt{\mathrm{Re}_x}} \left(\frac{KF}{1-K}\right) \right|_{K=K_b} , \qquad \text{(B-33)}$$

which is numerically identical to Eq. (C-19).

Using four different definitions of δ_i , it is seen in Table I that despite large numerical differences in the values of $F(K)$, K , and $C(K)$, the terms $C(K)(1 - K)^2$ and $(KF/1-K)$ are identical, showing that the physical quantity, ε_b , is independent of the definition of δ_i . The four definitions of δ_i were the following:

(1) δ_i defined by the maximum method (present study)

(2) δ_i defined by $u(\delta_i)/u_{ie} = .95$

(3) δ_i defined by $u(\delta_i)/u_{ie} = .99$

(4) δ_i defined by $u(\delta_i)/u_{ie} = .998$.

The values of the quantities F, K , and C(K) defined by the several values of $u(\delta_i)/u_{ie}$ were read from curves given in Reference 19, and it is found that the agreement of the two terms investigated is within the ability to read the values from the curves. Since the values of ε_b given by earlier investigations[33, 34], the Cohen and Reshotko method[16], and the Crocco-Lees method for several definitions of δ agree, the artificiality of δ has been demonstrated for a case in which an explicit physical result can be obtained in a simple analytic form, not requiring numerical integration.

TABLE I

Definition of δ_i	K_b	$F(K_b)$	$C(K_b)$	$C(K_b)(1-K_b)^2$	$\frac{K_b F(K_b)}{1-K_b}$
Maximum Method	.6930	1.591	2.341	0.2206	3.592
$u(\delta_i)/u_{ie} = .95$	.700	1.557	2.42	0.218	3.63
$u(\delta_i)/u_{ie} = .99$	.794	.945	5.15	0.220	3.64
$u(\delta_i)/u_{ie} = .998$	.834	.719	7.97	0.220	3.61

APPENDIX C

COHEN-RESHOTKO METHOD

In this section, the method of Cohen-Reshotko[16] will be used to calculate the pressure distribution over a flat plate up to separation for the case of steady two-dimensional laminar supersonic flow in which the Prandtl number is equal to unity and the heat transfer is zero. The external streamline direction will be set equal to the gradient of the displacement thickness, and in the present analysis, it will be assumed that $\mathcal{E}$, the deviation of the local Mach number from the free stream Mach number, will be small compared to the free stream Mach number.

From Eqs. (33) and (34) in Reference 16, we have

$$n = \frac{A}{\gamma p}\frac{dp}{dx}\left(\frac{T_t}{T_e}\right)^{1+K} M_e^{-(1+B)} \int_0^x \left(\frac{T_e}{T_t}\right)^{K} M_e^{B-1}\, dx \quad , \quad \text{(C-1)}$$

where $n \equiv \frac{\rho_w}{\mu_w}\theta^2\left(\frac{T_t}{T_e}\right)^3 \frac{du_e}{dx}$, $K \equiv \frac{(3\gamma - 1)}{2(\gamma - 1)}$, and A and B are constants.

From the isentropic Bernoulli equation, we have

$$(1/p)(dp/dx) = - \frac{\gamma M_e}{(1 + \frac{\gamma-1}{2} M_e^2)} (dM_e/dx) \quad . \quad \text{(C-2)}$$

Thus

$$n = - A M_e^{-B} (1 + \tfrac{\gamma-1}{2} M_e^2)^K \frac{dM_e}{dx} \int_0^x (1 + \tfrac{\gamma-1}{2} M_e^2)^{-K} M^{B-1}\, dx \quad . \quad \text{(C-3)}$$

Let $M_e = M_\infty + \mathcal{E}$ where M_∞ = free stream Mach number $>> \mathcal{E}$.
Substituting M_e in the above expression for n and keeping only first order terms in $\mathcal{E}$, we obtain

$$n = - (A/M_\infty)(d\mathcal{E}/dx)\, x \quad . \quad \text{(C-4)}$$

From Eqs. (34), (39), and (40) in Reference 16, we have for Pr = 1 and no heat transfer:

$$\frac{\delta^*}{H_i + \frac{\gamma-1}{2} M_e^2 (H_i+1)} = \frac{1}{\sqrt{Re_w}} \frac{T_e}{T_t} \sqrt{- \frac{n X M_e}{\frac{dM_e}{dX}}} \qquad \text{(C-5)}$$

where $Re_w \equiv \frac{\rho_w u_e x}{\mu_w}$.

But using Eq. (C-4) for n, it is found that

$$\frac{\delta^*}{H_i + \frac{\gamma-1}{2} M_e^2 (H_i+1)} = \frac{1}{\sqrt{Re_w}\left(1 + \frac{\gamma-1}{2} M_e^2\right)} \sqrt{\frac{A X^2 M_e}{M_\infty}} \qquad \text{(C-6)}$$

Thus

$$\delta^* = \left[H_i + 1 - \frac{1}{1 + \frac{\gamma-1}{2} M_e^2} \right] \sqrt{\frac{A X \mu_w}{M_\infty \rho_w a_e}} \qquad \text{(C-7)}$$

To terms of order ε , it can be shown that

$$\delta^* = k_3 \sqrt{x} \left[\bar{g} + \bar{f} \varepsilon \right], \qquad \text{(C-8)}$$

where

$$k_3 \equiv \left(1 + \frac{\gamma-1}{2} M_\infty^2\right) \sqrt{\frac{A \mu_\infty}{\rho_\infty u_\infty}}$$

$$\bar{f} \equiv \frac{(\gamma-1) M_\infty}{\left(1 + \frac{\gamma-1}{2} M_\infty^2\right)^2} + \frac{(3\gamma-1) M_\infty}{4 \left(1 + \frac{\gamma-1}{2} M_\infty^2\right)} \bar{g}$$

$$\bar{g} \equiv H_i + 1 - \frac{1}{1 + \frac{\gamma-1}{2} M_\infty^2} \, .$$

Thus,

$$\frac{d\delta^*}{dx} = \frac{k_3}{2\sqrt{x}} \left[\bar{g} + \bar{f} \varepsilon \right] + k_3 \sqrt{x} \left[\frac{d\bar{g}}{dn} \frac{dn}{dx} \left(1 + \frac{(3\gamma-1) M_\infty \varepsilon}{4\left(1 + \frac{\gamma-1}{2} M_\infty^2\right)} \right) + \bar{f} \frac{d\varepsilon}{dx} \right] \qquad \text{(C-9)}$$

But

$$(d\delta^*/dx) = - \frac{\sqrt{M_\infty^2 - 1}\ \varepsilon}{M_\infty \left(1 + \frac{\gamma-1}{2} M_\infty^2\right)} \quad , \tag{C-10}$$

from the Prandtl-Meyer relation and the assumption that $d\delta^*/dx$ equals the outer streamline direction. Therefore,

$$\frac{dn}{dx} = - \frac{\frac{1}{k_3\sqrt{x}}\left[\frac{\sqrt{M_\infty^2-1}\ \varepsilon}{M_\infty(1+\frac{\gamma-1}{2}M_\infty^2)} + \frac{k_3}{2\sqrt{x}}(\bar{g} + \bar{f}\varepsilon)\right] + \frac{\bar{f} M_\infty n}{Ax}}{\frac{d\bar{g}}{dn}\left[1 + \frac{(3\gamma-1)M_\infty \varepsilon}{4(1+\frac{\gamma-1}{2}M_\infty^2)}\right]} \tag{C-11}$$

$$\frac{d\varepsilon}{dx} = - \frac{M_\infty n}{Ax} \quad .$$

These two non-linear first order ordinary differential equations can be integrated numerically since the right-hand sides are known functions of n, ε, and x. Such an integration has been carried out for the $M_\infty = 2.0$, $Re_{x_s} = 2.87 \times 10^5$ shock wave-laminar boundary layer interaction case, and the results are shown in Figure 8. In the calculation, the $n(H_i)$ relation given in Reference 16 has been approximated by the following polynomial:

$$n = - 1.4992 + 1.1845\ H_i - 0.29950\ H_i^2 - 0.025327\ H_i^3 \quad . \tag{C-13}$$

Weak Hypersonic Interaction

It is interesting to note that if the boundary layer approaches the Blasius flat plate condition, corresponding to $n = 0$, the equation $dn/dx = 0$ gives the weak hypersonic interaction result in the same way as the Crocco-Lees method does when $K = K_b$ and $dK/dx = 0$. If $n = 0 = dn/dx$, we have

$$\frac{\sqrt{M_\infty^2 - 1}\ \ \varepsilon_b}{M_\infty \left(1 + \frac{\gamma-1}{2} M_\infty^2\right)} + \frac{k_3}{2\sqrt{x_b}}(\bar{g}_b + \bar{f}_b\, \varepsilon_b) = 0 \quad . \tag{C-14}$$

Solving for $\mathcal{E}_b$, we obtain

$$\mathcal{E}_b = - \frac{k_3 \bar{g}_b}{2\sqrt{x_b}\left[\frac{\sqrt{M_\infty^2-1}}{M_\infty(1+\frac{\gamma-1}{2}M_\infty^2)} + \frac{k_3}{2\sqrt{x_b}}\bar{f}_b\right]} \quad . \text{(C-15)}$$

Substituting values for $\bar{g}_b$, $\bar{f}_b$, and k_3, we have

$$\mathcal{E}_b = -\frac{\left[(H_{ib}+1)(1+\frac{\gamma-1}{2}M_\infty^2)-1\right]M_\infty(1+\frac{\gamma-1}{2}M_\infty^2)\sqrt{A}}{2\sqrt{Re_{x_b}(M_\infty^2-1)}\left\{1+\frac{M_\infty(1+\frac{\gamma-1}{2}M_\infty^2)\sqrt{A}}{2\sqrt{Re_{x_b}(M_\infty^2-1)}}\left[(H_{ib}+1)(1+\frac{\gamma-1}{2}M_\infty^2)-1\right]\left[\frac{(\gamma-1)M_\infty}{(1+\frac{\gamma-1}{2}M_\infty^2)^2\bar{g}_b}+\frac{(3\gamma-1)M_\infty}{4(1+\frac{\gamma-1}{2}M_\infty^2)}\right]\right\}} \quad \text{(C-16)}$$

If we let

$$\bar{\mathcal{E}} \equiv -\frac{\left[(H_{ib}+1)(1+\frac{\gamma-1}{2}M_\infty^2)-1\right]M_\infty(1+\frac{\gamma-1}{2}M_\infty^2)\sqrt{A}}{2\sqrt{Re_{x_b}(M_\infty^2-1)}} \quad , \text{(C-17)}$$

then,

$$\mathcal{E}_b = \frac{\bar{\mathcal{E}}_b}{1 - \bar{\mathcal{E}}_b\left[\frac{(\gamma-1)M_\infty}{(1+\frac{\gamma-1}{2}M_\infty^2)^2\bar{g}_b}+\frac{(3\gamma-1)M_\infty}{4(1+\frac{\gamma-1}{2}M_\infty^2)}\right]} \quad . \text{(C-18)}$$

This result holds for all Mach numbers if $\mathcal{E}_b << M_\infty$. However, if $M_\infty >> 1$, it is seen that $\mathcal{E}_b \longrightarrow \bar{\mathcal{E}}_b$. Therefore,

$$\lim_{M_\infty >> 1} \mathcal{E}_b = \frac{-(H_{ib}+1)(\frac{\gamma-1}{2})^2 M_\infty^4 \sqrt{\gamma A}}{2\sqrt{Re_{x_b}}} \quad , \quad \text{(C-19)}$$

where

$$A = 0.44$$

$$H_{ib} = 2.591 \quad .$$

Using Eqs. (C-2) and (C-19), we obtain

$$\lim_{M_\infty >> 1} (\Delta p/p_\infty) = \frac{0.119\ \gamma \left(\frac{\gamma-1}{2}\right) M_\infty^{\ 3}}{\sqrt{Re_{x_b}}} \quad . \qquad \text{(C-20)}$$

For low supersonic Mach numbers, $\varepsilon_b \cong \overline{\varepsilon}_b$, if $\overline{\varepsilon}_b << 1$, since the bracketed term in the denominator of Eq. (C-18) is of order unity.

APPENDIX D

ALTERNATE C(K) CORRELATION

In this Appendix, an attempt is made to construct a C(K) relation that correlates the Falkner-Skan solutions with flows that have "histories", such as the Schubauer ellipse flow. The idea motivating this attempt is the removal of the term $\delta_i \, (d/d\xi)(\delta_i^*/\delta_i)$ since this term is identically zero for the Falkner-Skan solutions. (See Section II.) A new mass flux parameter, $\tilde{m}_i$, is defined as

$$\tilde{m}_i \equiv \frac{m_i}{1 - \frac{\delta_i^*}{\delta_i}} = \rho_t u_{ie} \delta_i$$

$$\tilde{k}_i \equiv \frac{1}{\rho_t u_{ie}} \frac{d\tilde{m}_i}{d\xi} = \frac{\tilde{C}(K)_i \mu_t}{\tilde{m}_i} \qquad . \quad \text{(D-1)}$$

It can be readily shown that

$$\tilde{C}(K)_i = \frac{\rho_t u_{ie}}{\mu_t} (\delta_i/\delta_i^*)^2 \; \delta_i^{*2} \; (d/d\xi)\left(u_{ie} \frac{\delta_i}{\delta_i^*} \delta_i^*\right) \qquad . \quad \text{(D-2)}$$

From the maximum correlation procedure, it is shown in Appendix A that

$$\delta_i/\delta_i^* = (H_i + 1)(H_i - 1) \qquad \text{(A-14)}$$

Therefore,

$$\tilde{C}(K)_i = \frac{\rho_t u_{ie}}{\mu_t}\left(\frac{H_i+1}{H_i-1}\right)^2 \delta_i^{*2} \frac{d}{d\xi}\left(\log u_{ie}\left(\frac{H_i+1}{H_i-1}\right)\delta_i^*\right) \qquad \text{(D-3)}$$

For the Falkner-Skan case, H_i = constant for each flow. Also, since $u_{ie} = a\xi^v$, where a and v are constants, and $\delta_i^* = b\xi \, Re_i^{-\frac{1}{2}}$, where $Re_i = \frac{\rho_t u_{ie} \xi}{\mu_t}$ and b is a constant, it can be shown that

$$d/d\xi \left(\log u_{ie} \frac{(H_i + 1)}{(H_i - 1)} \delta_i^* \right) = \frac{(n+1)}{2\xi} \quad , \tag{D-4}$$

so that

$$\tilde{C}(K)_i = \left(\frac{H_i+1}{H_i-1}\right)^2 \left(\frac{\delta_i^* \sqrt{Re_i}}{\xi}\right)^2 \frac{(n+1)}{2} \quad . \tag{D-5}$$

But $\Delta^* \equiv \frac{\delta_i^* \sqrt{Re_i}}{\xi} \sqrt{\frac{n+1}{2}}$ where Δ^* are values tabulated in Reference 34. Thus,

$$\tilde{C}(K)_i = \left[\left(\frac{H_i + 1}{H_i - 1} \right) \Delta^* \right]^2 \tag{D-6}$$

and

$$= \frac{(H_i + 1)}{2 H_i} \quad . \tag{A-12}$$

For Thwaites' treatment of the Schubauer ellipse[14],

$$\tilde{C}(K)_i = \left(\frac{H_i+1}{H_i-1}\right)^2 \frac{u_{ie}}{u_\infty} \left(\frac{\delta_i^* \sqrt{Re_i}}{L}\right) \frac{d}{d\bar{\xi}} \left[\log \frac{u_{ie}}{u_\infty} \left(\frac{H_i+1}{H_i-1}\right) \frac{\delta_i^* \sqrt{Re_i}}{L} \right] \tag{D-7}$$

where

$$Re_i \equiv \frac{\rho_t u_\infty \bar{L}}{\mu_t}$$

$$\bar{\xi} \equiv (\xi/\bar{L}) \quad .$$

Using these formulae for $\tilde{C}(K)_i$, the correlation curves have been computed and are shown in Figure 21. It is seen that although the curves diverge toward separation, the agreement is better than that obtained with the conventional $C(K)$ formulation shown in Figure 5, and the improvement expected by removing the δ_i^*/δ_i term has therefore been largely realized. Also, δ_i^*/δ_i is seen to be a universal function of K using the maximum correlation procedure, and it can be readily shown that

$$\left(1 - \frac{\delta_i^*}{\delta_i}\right) = \frac{2K - 1}{K} \quad . \qquad \text{(A-14)}$$

Therefore, we can write

$$\overline{m}_i = \frac{(2K - 1)}{K} \tilde{m}_i \quad . \qquad \text{(D-8)}$$

Thus,

$$\frac{d\overline{m}_i}{d\xi} = \frac{\overline{m}_i}{K(2K-1)} \frac{dK}{d\xi} + \frac{(2K-1)^2 \tilde{C}(K)_i}{K^2 \overline{m}_i} \mu_t \rho_t u_{ie} \quad , \qquad \text{(D-9)}$$

since

$$k_i \equiv \frac{1}{\rho_t u_{ie}} \frac{d\overline{m}_i}{d\xi} = \frac{C(K)_i \mu_t}{\overline{m}_i} \quad .$$

It therefore follows that

$$C(K)_i = \frac{(2K-1)^2}{K^2} \tilde{C}(K)_i + \frac{\overline{m}_i^2}{K(2K-1)} \frac{dK}{d\xi} \frac{1}{\rho_t \mu_t u_{ie}} \quad . \qquad \text{(D-10)}$$

Let us define: $\overline{C(K)}_i = \left(\frac{2K - 1}{K}\right)^2 \tilde{C}(K)_i$ and transform the results to the compressible plane. It is easily shown that $C(K)_i = C(K)$ and $\overline{m}_i = \overline{m}$ (See Reference 1.). Therefore,

$$C(K) = \overline{C(K)}_i + \frac{\overline{m}^2}{K(2K-1)} (dK/dx) \frac{1}{\rho_e u_e \mu_e} \quad . \qquad \text{(D-11)}$$

Clearly, if Falkner-Skan solutions are used, $dK/d\xi = dK/dx = 0$, so that

$$C(K) = \overline{C(K)}_i \quad , \qquad \text{(D-12)}$$

and the $C(K)$ relation is the same in the compressible and associated incompressible cases. However, for the general case, the term $\frac{\overline{m}^2}{K(2K-1)} \frac{dK}{dx} \frac{1}{\rho_e u_e \mu_e}$ is not zero, but generally depends on a

numerical integration of a specific case, and the $C(\kappa)$ relation is therefore not known a priori. It is thus seen that this attempt to improve the universality of the $C(\kappa)$ formulation has increased the mathematical complexity of the method. No systematic procedure for trying other $C(\kappa)$ formulations in order to obtain an optimum is known, and it is not even clear how to express the optimum condition since universality and mathematical simplicity are both important.

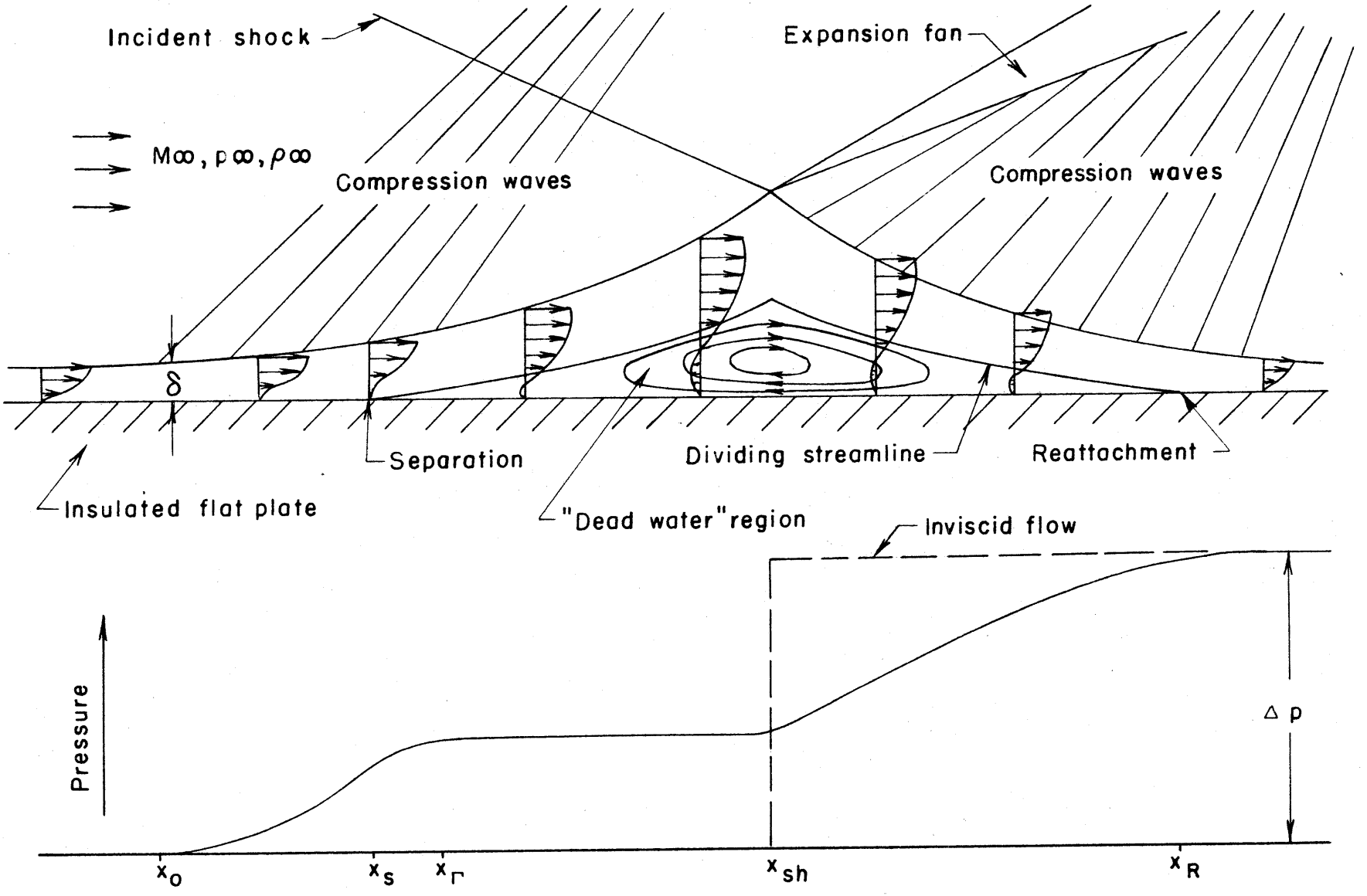

FIG. I – SHOCK WAVE – LAMINAR BOUNDARY LAYER INTERACTION

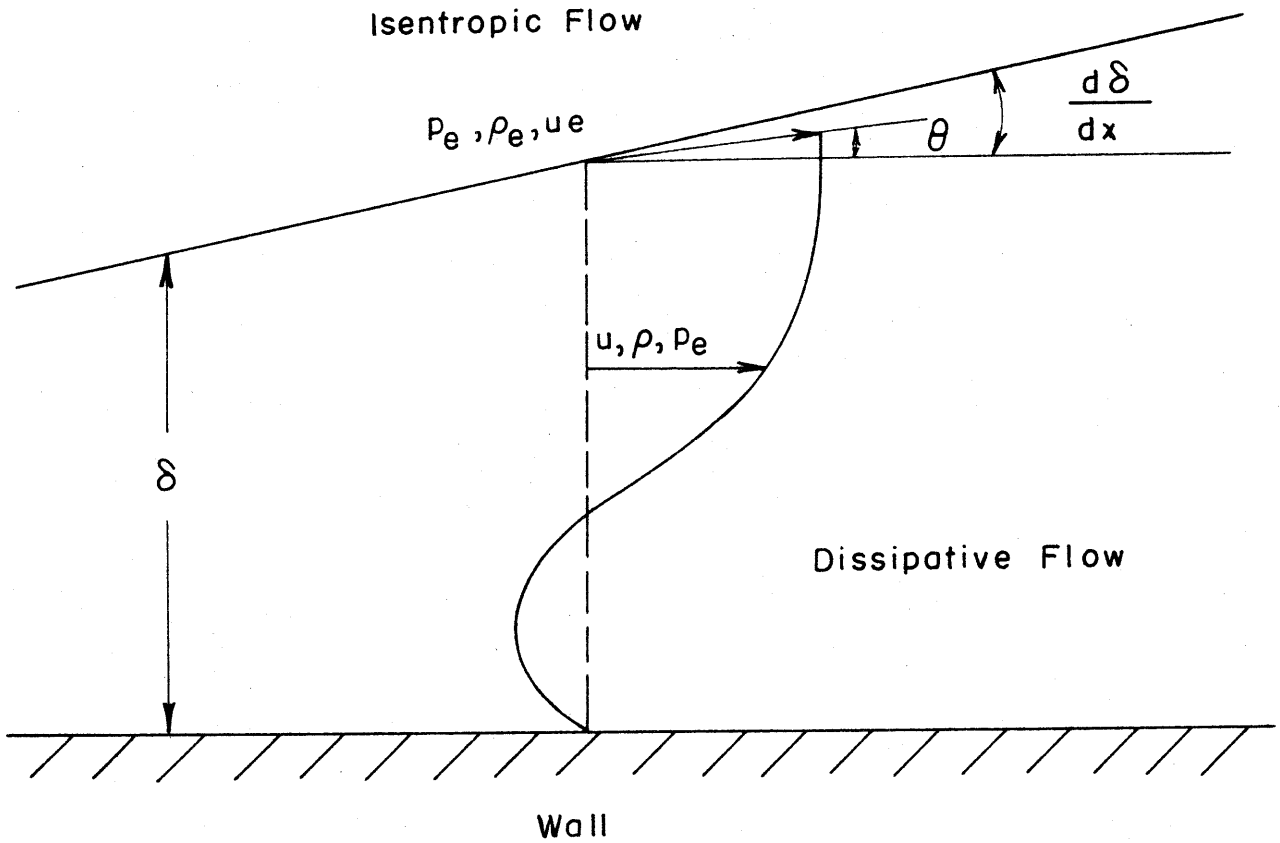

FIG. 2 – THE FLOW REGIONS

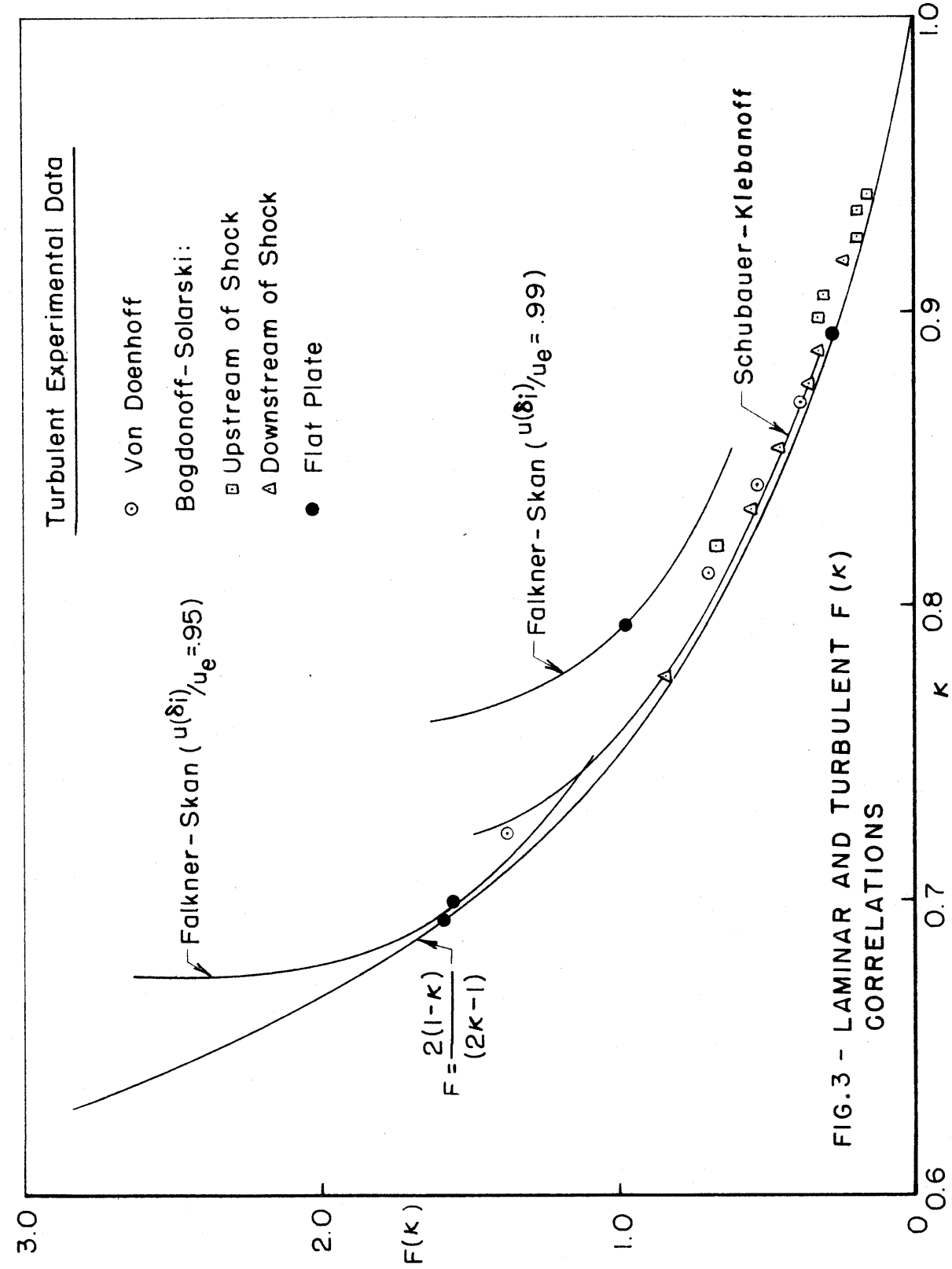

FIG. 3 - LAMINAR AND TURBULENT F(κ) CORRELATIONS

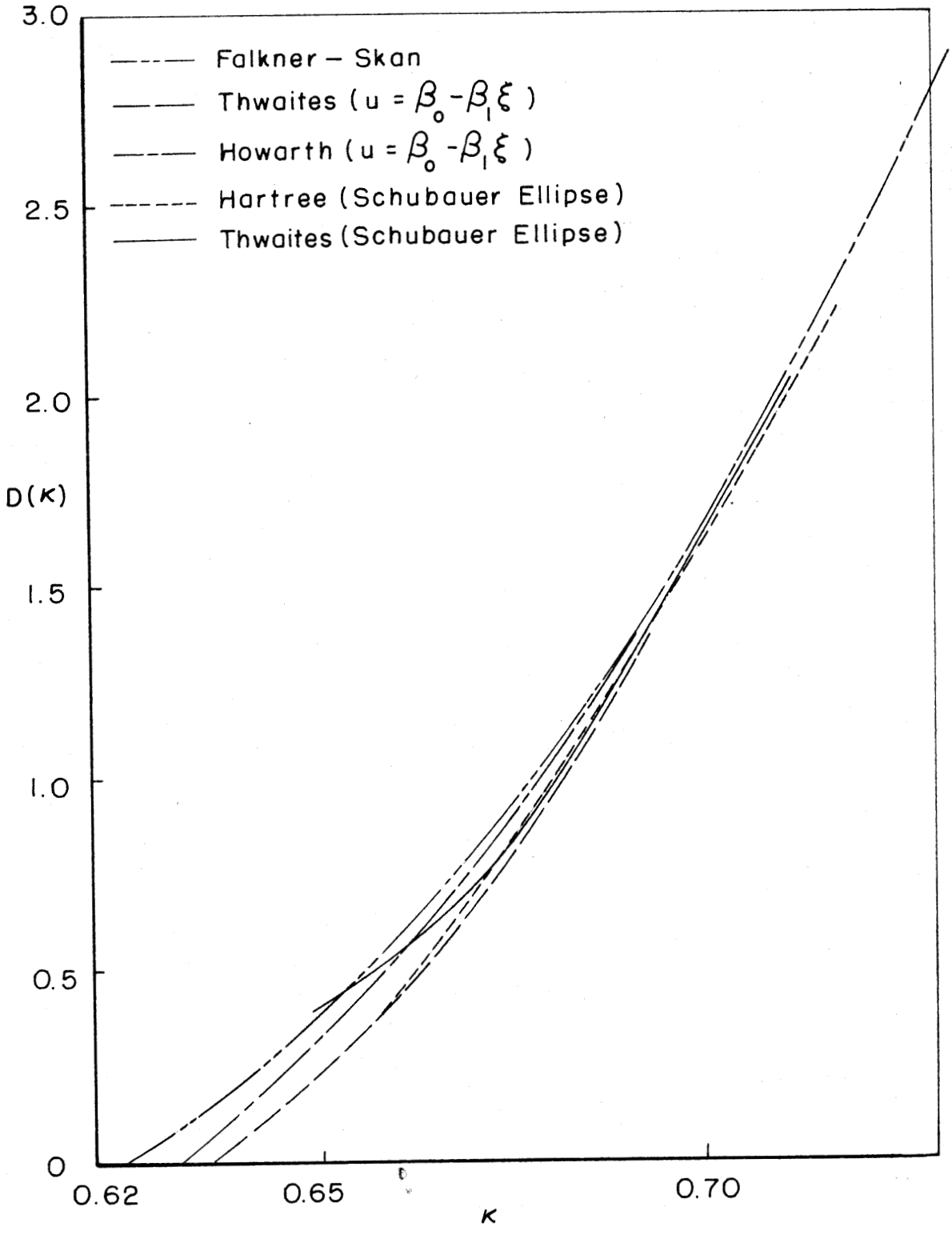

FIG. 4 - THEORETICAL D (κ) CORRELATIONS

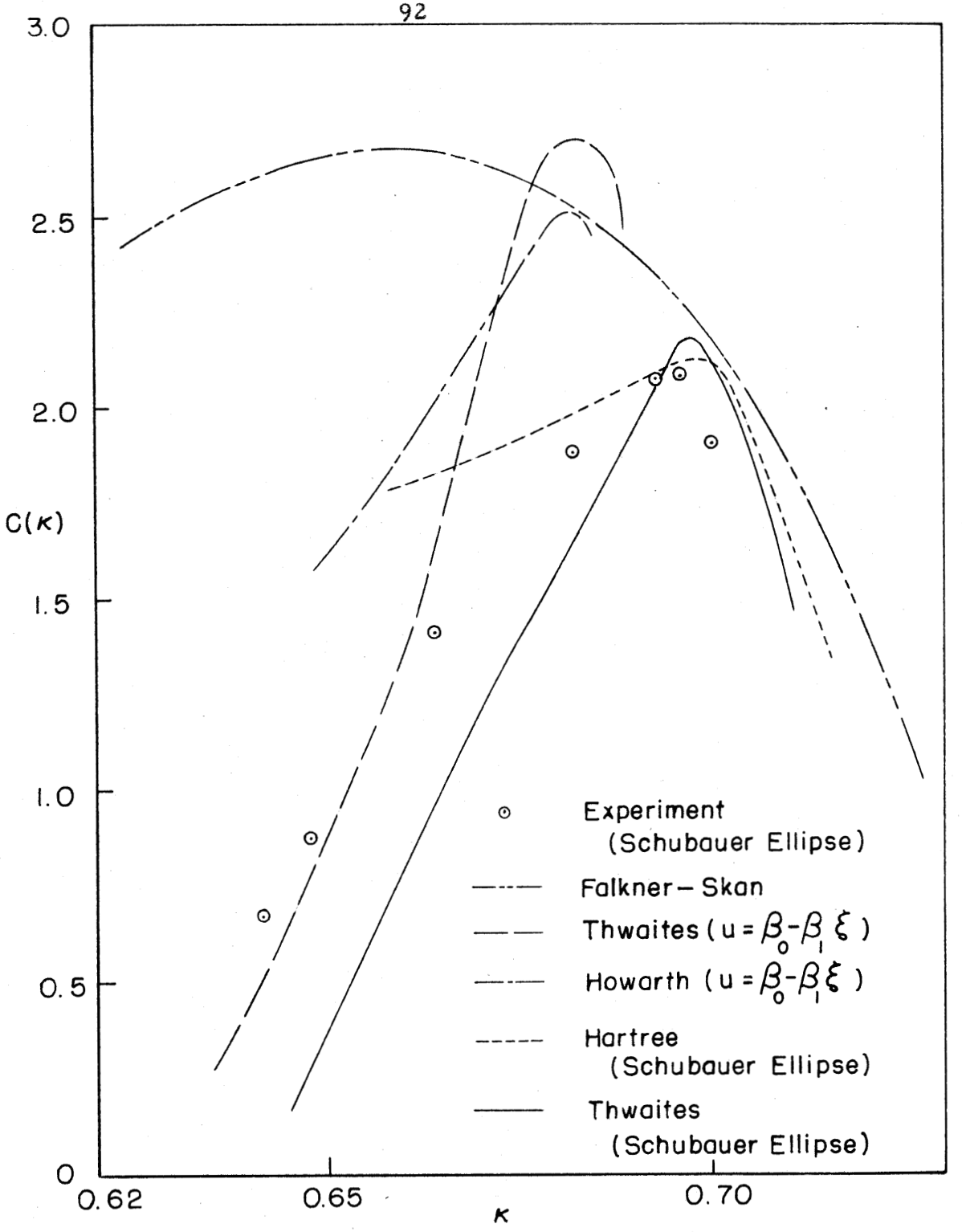

FIG. 5 – EXPERIMENTAL AND THEORETICAL C(κ) CORRELATIONS

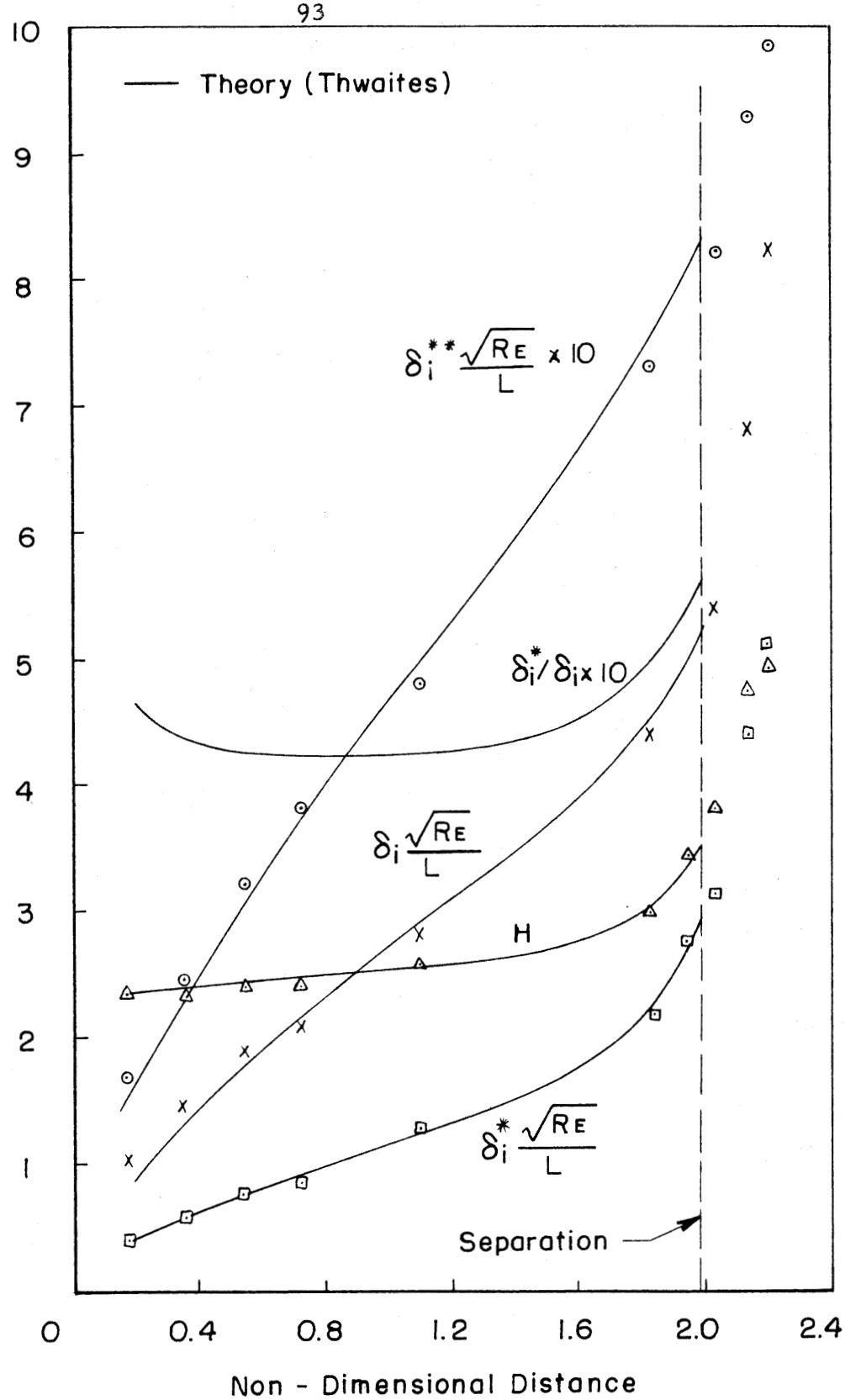

FIG. 6 - EXPERIMENTAL AND THEORETICAL BOUNDARY LAYER PARAMETERS FOR SCHUBAUER ELLIPSE

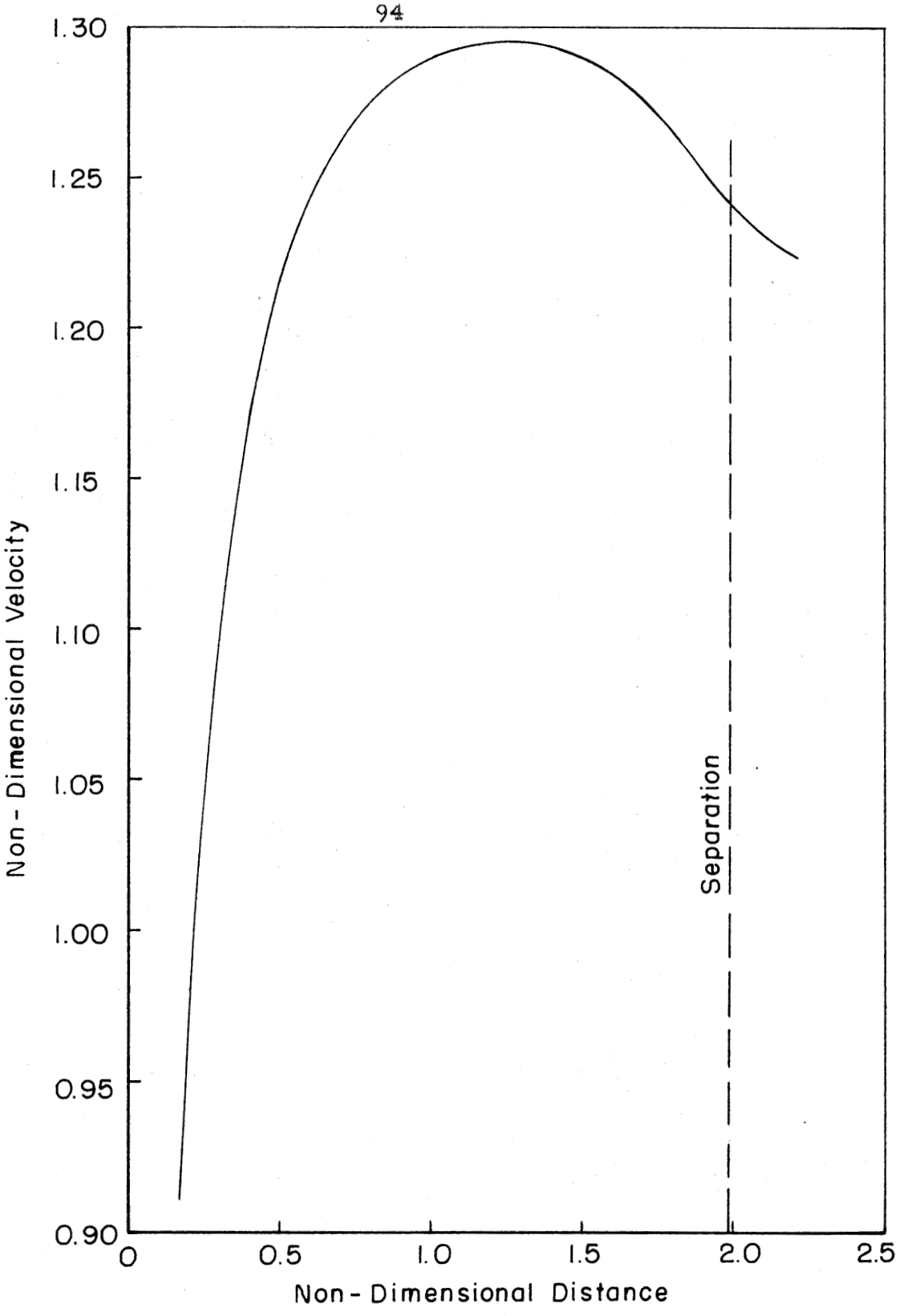

FIG. 7 – VELOCITY DISTRIBUTION OF SCHUBAUER ELLIPSE

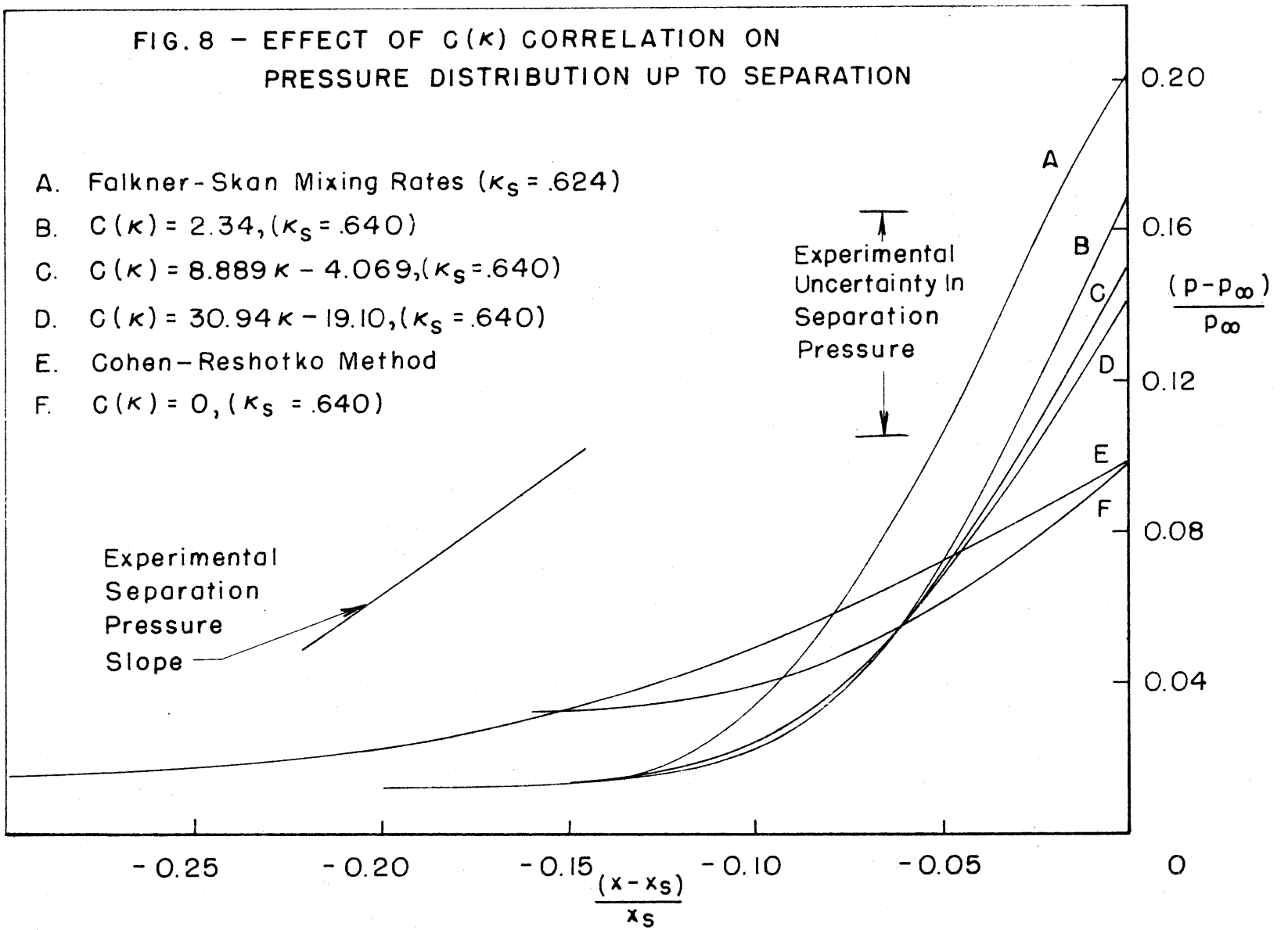
FIG. 8 – EFFECT OF C(κ) CORRELATION ON PRESSURE DISTRIBUTION UP TO SEPARATION
A. Falkner-Skan Mixing Rates (κ_s = .624)
B. C(κ) = 2.34, (κ_s = .640)
C. C(κ) = 8.889κ – 4.069, (κ_s = .640)
D. C(κ) = 30.94κ – 19.10, (κ_s = .640)
E. Cohen–Reshotko Method
F. C(κ) = 0, (κ_s = .640)
Experimental Uncertainty In Separation Pressure
Experimental Separation Pressure Slope
A
B
C
D
E
F
0.20
0.16
0.12
0.08
0.04
$\frac{(p-p_\infty)}{p_\infty}$
-0.25
-0.20
-0.15
-0.10
-0.05
0
$\frac{(x-x_s)}{x_s}$

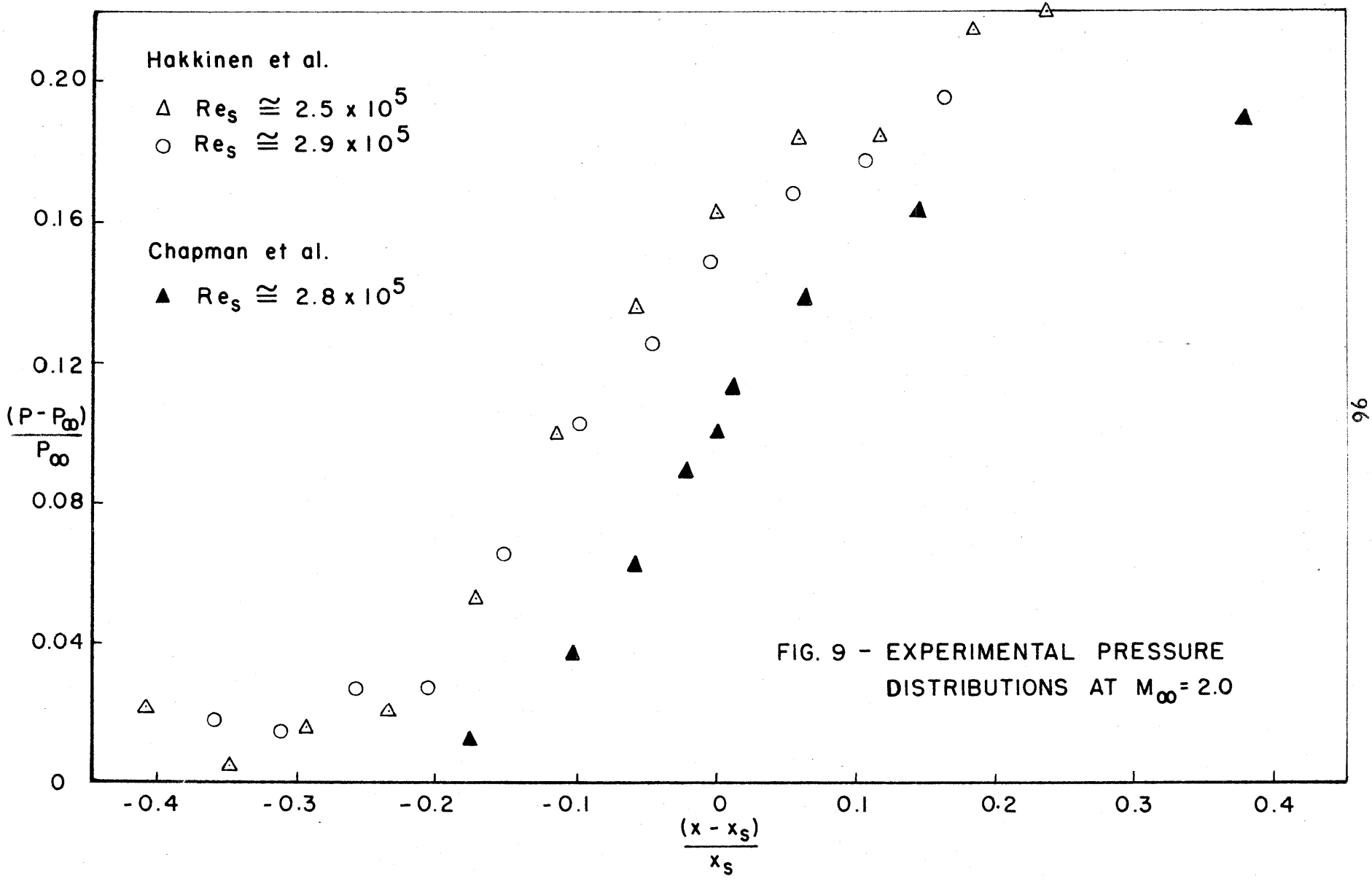

FIG. 9 - EXPERIMENTAL PRESSURE DISTRIBUTIONS AT $M_\infty = 2.0$

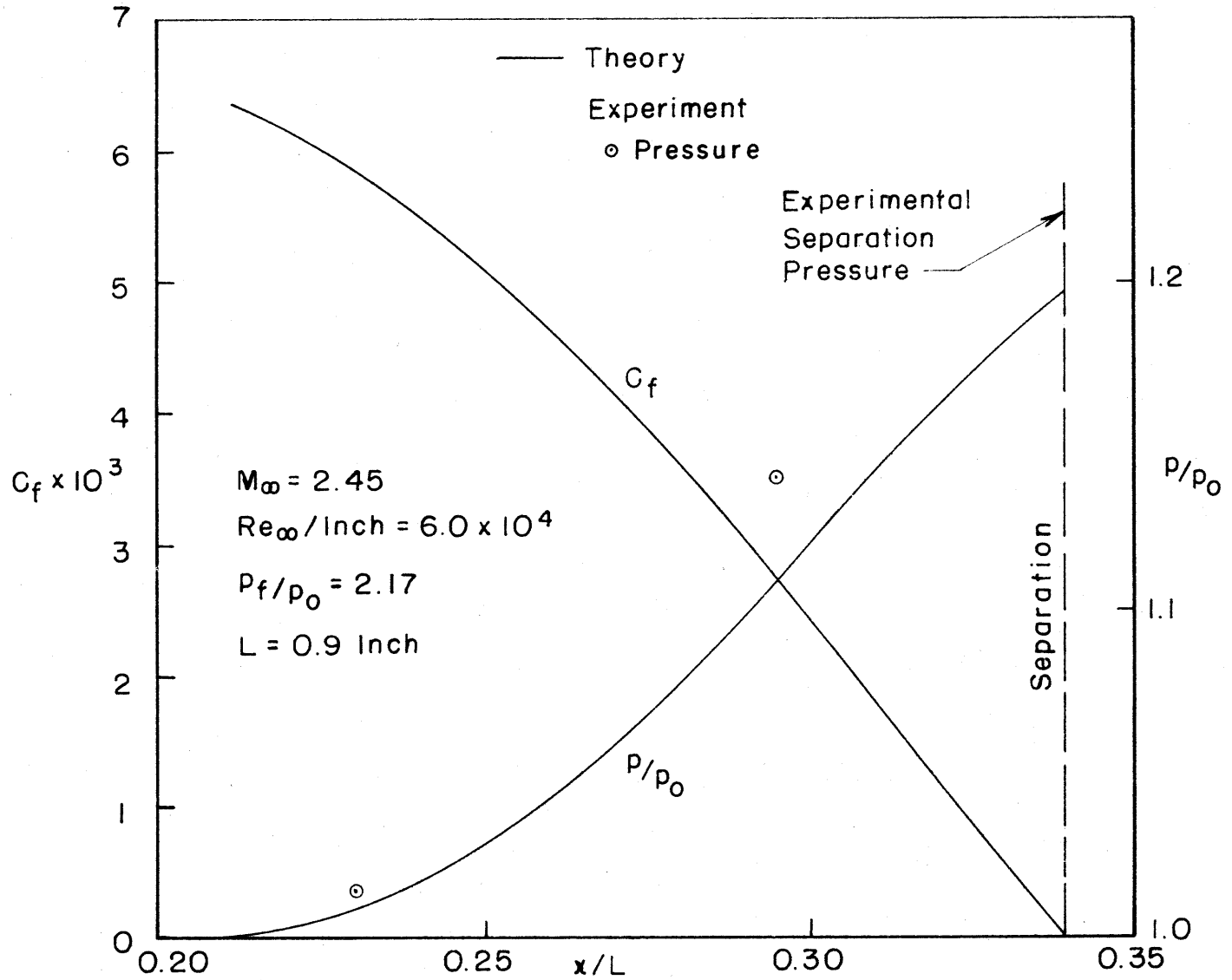

FIG. 10 - PRESSURE AND SKIN FRICTION DISTRIBUTIONS UP TO SEPARATION AT $M_\infty = 2.45$

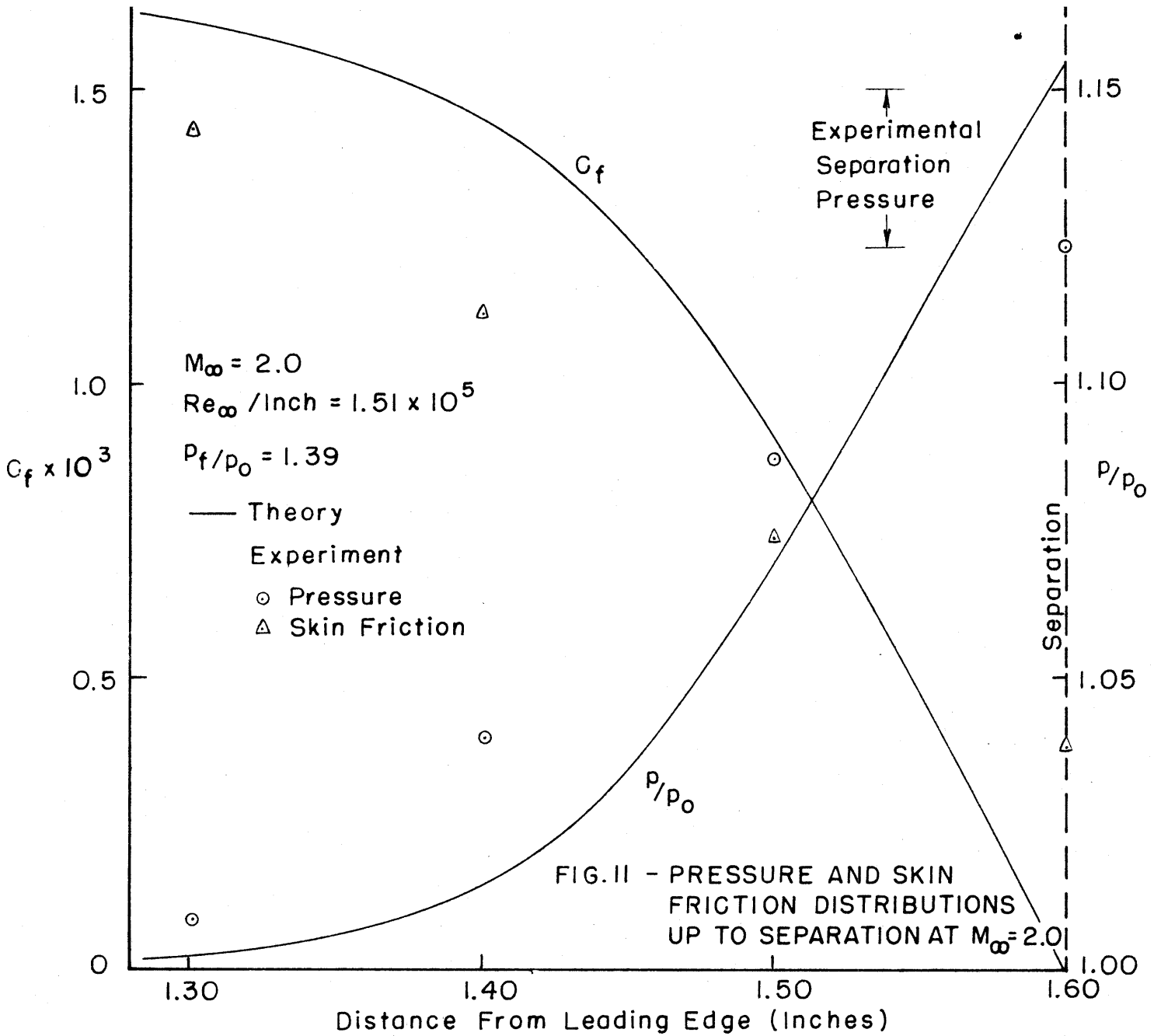

FIG. 11 - PRESSURE AND SKIN FRICTION DISTRIBUTIONS UP TO SEPARATION AT $M_\infty = 2.0$

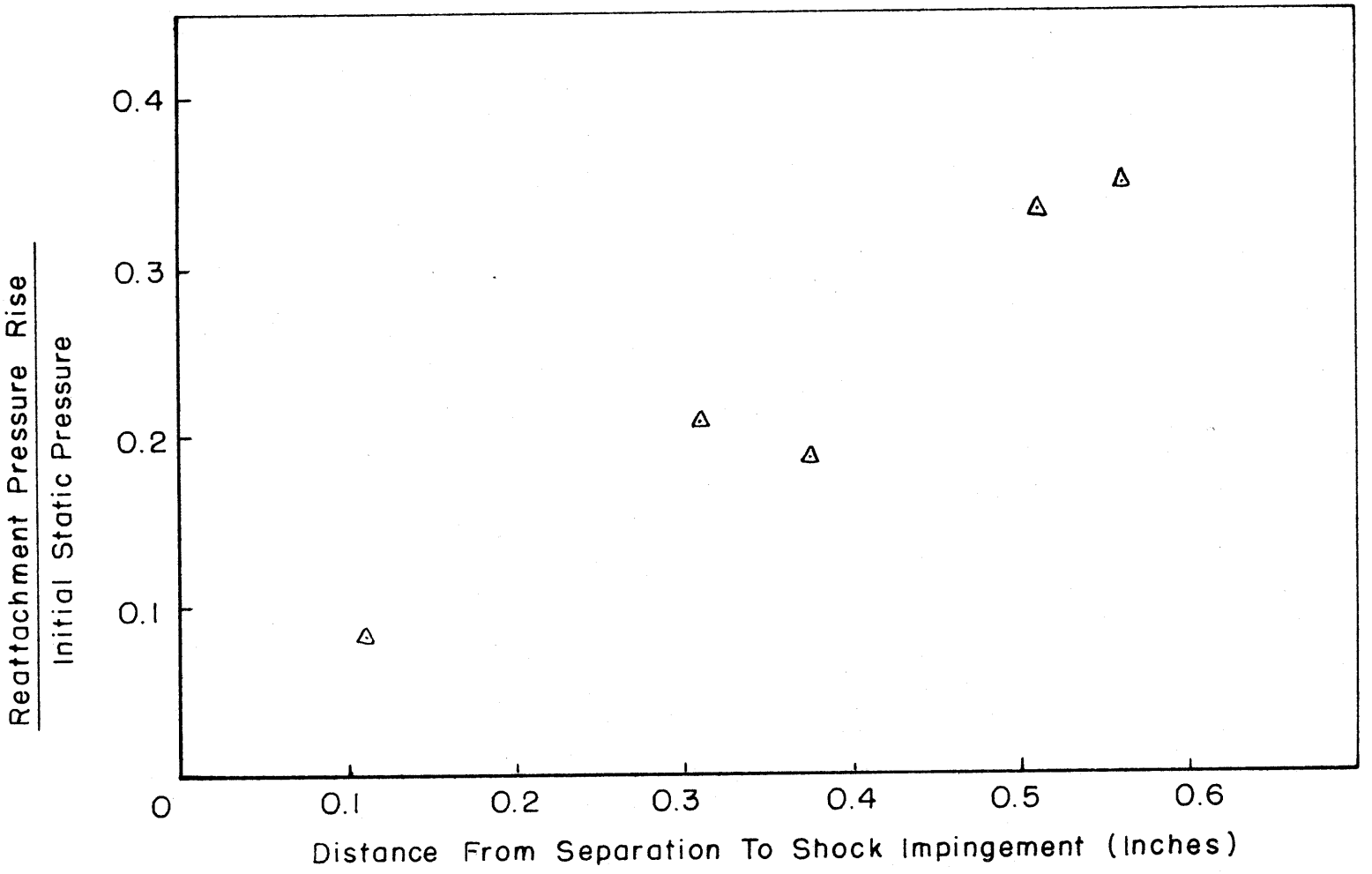

FIG. 12 - EXPERIMENTAL REATTACHMENT PRESSURE RISE AS FUNCTION OF DISTANCE BETWEEN SEPARATION AND SHOCK IMPINGEMENT

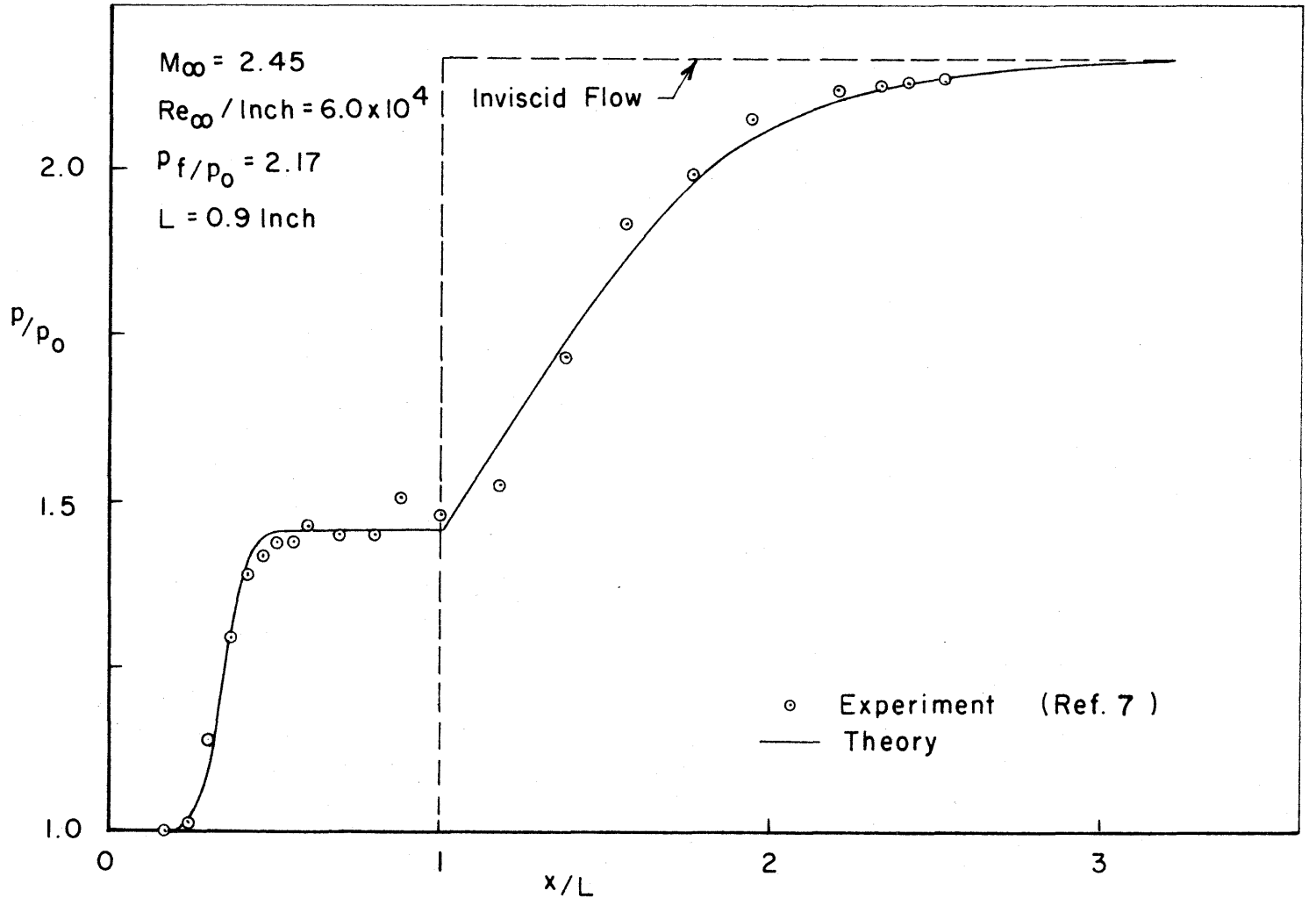

FIG. 13 - EXPERIMENTAL AND THEORETICAL PRESSURE DISTRIBUTIONS AT M_∞ = 2.45

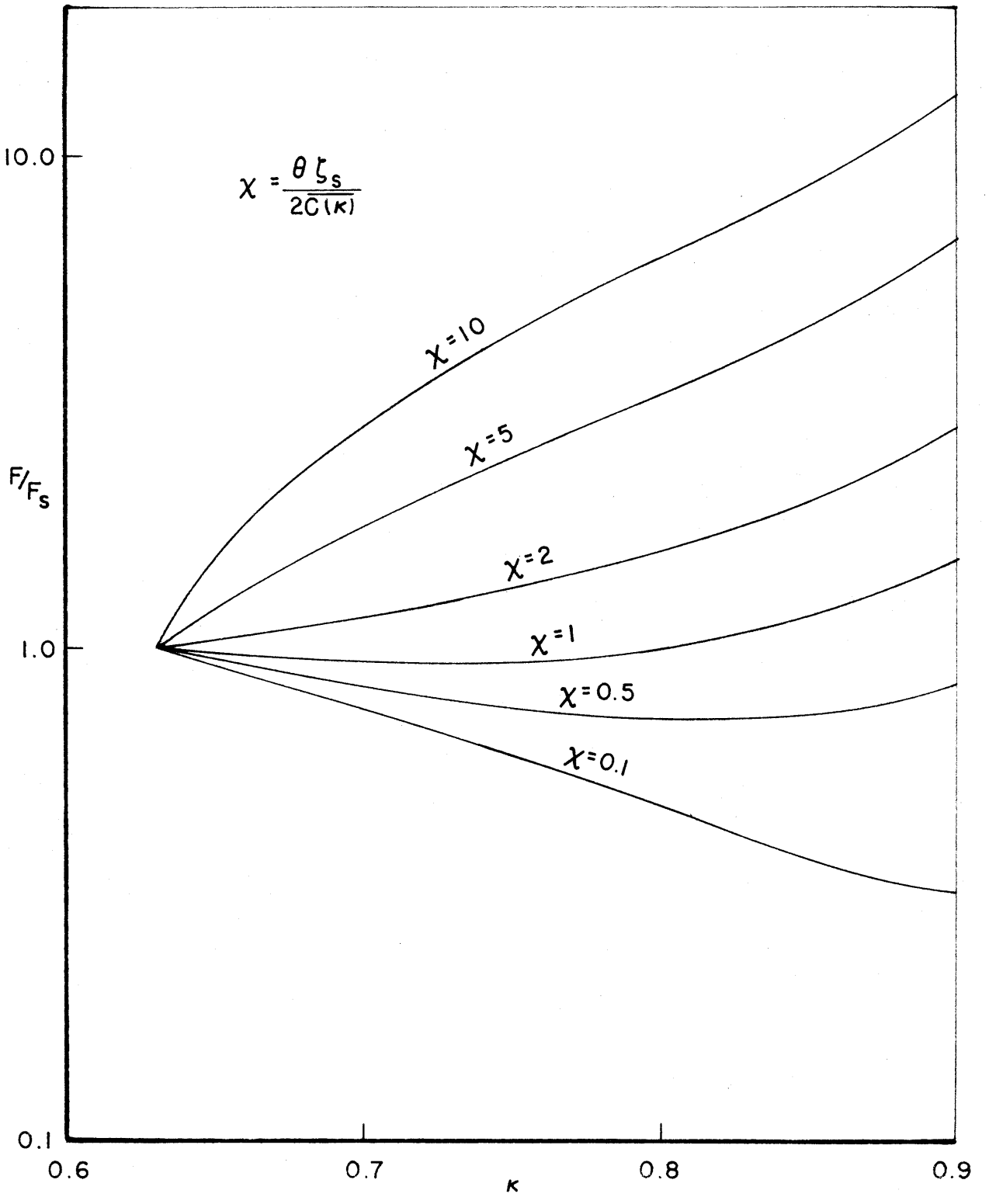

FIG. 14 - CONSTANT PRESSURE F(κ) RELATION

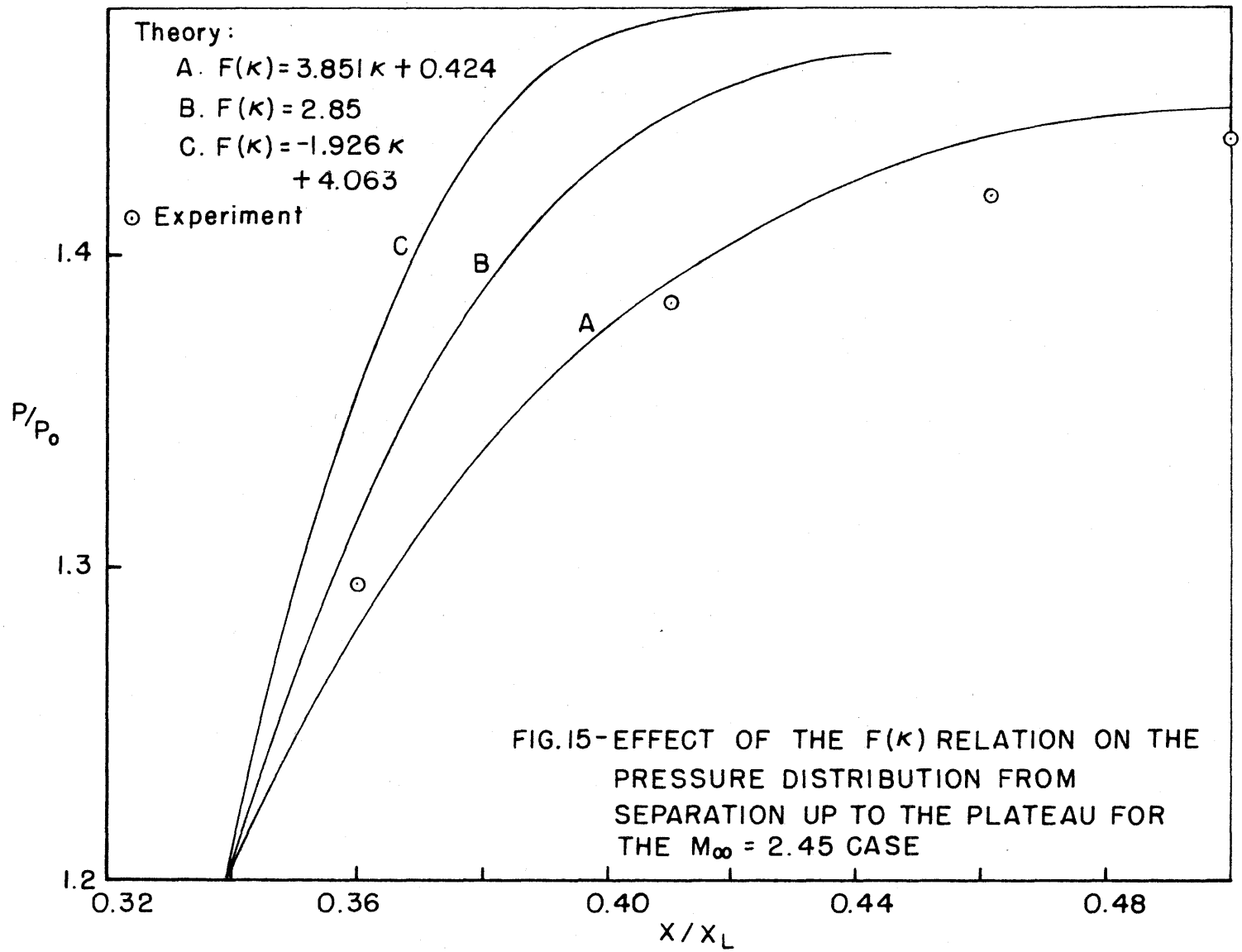

FIG. 15 - EFFECT OF THE F(κ) RELATION ON THE PRESSURE DISTRIBUTION FROM SEPARATION UP TO THE PLATEAU FOR THE $M_\infty = 2.45$ CASE

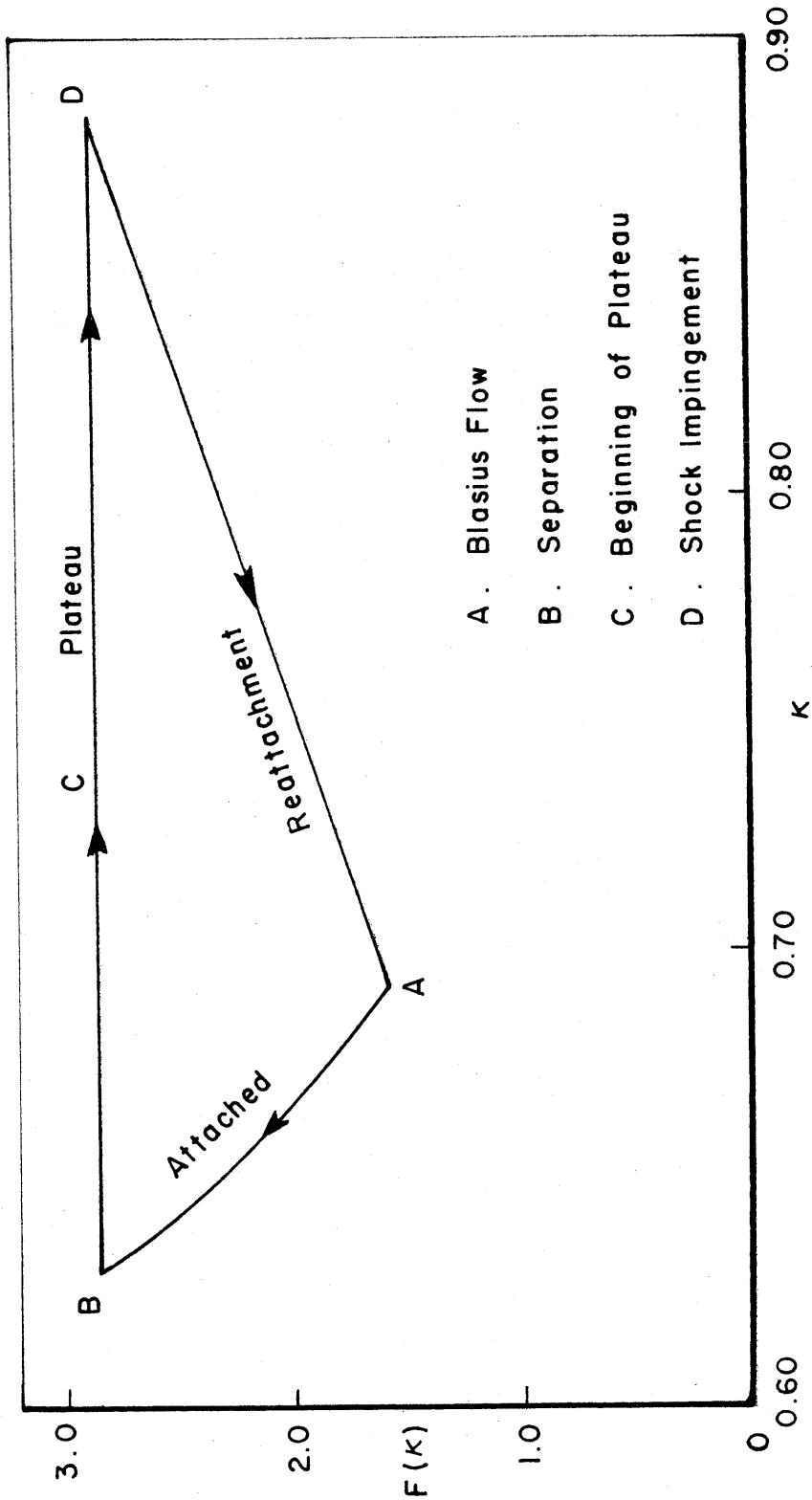

FIG. 16 - F(K) TRAJECTORY FOR SHOCK WAVE-LAMINAR BOUNDARY LAYER INTERACTION CASE AT $M_\infty = 2.45$

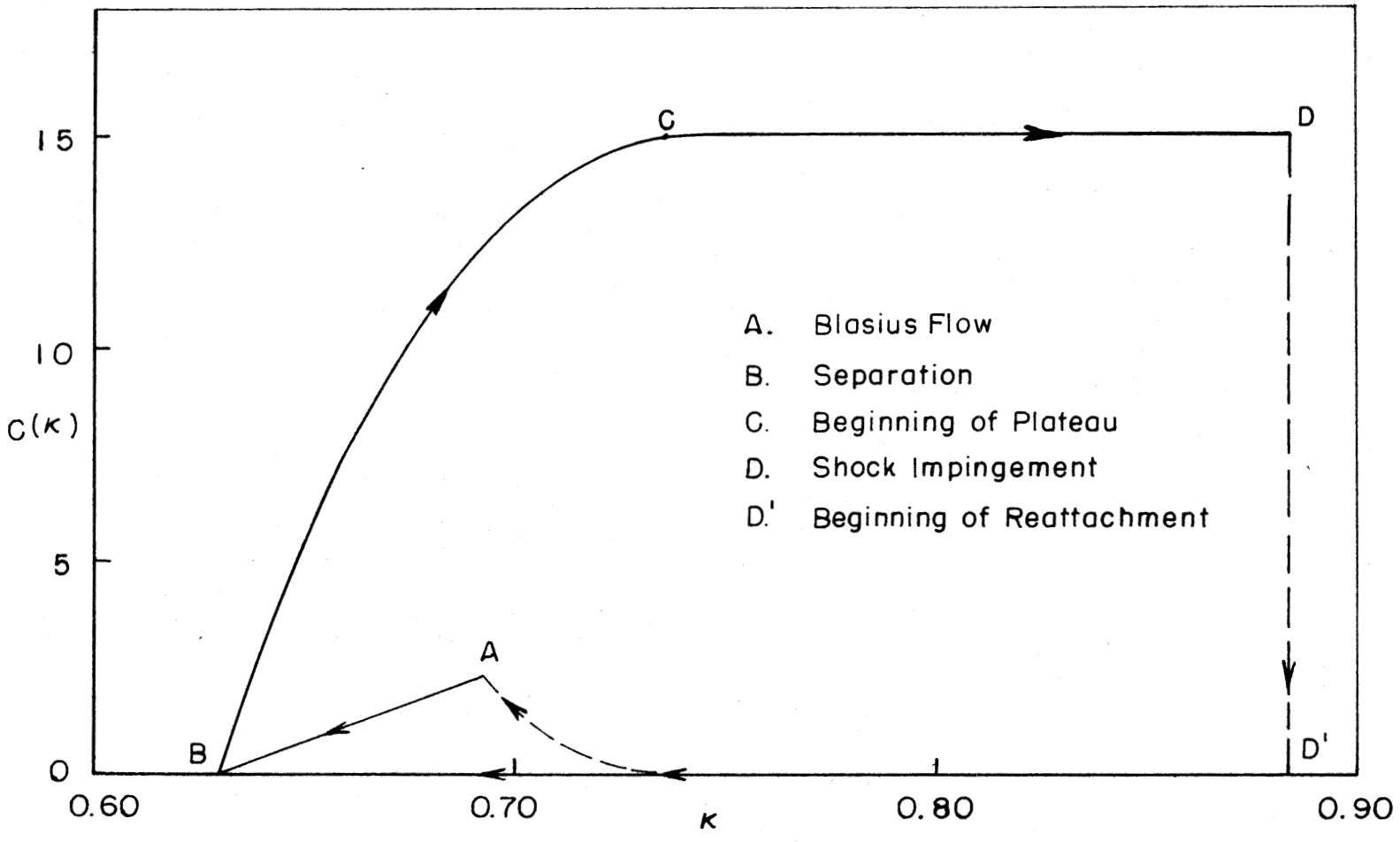

FIG. 17 - C(κ) TRAJECTORY FOR SHOCK WAVE-LAMINAR BOUNDARY LAYER INTERACTION CASE AT $M_\infty = 2.45$

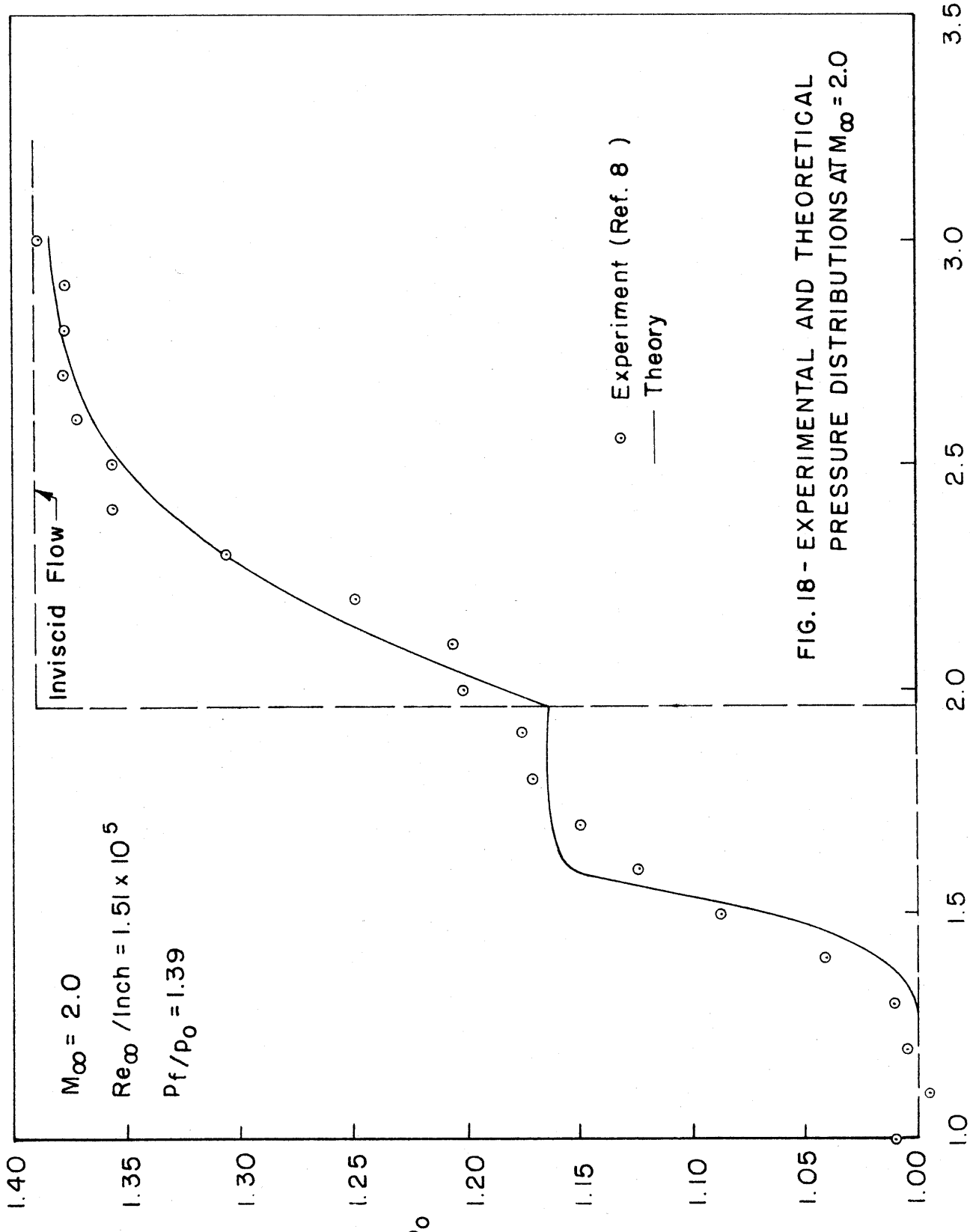

FIG. 18 - EXPERIMENTAL AND THEORETICAL PRESSURE DISTRIBUTIONS AT $M_\infty = 2.0$

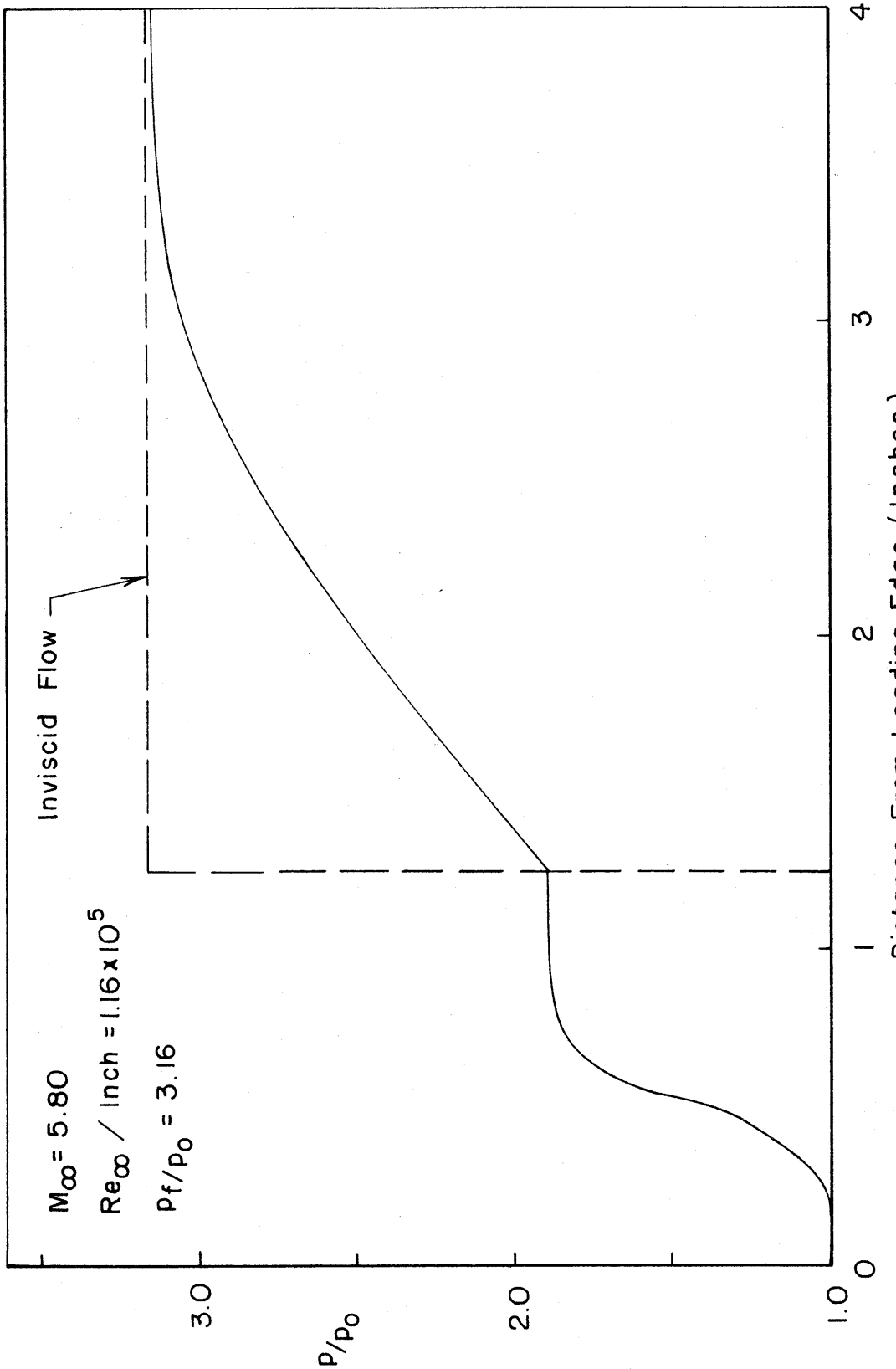

FIG.19 - THEORETICAL PRESSURE DISTRIBUTION AT $M_\infty = 5.80$

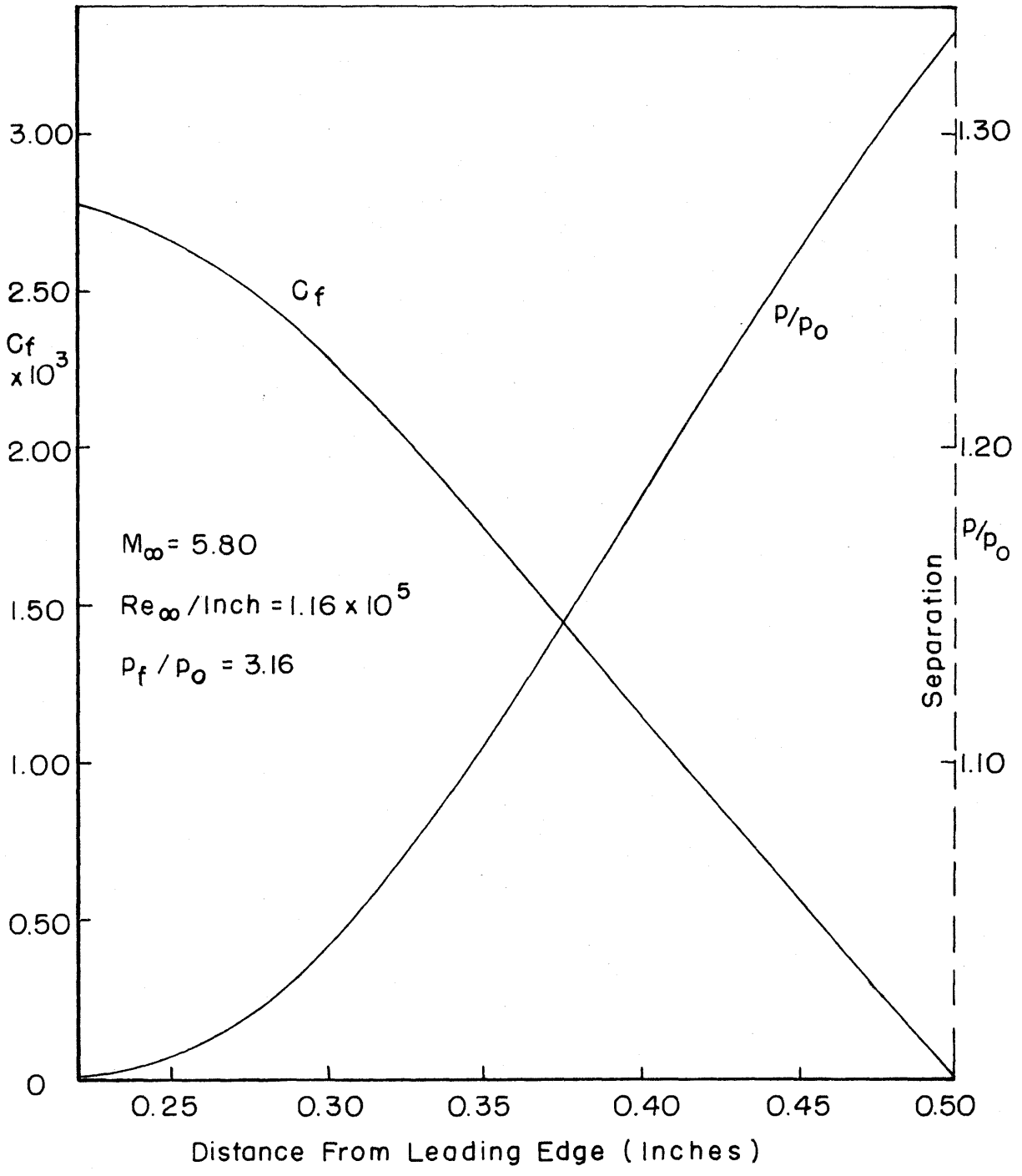

FIG. 20- THEORETICAL PRESSURE AND SKIN FRICTION DISTRIBUTIONS UP TO SEPARATION AT $M_\infty = 5.80$

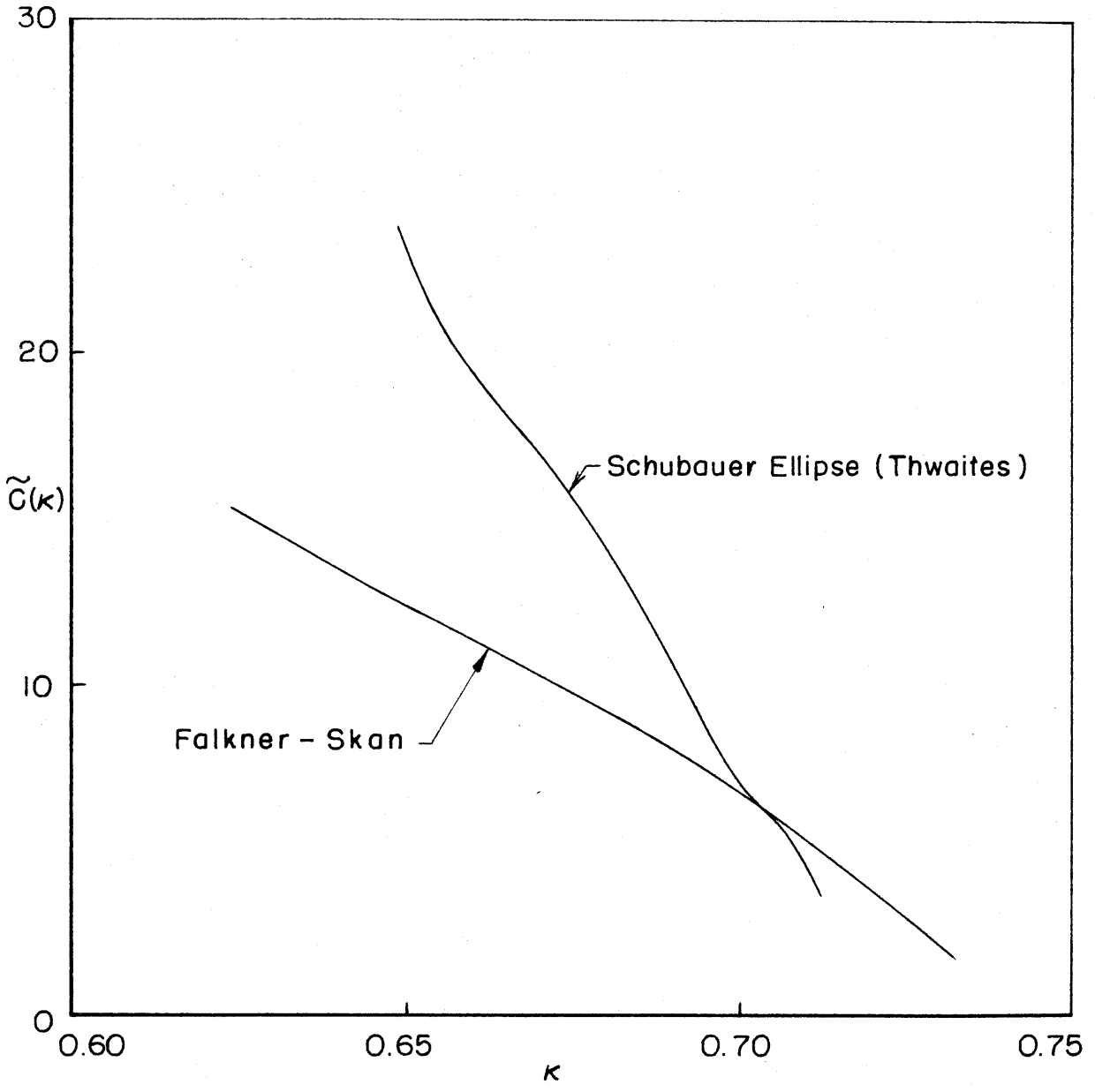

FIG.21 - THEORETICAL $\tilde{C}$ (κ) CORRELATIONS